Author response to editor and reviewers

We thank the reviewers for their comments to the paper, and have revised the paper accordingly.

Main revisions include the following:

- The paper has been thoroughly revised, restructured and written for brevity.
- The volcanic matching between RICE and WAIS Divide has been revised:

  The revision was based on a new conductivity-to-Ca excess depth profile, directly calculated from the two CFA records. Due to slight differences in depth assignment of the two records, we previously refrained from calculating their differences, and instead compared the two records visually. However, having a directly calculated record of the non-sea-salt conductivity simplified the volcanic matching between the two cores.

  The main difference from the previous matching is that we have removed some of the volcanic matches that we did not consider to be completely certain. Using the new non-sea-salt conductivity record, we were also able to identify and match up many more of the volcanic peaks in RICE to a counterpart in WAIS Divide.
- The new RICE volcanic record (Table 2) only includes volcanic events that are visible both in the RICE and WAIS Divide ice cores. We therefore do not attribute peaks in the RICE acidity records that do not exist in WAIS Divide as clear evidence of volcanic eruptions.
- We corrected an error in the calculation of uncertainty on the RICE accumulation rates. With this correction, the uncertainty bounds on the accumulation rates become much smaller going back in time, allowing us to infer past trends in accumulation rate with greater certainty.
- The connection between climate drivers and RICE accumulation rates have been described in more detail.

Point-by-point replies to the two reviewers' comments are provided separately.

With these changes, we hope that you will agree to the submission of a revised version of the paper.

On behalf of the authors,

Mai Winstrup

Answers to reviewer 1:

We thank the reviewer for the extensive comments and suggestions to the paper. Based on the reviewer comments, we have significantly restructured and revised the paper. We will not provide a detailed summary of these structural revisions below, but hope to be allowed to submit a revised version of the paper.

A point-to-point reply to the reviewer's comments are provided below (in blue), along with a short description of the adjustments to the paper relating to these comments.

The manuscript is poorly written, too long with several repetition redundant, several contradictions between the same paragraph or other paragraphs, the data and the result are inaccurate present (see example tephra layers).

The manuscript has been thoroughly restructured and revised, and redundancies have been removed.

We do not agree with the reviewer that we contradict ourselves, or that the data and result have been inaccurately presented, and we believe that this rely on misunderstandings. We hope that the reviewer agrees upon reading the revised version of the manuscript.

The methods chapter are not well structured with several information reported two three times and not in the appropriate chapter as result and discussion. Most of the information about the methods is reported in the supplementary material, where are more clearly presented. The manuscript must be completely revised and shortening significantly.

The manuscript has been thoroughly restructured and revised, and its content has been rewritten more concisely. Since the reviewers requested several expansions of the manuscript, the final version of the paper is, however, about the same length as the original version.

In the revised version of the manuscript, we have e.g. moved the section on timescale validation by comparison to WAIS Divide from "Method" to "Results". We believe that with this structural change, it should also become clearer that the RICE17 timescale is NOT synchronized to WAIS Divide, and that our matching of the two cores is only a basis for comparing the two timescales.

Some references are uncorrected or mismatched.

We have gone through all references and corrected these.

Five accompanied papers of RICE core are submitted or in preparation, but their result are used to validate or as source of the result of the manuscript (ex. Lee et al., in preparation).

It is correct that the Lee et al paper on methane matching of the RICE and WAIS Divide ice cores has not yet been submitted. We hope that this paper will be submitted very soon and will then be accessible as a discussion paper in Climate of the Past Discussions. In the present manuscript, we have revised the wording of the section on methane matching to improve its readability as a stand-alone text.

All other papers have been submitted and/or published now.

To make this manuscript a significant contribution to the literature, the authors need to better justify their time scale and snow accumulation records.

We hope that the reviewer will approve of the revised version.

Clarify the use of the WAIS volcanic signal and methane with RICE17 chronology, in the text look like that is use as synchronisation (see 3.3.1.3), but several point is stressed that the accuracy is low and it is use only at posteriori as validation. All the process of comparison between RICE and WAIS must be clarify, it is repeated several time in different way.

The RICE17 timescale is NOT synchronized to WAIS Divide.

We believe that part of the misunderstanding may be due to us inappropriately using the word "volcanic synchronization", where it more correctly should have been called "volcanic matching". This has been corrected in the new version of the manuscript.

If the two records are synchronised by volcanic the age error must be the same closer the tie points, between one tie point to other can increase. The process must be revised.

Since the two ice cores have not been synchronized (although they have been matched), the ages of the volcanic markers are not expected to be identical in the RICE and WAIS Divide records.

The tephra layers where used to fix the chronology, but it is not reported the analysis of tephra particles (Raboul 1964 CE and Pleaide 1252 CE) and the analysis on WAIS ice record (up to now never published on my knowledge), that can be permit an unequivocal attribution.

Results from geochemical analysis of the Pleiades tephra layers have been made available from the AntT database (http://antt.tephrochronology.org/I.html?id=AntT-15, http://antt.tephrochronology.org/I.html?id=AntT-16), which are now referenced in the text. Geochemistry of the Pleiades tephra horizon in the RICE and WAIS Divide ice cores is reported and discussed in Kalteyer (2015) and Dunbar et al (2010), which have now been included in the references:

Kalteyer, D.A., 2015. *Tephra in Antarctic Ice Cores*. Master Thesis, University of Maine. Available at: http://digitalcommons.library.umaine.edu/etd/2381/.

Dunbar, N.W., Kurbatov, A.V., Koffman, B.G., Kreutz, K.J., 2010. Tephra Record of Local and Distal Volcanism in the WAIS Divide Ice Core. 2010 WAIS Divide Science Meeting September 30-October 1, La Jolla, CA.

The 1965CE (Raoul) tephra layer from RICE and WAIS Divide is available from the Interdisciplinary Earth Data Alliance (IEDA) database (e.g. https://app.geosamples.org/sample/igsn/IESDW0026 and https://app.geosamples.org/sample/igsn/IESDW0016) with data reference Kurbatov (2015).

Results from the tephra analysis will be reported on in forthcoming publications, which we now refer to (see also comments below).

The explanation because nssSO4 signal or acidity peak of major eruption reconnaissance in WAIS (Tambora, Unknow etc.) are not recorded in the RICE records is questionable, but Authors have attributed as unknown more than hundreds chemistry signal to volcanic eruption (123 event Table 2) and those are not observed in WAIS or others ice core in Ross Sea (Siple Dome, Taylor Dome, Talos Dome). Why RICE records is able to record 193 volcanic event, with all the problems pointed out in paragraph 3.3?

We observe many small acidity peaks in the RICE records, which we in the previous draft related to volcanic events, despite these not being correlated to volcanic events in other ice cores. As the reviewer correctly points out, there is, however, a risk that we in Table 2 included acidity peaks derived from other events, e.g. extreme biogenic emission events.

For the new version of the manuscript, we have gone through the volcanic signatures in RICE and their matching to WAIS Divide, and have made the following changes:

- We established a new conductivity-to-Ca excess depth profile, directly calculated from the two CFA records. Previously, we only compared the two records visually, and refrained from calculating their differences, due to issues related to e.g. slight differences in depth assignment of the two records. However, as it turned out, having a directly calculated record of the non-sea-salt conductivity greatly simplified the volcanic matching between the two cores.

- With help of the new depth profile of non-sea-salt conductivity, we were able to match most of the prominent acidity peaks in WAIS Divide to volcanic peaks in RICE. The majority of the signals that were found in both cores corresponds to bipolar volcanic signals. This strengthens our trust in the reliability of the volcanic matching, since these are expected to deposit acidic material over an extended period, and therefore be most easily recognizable from the RICE records.

- The RICE acidity record still contains a large number of acid peaks that do not have a counterpart in WAIS Divide, but we refrain from stating that all these originate from volcanic events. Table 2 now only includes the acidity peaks that could be matched to a corresponding sulfate peak in WAIS Divide (65 acidity match points).

We consider the new volcanic matching to be very robust, and the main difference from the previous matching is that we have removed matches that we do not consider to be completely certain. However, the new depth profile of the conductivity-to-Ca excess allowed us to also identify a few new match points between RICE and WAIS Divide.

The text regarding the volcanic matching of the two cores has been revised accordingly.

Black Carbon, on the base of figure 4 does not appear the best proxies of seasonal signal, H+ appear more conservative and less misleading of BC

During development of the RICE17 timescale, we used all available proxies with annual signal, including black carbon and H+ (P. 9, line 26-27). Using multiple proxies will give us the most accurate timescale, as both records includes non-annual features that make annual layer interpretation based on a single record questionable.

Authors report strong gradient in snow accumulation spatially ranged from 0.09 to 0.30 m we/yr and migration of the dome from 500 to 900 m. Can the Authors exclude any impact on the snow accumulation history due to migration of the dome ? and/or on thinning function?

Over the last 2700 years, the Roosevelt Island ice divide has migrated only 500m from its present position (P13, L41), not 900m. We account for the migration of the ice divide in our derivation of the thinning function for the ice core, in that we vary the vertical velocity profile through time (P14, L11-20).

As suggested, we have added to the manuscript a brief discussion on how the migration of the ice divide could influence the obtained accumulation rate history:

The recent period (~1500-1750 CE) of divide migration at Roosevelt Island may impact interpretation of the climate records from the RICE core. Present accumulation rates across Roosevelt Island show a distinct decrease on the downwind (western) side of the ice divide, with a gradient of ~0.5 cm/km yr^{-1}, although the trend is muted around the summit area. Ice recovered in the deeper part of the RICE core, deposited before divide migration, have originated west of the ice divide. Assuming a stable snowfall pattern through time relative to the divide, its migration would have caused reduced accumulation rates to be observed during the early part (until 1500 CE) of the RICE accumulation history. With an origin of the ice recovered in RICE of up to 500m west of the divide at time of deposition, our estimates of Roosevelt Island accumulation rates during this early period would therefore have a small negative bias of up to 0.25 cm/yr.

Correcting for the influence of ice divide migration, the main impact on the Roosevelt Island accumulation history is an earlier onset of the period with more rapid decrease in accumulation rates. The differences are small, however, and the overall pattern of trends in accumulation rate through time remains the same. In particular, ice divide migration has no impact on accumulation rate trends observed before and after the migration period.

As mentioned, the impact on the accumulation history is small, and ice divide migration would have no impact on e.g. recent trends in accumulation rates.

Paragraph 5.3 "Current mass balance. . .. "does not report any new valuable information for the mass balance of the RIS

We have deleted this section from the manuscript.

P. 3, line 44-47: How could explained stable ice divide flow with a migration of the ice divide position of around 500-900m?

First of all, the ice divide has migrated only 500m, and this migration took place over a period of a few hundred years (roughly 1750-1500CE). During periods before and after, i.e. during the majority of the period, the ice divide flow was stable. We have accounted for the change in ice divide location over time in our modelling of the thinning function (P. 14, line 11-20).

We have revised the text to clarify this:

To account for the changes in vertical strain rates at the drill site over time, we assumed the following divide-migration history, informed by the architecture of the Raymond stack (Fig. 6b): Until 500 years before ice core drilling (1512 CE), the divide was located 500 m east of the present position, as indicated by the position of the deeper Raymond arches. Since 500 years ago, the divide migrated westward, reaching its current position approximately 250 years ago (1762 CE), where it has since been stable.

P.4, line 33-34: RICE would be representative of East Ross Sea, not of Victoria Land, see accompanied RICE paper (Bertler et al, submitted)

We have removed this sentence from the paper.

Chapter methods: This part is too long and inappropriate as method chapter and most of the text must be moved to result chapter.

As suggested by the reviewer, we have significantly restructured the paper.

The content of the methodology chapter is now split up into three parts: "Ice core processing and impurity analysis", "Constructing the Roosevelt Island Ice Core Chronology, RICE17, for the last 2700 years", and "Reconstructing past accumulation rates". We further have removed the section on comparison of the RICE17 timescale to WD2014 to the Results. We hope that this restructuring has made the paper more easily accessible.

The does not provide information about the sample resolution along the core and the analysis performed and at which resolution ice (cm) and sample per year.

Sample resolution of the various records is provided in Table 1. Further, as the CFA records are measured continuously, a discussion of their effective depth resolution is made on P.5, line 47 – P.6, line 5. We have made a slight addition to this paragraph to clarify the distinction between the two, so that it now reads:

The CFA chemistry records are very densely sampled (1 data point per mm). Mixing in the tubing, however, as the meltwater sample travels from melthead to the analytical systems caused individual measurements to be correlated, and hence the effective depth resolution of the system is significantly less than the sampling resolution. This was especially the case for the RICE CFA set-up due to the relatively small fraction of total meltwater directed to the continuous measurement systems. Following the technique used in Bigler et al. (2011), we estimate the effective depth resolution for the CFA measurements to range from 0.8 cm (for conductivity) to 2.4 cm (for calcium) (see supplementary Table S1).

The layer thickness is decreasing with depth, causing the number of independent samples per year to also change with depth (and varying between the individual chemical species). We therefore prefer to refrain from providing a general value for the number of samples per year in the manuscript.

Instead, in the section "Overview of the annual-layer counting strategy", we now mention the number of independent data points per year in the best resolved record in the very deepest part of the layer-counted timescale:

At this depth, the annual layers are too thin (<6 cm, i.e. less than 8 independent data points/year in the best resolved records) for reliable layer identification in data produced by the RICE CFA set-up.

Percentage of missing record of CFA example must be reported and show.

We have added the following paragraph to the paper (P. 5, line 46):

Core breaks and/or contamination in the system caused some sections of missing data. The percentage of affected core varied between chemistry species, ranging from <1% (BC) to 15% (H^+), the majority being small sections of missing data that did not severely impact annual layer interpretation of the records.

Most of the information about methods is relegate in the supplementary info.

We are not sure whether the reviewer would like us to move more of the material in these three paragraphs into the supplementary, or if he/she would like us to include some of the supplementary material into the paper itself.

In our endeavor to shorten the paper, we have decided to keep the division between the two more or less as is. We have transferred some of the technicalities on the StratiCounter set-up to the supplementary.

However, we have included into the main paper the discussion of the annual layer signals observed in the various CFA records, as we consider these to be of general interest.

P. 6, line 21-24: This paragraph present contraindiction in several points, along the entire text, correlation between RICE and WAIS "volcanic event" are used or not to tune the RICE scale? Ex. See line 29-30 of pag 6

Apart from the top 42m (where the timescale can be constrained by historical events), the RICE17 timescale is a fully independent layer-counted timescale, i.e. it has not been tuned to the WAIS Divide timescale. The correlation to WAIS volcanic events is only used for subsequent comparison of the timescale to WD2014. We recognize that this essential aspect was not sufficiently clear from the manuscript, and, as previously mentioned, we have made several revisions to the paper for clarification, including the following:

- We have moved the comparison of the RICE17 timescale to WD2014 to the results section.
- A few instances of incorrect use of the word "synchronizing" has been removed, and the word "tiepoints" has been replaced with "matchpoints".

We have further revised the section "Overview of the annual-layer counting strategy" on page 6, so that it now reads as follows:

The uppermost section (0-42.34 m) of the core was dated by manual identification of annual layers in records of water isotopes and ice impurities from the RICE main core as well as the RICE-12/13B shallow core. For this most recent period, several distinct marker horizons from well-known historical events were used to constrain the chronology.

Below 42.34m (1885 CE), the timescale was augmented using the StratiCounter layer-counting algorithm (Winstrup et al. 2012) applied to multiple CFA impurity records from the RICE main core. A previously-dated tephra layer at 165 m (Pleiades; 1251.6±2 CE according to WD2014) was used to optimize the algorithm settings, but other than that, RICE17 is a fully independent layer-counted ice-core chronology.

Page 6, line 24: The Raoul tephra is a unequivocal volcanic event or not?

The Raoul tephra is an unequivocal tephra horizon, but as it is located above 42m it is not mentioned here. In the revised version of this paragraph (see above), we have removed the reference to unequivocal volcanic events.

Page 6, line 31-32: The layer counting stops at 343.72, because the annual layer is to fine (<6cm), to identify seasonal signal needs at least 10-12 sample per year, a graph showing the number of sample analysed per year must be show, from the surface to the 344m

As the CFA measurements are made continuously on the melt water stream, the notion of the number of samples per year is not a straight-forward measure for such data sets. Further, due to different amount of mixing in the various chemistry melt-water lines in the CFA set-up, the effective depth resolution differs between data sets. Instead of showing these in a graph, we have elected to mention the number of data points per year in the best resolved record in the very deepest part of the layer-counted timescale (P.6, line 31-32), as also mentioned above.

In the bottom part, we have less than 8 independent data points/year in the best resolved records. We note that this number is less than ~10-12 independent samples per year, mentioned by the reviewer to be required for annual layer identification. This lower number is somewhat counteracted by the near-continuity of the CFA records, which was employed on a depth scale with ~1mm resolution (i.e. resulting in 60 correlated samples/year in the deepest part of the timescale).

Page 6, line 44-46: The record of overlap section must be shown to see the ratio noise/signal in the two cores

As the reviewer also requests a significant shortening of the paper, we have elected not to extend the manuscript with such figure.

Page 7, line 10: Several other records also displayed annual variability, but much less reliability" Why do use BC instead of H+ or both

This is a misunderstanding. For all depth intervals, annual layer interpretation in the RICE17 chronology is based on the complete set of available chemistry and isotope records, as also mentioned in the section "Overview of the annual-layer counting strategy".

Our intention with the remark on page 7, line 10, was simply to note that some data series displayed a more reliable annual signal than others. In the deeper part, BC is the record with the most reliable annual signal, partly because of the high resolution of the record. Yet, also here annual layer counting is based on all CFA records, including H+.

Page 7, line 11-16: The peak of proxies seasonality are quite different in time (isotope versus sea ice proxies, or photolysis), and most depend from the occurrence of snow fall. The use of ERA model does not look appropriate and the reference is still not published

We observe from the data records that water isotopes and acidity signals peak simultaneously in most years (Figure 4), which we interpret as the maximum annual temperature and lowest sea ice extent taking place approximately at the same time. We have assigned the depths of these peaks to correspond to January 1st. Seasonal variations in snowfall will influence the precise depth location of the peaks in the various records, but it will do so similarly for all records.

In the text, we have shortened and reorganized the section, and removed the reference to ERA-interim data, so that the paragraph now reads:

Summers could be identified as periods with high stable isotope ratios, high concentrations of nss-SO_4^{2-} and associated acidity [originating from phytoplankton activity in the surrounding ocean during summer (Legrand et al. 1991; Udisti et al. 1998)], and low iodine concentrations [due to summertime photolysis of iodine in the snowpack (Frieß et al. 2009; Spolaor et al. 2014)]. Layer marks were placed according to the depths of concurrent summer peaks in water isotope ratios, nss-SO_4^{2-} concentrations, and acidity levels, and assigned a nominal date of January 1st.

Page 8, line 17-21: Geochemical composition of the tephra at RICE-WAIS and source must be show before any attribution of a tephra never reported in Antarctica before (Raoul 1964)

Results from the geochemical analysis of the Raoul tephra from RICE and WAIS Divide is available from the IEDA database, with data reference Kurbatov et al 2015 (which unfortunately had dropped out of the previous version of the manuscript):

Kurbatov, A. V. et al., 2015. Major element analyses of visible tephra layers in the Roosevelt Island Climate Evolution Project ice core (Antarctica). *Interdisciplinary Earth Data Alliance (IEDA)*. Available at: https://app.geosamples.org/sample/igsn/IESDW0025

The attribution to Raoul will be reported in a paper currently in preparation.

We have added these references to the text:

A couple of volcanic horizons in RICE during this most recent part could be unambiguously related to well-known volcanic eruptions. Rhyolitic tephra located between 18.1-18.2m (Kurbatov et al. 2015) was found to have a similar geochemical composition as a tephra layer found in the WAIS Divide core, with a depth corresponding to late 1964 CE. The tephra likely originates from Raoul Island, New Zealand (Wheatley et al, in prep), which erupted from November 1964 to April 1965. This is consistent with the RICE17 chronology, according to which the tephra is located in early 1965 CE (Table 2).

Page 8, line 21-36: It is not clear why some sulphate deposition is attributed to eruption and others no, and correlated to WAIS

For this most recent part of the timescale, for which historical volcanic eruptions constrained the timescale, we used all available unambiguous volcanic horizons. Apart from the Raoul tephra, however, we were only able to identify two volcanic horizons during this time interval: Santa Maria and Krakatau. We note that the ages of these volcanic horizons are constrained from historical records, and not because of synchronization to the WAIS Divide core, but agree with the reviewer that this was not clear from the previous version of the manuscript.

We have shortened this section, removed the references to WAIS Divide ages, and revised the wording to clarify these aspects. It now reads:

Only two volcanic eruptions could be unambiguously identified in the acidity records over this period, namely the historical eruptions of Santa Maria (1902 CE; 37.45m) and Krakatau (1883 CE; 42.34m). These two horizons were used to constrain the deeper part of the manually-counted interval of RICE17, which terminates at the Krakatau acidity peak (Table 2). Deposition age of volcanic material for these events was assumed identical to observed in the WAIS Divide ice core (Sigl et al. 2013). Imprints from other large volcanic eruptions taking place during recent historical time, such as Agung and Pinatubo, did not manifest themselves sufficiently in the RICE records to be confidently identified.

Page 8: Analysis of comparison between manual and automated annual counting must be performed and show

The manual counting performed was only a rough preliminary counting, with the sole purpose of producing a set of templates for the annual layers in the chemistry records, as required for initialization of StratiCounter. We therefore refrain from performing an analysis between the manual counts and the automated layer counts in the paper.

We have revised the wording in this section to ensure that the preliminary nature of the manual layer counts is better conveyed to the reader:

StratiCounter was initialized based on a rough set of manual layer annotations in a short section of the data (40-150m). The manual annotations were used to produce a template for an annual layer in the various impurity records. To increase the independence of the StratiCounter timescale from the preliminary manual interpretation, in a final step the entire timescale was reevaluated using an improved set of layer templates derived from the output of the algorithm itself.

In order to shorten the paper, these and other details regarding how the StratiCounter software was run has been moved to the Supplementary.

Page 9, line 14-15: BC is used to date the 90% of the core analyzed, but on base of fig 4, is not the best proxies of seasonality, also as reported by Author pag 7 line 10. At line 26-27 is reported different use of the proxies the Authors contradict themselves

This is a misunderstanding. We always use all available proxies for the dating (see e.g. P9, L25-27), see also our answer to the question reg. P7, L10.

We do not have IC or ICP-MS measurements (of e.g. S, as shown in figure 4) in sufficiently high resolution that these can be used for identifying layers below 40m. Fortunately, in the deeper part of the core, the annual signal in BC is better than for the top part, and, due to its high effective resolution, it maintains a good annual signal with depth.

We have now included a discussion on the annual layer signal in the various chemistry series in the main paper, along with figure S2 (now: figure 7), which shows the evolution in annual signal with depth of the various CFA species. See an updated version of the figure below.

The reason for the misunderstanding may lie in the paragraph on P9, L15-16, where we mention that we use the peak in BC for the annual markers. However, this is simply a matter of where the layer marks are placed, and it does not imply that BC is the only chemistry series used to identify the layers. To avoid misunderstandings, we have removed this sentence from the revised version of the paper.

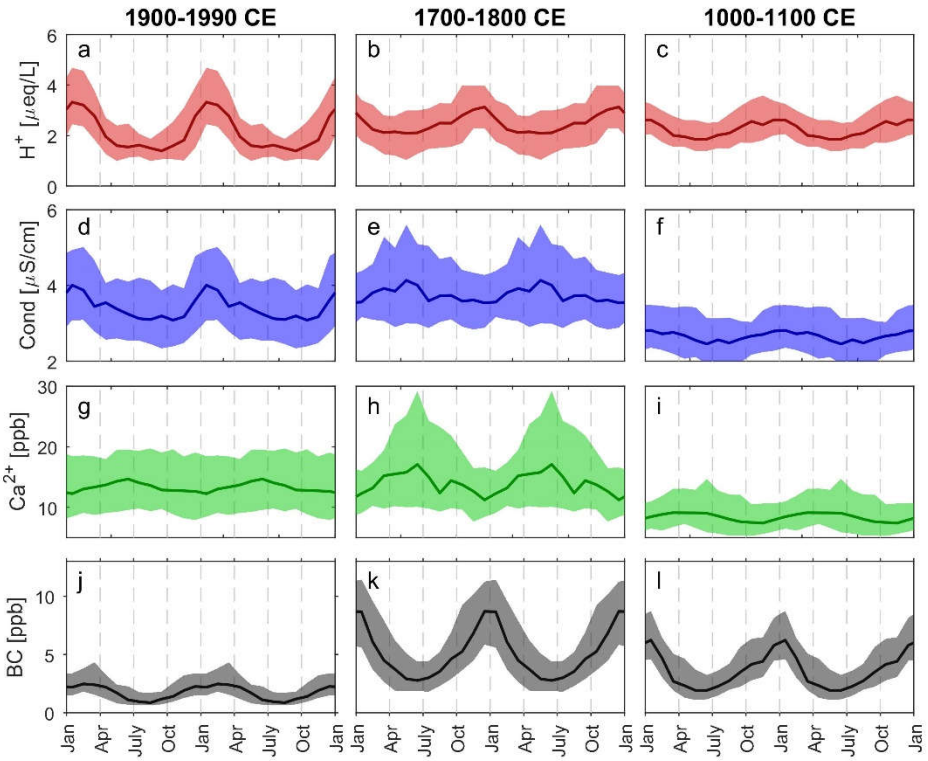

Figure 7: *Average annual signals of 2 successive years in* ***a-c)*** *RICE acidity (H^+),* ***d-f)*** *conductivity (Cond),* ***g-i)*** *calcium (Ca^{2+}), and* ***j-l)*** *black carbon (BC) over three 100-year periods, calculated under the assumption of constant snowfall through the year. The line shows monthly-averaged median value of measured concentrations, and colored area signifies the 50% quantile envelope of the value distribution.*

Page 9, line 39-40: The geochemistry is not show; Pleiades volcano is not West Antarctica, but in Northern Victoria Land; Kurbatov et al, 2015 is not reported in reference, and it is not present in any database as reference for tephra layer reported; the 1252 tephra attributed to The Pleiade was iscovered the first time at Talos Dome and dated at 1254+-2 by Narcisi et al, 2001; on my knowledge the analysis of the tephra at WAIS is still not published

We have changed "West Antarctica" to "Northern Victoria Land".

Kurbatov (2015) has been added as reference, see also previous comments.

We have elected to shorten the discussion involving tephra in the manuscript, as this will be the focus of forthcoming publications. We have further moved the discussion about the Pleiades tephra layer to the Results, as it was primarily used during the matching of RICE to the WAIS Divide ice core. We have revised the text, and added additional references for the geochemistry analyses of the tephra.

Results from geochemical analysis of the Pleiades tephra layers have been made available from the AntT database (http://antt.tephrochronology.org/I.html?id=AntT-15, http://antt.tephrochronology.org/I.html?id=AntT-16), which are now referenced in the text. Geochemistry of the Pleiades tephra horizon in the RICE and WAIS Divide ice cores is reported and discussed in Kalteyer (2015) and Dunbar et al (2010), which have now been included in the references.

We also mention that tephra of similar composition has been found in Talos Dome (Narcisi et al, 2001), and TALDICE (Narcisi et al, 2012).

The section now reads:

A visible tephra layer was found in RICE at 165m depth, with a RICE17 age of 1251.5±13 CE. Geochemistry of the tephra particles is consistent with an eruption from the Pleiades (Kalteyer 2015), a volcanic group located in Northern Victoria Land, Antarctica (Fig. 1). Tephra of similar geochemistry has been found in several other Antarctic cores dated to approximately the same time, including WAIS Divide (1251.6±2 CE; Dunbar et al. 2010) and Talos Dome/TALDICE (1254±2 CE; Narcisi, Proposito, and Frezzotti 2001; Narcisi et al. 2012). The Pleiades tephra horizon allowed a firm volcanic matching of the RICE and WAIS Divide ice cores at this depth (Fig. 8).

Page 10, line 5-18: RICE site is farer than other cores (WAIS-Byrd-Siple Dome and Talos Dome) from "many active volcanoes", it is very difficult to understand why RICE record is able to identify volcanic eruptions those are not identified in the ice cores of the region with much lower ratio in noise/signature due to marine biogenic sulphate emissions

This is a good point. In the previous version of the manuscript, we had included several minor acidity peaks. There is, however, a risk that we had included acidity peaks of non-volcanic origin, e.g. extreme biogenic emission events. In the new version of the manuscript, we only include RICE acidity peaks that could be matched to the WAIS Divide volcanic record.

We note that one reason why we might observe more regional volcanoes in the RICE core is our use of acidity records to identify volcanic eruptions. By using acidity rather than sulfate, we might better observe the signals from regional eruptions, as discussed on P. 11, L1-9. This section has been moved to the discussion.

Page 10, line 19-25: Methane gas synchronization less precise than volcano matching, after 4 line "but methane it is better than volcanic matching", clarify

As described on P10, L5-31, the two methods are complementary: Methane matching is less precise (i.e. relative age differences is much better resolved using volcanic matching), but it provides better absolute age control, since there is less risk of misalignment of the records. The text has been revised to clarify this aspect.

Paragraph 3.3.1.1: The use of acidity and ECM to detect volcanic signal is not a new tools. Hammer have used H+ in 1980 as proxies of volcanic signal

Agreed. However, the volcanic record here is based on direct measurements of H+ in the ice core, whereas H+ used by Hammer (1980) was estimated from the ECM signal. Further, the volcanic proxy developed based on non-sea-salt conductivity is new. We have changed the title of the paragraph to "New and traditional ice-core tracers for volcanic activity" to reflect that it is not new to use ECM to detect volcanic signals.

Page 10, line 43: A resolution of 9.5 cm (about 4 sample per yr) is very low to observe the seasonal variation, but enough to detect the important volcanic signal like Tambora, Kauve etc present a signal for 2-3 yr in Antarctic cores (from 8 to 12 sample)

We agree with the reviewer that with this resolution, we would expect to be able to see some signal in discretely-sampled S record from large bipolar volcanoes that deposit material over several years. However, we observe from the retrieved sulfate records that it is usually very hard to distinguish volcanic eruptions in these. This is likely due to the large inter-annual variability in biogenic sulfate influx, shading the volcanic signatures. The volcanic eruptions are easier to identify from higher-resolution records, such as acidity.

We have added the following to the paper:

Resolution of the discretely-sampled sulfur record was too low (below 67m: 5 cm, i.e. less than 4 samples/year), and even large volcanoes only left a vague imprint in form of slightly increased sulfur levels over a multi-year period (Fig. 8a). Detection of volcanic horizons in the RICE core therefore primarily relied on two new high-resolution tracers for volcanic activity; direct measurements of total acidity and estimated non-sea-salt liquid conductivity.

To illustrate our point, we have added the sulfur records to figure 7 (now: figure 8), see below, so that the reader can verify our statements. We note that exactly this section is actually where the sulfur record displays the most distinct volcanic signal.

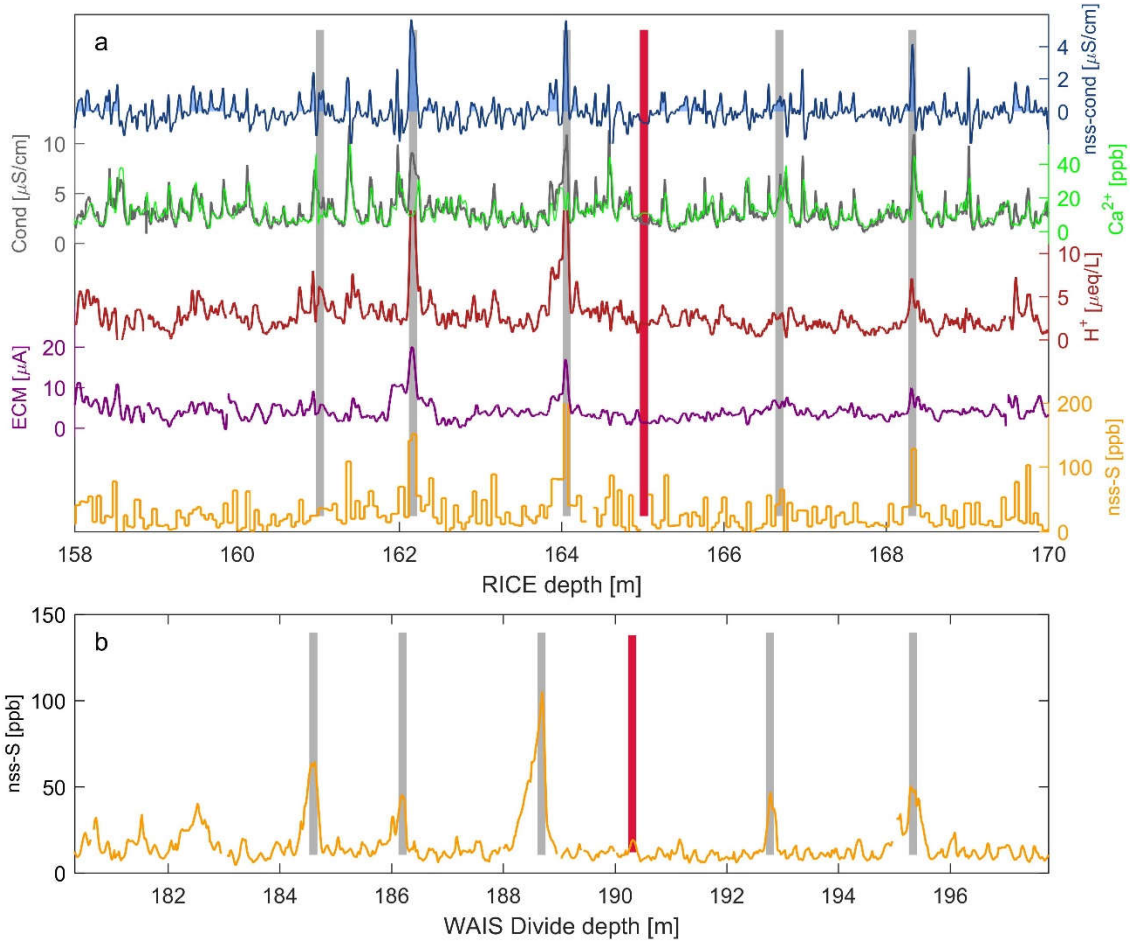

*Figure 8: **a)** The RICE volcanic proxy records: non-sea-salt-sulfur (nss-S; orange), ECM (purple), acidity (H^+; red), and non-sea-salt conductivity (nss-cond; blue) based on the conductivity-to-calcium excess (grey and green). **b)** Matching of the RICE records to the WAIS Divide non-sea-salt sulfur record (Sigl et al. 2015). Vertical bars indicate volcanic match points (Table 2), with the red bar being the Pleiades tephra horizon (1251 CE).*

Page 10, line 25-32: On the base of figure 7a and Table 2 the volcanic events identified in RICE at 158.15m and 160.77m do not present any clear evidence in ECM, H+, due to the high background of ssSO4 at RICE. It is very difficult to understand why a site with this high noise/signal ratio could record local eruption sulphate does not observed at other site core.

We agree that these two volcanic eruptions are hard to identify from the figure. During the process of re-evaluating the volcanic matching between RICE and WAIS Divide, we have removed the volcanic event at 158.15m, which was not matched up to a volcanic horizon in WAIS Divide. In addition, we removed the volcanic event at 159.5m, as we did not consider this horizon to be a sufficiently clear-cut match to WAIS Divide, when considering all available volcanic proxies.

We have added to figure 7 (now: figure 8, see previous comment) the newly developed non-sea-salt conductivity record, which facilitates identification of volcanic eruptions from the difference between the conductivity and calcium records.

At 160.77m, the non-sea-salt conductivity record has predominantly positive values over a significant section, indicative of a volcanic event. This is backed up by significant, albeit small, peaks in the other volcanic proxies. We note that the age differences between this and surrounding volcanic events are identical to those obtained from matching this peak to the significant non-sea-salt sulfur peak in WAIS Divide at 184.5m. We hence consider this peak to be well-qualified as match point between the two cores.

We note that we do not believe that RICE records volcanic sulfate peaks not observed at other sites (such as WAIS Divide). However, by identifying volcanic eruptions based on the acidity rather than sulfate, we may be able to better identify regional eruptions, which also deposit other acids than sulfuric acids.

Paragraph 3.3.1.2 The Pleiades horizon is discussed in several part of the manuscript (parag 3.2.1, 3.2.4, and 3.3.1.2), but without provide any evidence on the base of geochemistry analysis. This tephra layer was reported for the first time in Talos Dome 1996 ice core and dated by Narcisi et al, 2001, at 1254+-2 and attributed as source to Melbourne Volcanic Providence, probably "The Pleiades", located about 250km from Talos Dome. This tephra was than identified in Siple Dome and Taylor Dome by Dunbar et al, 2003. Moreover, Narcisi et al, 2012 pointed out that at TALDICE (a core drilled from 2004 to 2007) is present the tephra of 1254 as TD87a (86.2m depth) close in composition to the previous found in the ice core on 1996. However a subordinate set of glass shards (TD87b) is also trachytic but with a chemical signature inconsistent with The Pleiades products. Mount Berlin could thus be a suitable source of ash (Narcisi et al, 2012). Moreover an other tephra layer TD85 at 84.37m depth younger than 25 yr has been reported by Narcisi et al, 2012 and the suggest source is Mt Melbourne volcanic province. Without any geochemical analysis is impossible attribute unequivocally the tephra found in RICE"

We now discuss the tephra horizon attributed to the Pleiades only in a single paragraph in the manuscript. In this paragraph, we now also mention that it has previously been found in other ice cores in the region, and provide additional references, see our reply to previous comments.

We prefer to not go into the tephra geochemistry in details here, as this will be the topic of forthcoming publications. As previously mentioned, geochemical analysis of this tephra layer is now published in the AntT database.

Page 11, line 41-42: If the tephra layer identified is 1252+-2 yr, why use 1252+-13 for this horizon in RIC17?

RICE17 is an independent timescale, and thus the uncertainty on the age of this tephra horizon reflects the uncertainty in layer counting in the RICE records.

Page 12, line 9-18: See above, more than 170 volcanic event most of them never see in closer core

This number has been reduced, see our previous comments.

Page 12, line 19-42: Volcanic event and Methane records are used for Synchronization or validation?

They are only used for validation, see our previous comments.

Page 13, line 9-10: Which is the gas-age at RICE? And compared to closer site as Siple and WAIS?

For the period discussed in the paper, Δage values for RICE is 145-171 years. This is slightly less than Δage values for the WAIS Divide ice core (174-206 years), and somewhat smaller than those for Siple Dome (233-255 years). TALDICE has significantly larger values of Δage.

Page 13, line 24-29: What is the source of surface temperature of -22oC? Why is used this instead of 27.4oC, this value is also proposed in accompanied paper of Bertler et al, submitted. Why do you use a warmer temperature of 5.4oC? Which implication on density and thinning model using 5.4oC warmer?

We thank the reviewer for pointing out this inconsistency regarding the current surface temperature at RICE. The -27.4^{o}C temperature is derived from ERA-interim data, obtained for a location slightly south of the Roosevelt Island. It seems that there is a large temperature difference between this location and the RICE drill site, with borehole temperatures and AWS data from the RICE site showing an average temperature of -23.5^{o}C. This difference in mean temperature based on the two methods is also discussed in Bertler et al. 2018 (published version). In the new version of the manuscript, we refrain from mentioning the too-cold ERA-interim temperatures.

As the surface temperature of -23.5^{o}C was always used for the density and Δage modelling, these are correctly calculated in the manuscript.

Page 13, line 30-40: Kingslake et al, 2014, instead of Raymond

We have moved the Raymond 1983 reference to immediately after the phrase “Raymond arches”.

Page 13, line 40-41: The recent migration of ice divide, could be attributed to change in snow accumulation variability at ice divide? Due to the snow accumulation variability between the flank of the ice divide, which is the influence have on snow accumulation record and thinning function of RICE core? Kingslake et al., 2014 report that near-surface strain rates are compressive at ice divide than in the flanks 90% higher at RICE. The migration of the ice divide respect to Raymond Bump position indicate a role of temporally changing in spatial snow accumulation distribution, as well as the role of along-ridge flow is un-clear and hampers a solid interpretation about thinning function and snow accumulation records

Neither the high frequency (shallow, <100m) or low frequency (deep, >50m) profiles suggest a significant change in accumulation pattern over time that could have driven the divide migration. Therefore, we believe the divide migration is likely caused by ice dynamics, potentially caused by changes in buttressing by the surrounding Ross Ice Shelf. The relatively small changes in divide position over time, however, suggest that neither has changed significantly over the past 2700 years. Since the reviewer has recommended a significant shortening of the manuscript, we have elected not to expand the discussion of the thinning function.

The applied thinning function takes account for the divide migration (see previous comments).

It is correct that the large gradient in accumulation rates across the ice divide could influence the obtained accumulation record from the ice core, and as previously mentioned, we now estimate this in the paper. Since the divide has only migrated a short distance, this does not significantly impact the derived trends in the accumulation rates.

Fig 8: The pRES measurement (Kingslake et al., 2014) was at ice divide and does not follow the Raymond bump features as reported in figure 8b

Correct. That is why we vary the vertical velocity profile through time (P14, L11-20).

Page 14, line 11-20: On the base of which data the Authors construct a vertical velocity profile along the Raymond Bump?

As stated, we are assuming that the ice in the core was not directly beneath the divide from 700BCE to 1450CE. The vertical velocity profile is allowed to change over time, based on a linear combination of the measured vertical velocity profiles from the flank and the topographic divide.

In the revised paper, this section has been clarified.

Page 15, line 14: "Control point… of atmospheric oxygen isotope" at page 12 "Given the stability of the d18Oatm record over the last millennia, the synchronization was solely constrained by the observed variability in the methane records" as in several other part of the text none coherence exist between the paragraphs and some times also in the same paragraph"

We used both $\delta^{18}O_{atm}$ and CH_4 for matching the two cores. However, given that the levels of $\delta^{18}O_{atm}$ were very stable over the last 3000 years, using this record did not provide many constraints to the synchronization. Essentially, therefore, the matching was based on the methane records. We have added the following to the text to make this clearer:

The feature matching routine employed discretely-measured records of methane as well as isotopic composition of molecular oxygen ($\delta^{18}O_{atm}$). Over recent millennia, however, the $\delta^{18}O_{atm}$ concentrations are stable, and hence provided minimal matching constraints.

Page 15: Along all the paragraph it is not clear the process of adjustments of the counting layer respect to matching between RICE and WAIS

RICE17 is an independent timescale, and hence we do not adjust the number of counted layers between match-points to fit the WD2014 timescale.

Page 16, line 13-16: High internal-annual variability in snow accumulation is normal issue (see eg Eisen et al, 2008 and reference within), 1.3% is very low value

We have removed this section from the manuscript.

Page 16, line 40-45: The three accumulation record of snow accumulation must be shown in the overlap time, the correlation coefficient of 0.85 and 0.87 indicate that the RICE annual are representative, but at pluriannual scale (see Eisen et al., 2008; Frezzotti et al., 2007). The comparison of the three cores can confirm only the stability of snow in the overlap time, not at secular or millennium scale

Agreed. However, while we can only say for certain that the accumulation is spatially consistent within the time period covered by these three cores, we still believe that the consistency between these records in the overlap period provides a basis for our general statement that the strong correlation between these indicates spatial consistency in accumulation rates.

We have added to the paper a figure comparing the accumulation records obtained from the three cores during their overlap period, see below. The three records show very similar inter-annual variability.

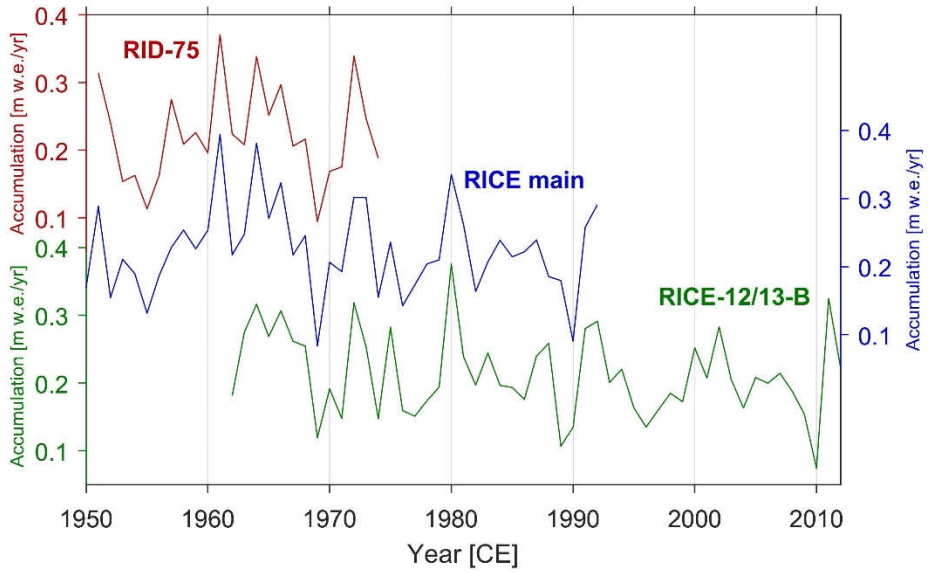

Figure 12: *Accumulation reconstructions for the three Roosevelt Island ice cores.*

Paragraph 4.3.2: "The inflection point in accumulation of fig 9 with a trend in decrease is closer to age of the hypothesis of the stabilization of the ice divide at present position 1450 EC (Pag 14). The uncertainty of change in accumulation must be taking in account also the spatial variability at ice divide. The topography position of ice divide is probably linked also to spatial variability of snow accumulation in a feedback mechanism (see Drews et al., 2013; King et al., 2004; Matsuoka et al., 2015; Lenaerts et al., 2014).

Firstly, we note that there was a small error in the previous version of the draft regarding our inferred timing of stabilization of the ice divide at its present location – we expect the migration to start 500 years ago, i.e. in 1512CE, not in 1450CE, and arrive to its present location 250 years ago (1762CE).

With these new ages, there is an even more significant difference in timing between the onset of a negative trend in the accumulation rates (1250CE) and the onset of divide migration (1512CE). As previously mentioned, the migration of the ice divide would give rise to a small negative bias in derived accumulation rates for the first part of the period. However, it does not significant impact the derived trends in the accumulation history.

Given the different timing as well as the small effect on the accumulation rates, we do not believe that migration of the ice divide has been the main cause behind the observed changes in accumulation rate over time.

The uncertainty due to age scale and thinning function and ice divide migration must be tacking in account when is analysed the trend, uncertainties is not small amounts

We note that the uncertainty associated with the change in ice divide migration (~0.25cm/yr) is small compared to the uncertainty in thinning function (~2 cm). Similarly, the small (correlated) uncertainties in the age scale do not significantly impact trends in the derived accumulation rates (P. 17, L10-15).

We have taken the approach to estimate uncertainty on the trend estimates based on a linear regression to the most likely accumulation rate history. We note that this is much more reasonable now that the uncertainties on the thinning function have been significantly reduced. Due to the high variability of the accumulation rate over time, we believe that this approach provides reasonable estimates for the uncertainty in observed trends.

Page 17, line 36-46: The interpretation of the reason of trend in accumulation differ from that hypothesis reported by Bertler et al., submitted paper

We now mention that the recent decline in accumulation at Roosevelt Island may be due to increased sea ice extent in the Eastern Ross Sea, as put forward by Bertler et al (2018).

Page 18, line 1-4: The decrease of 6.6 cm/yr per century is not agree since 1950 with the paragraph 5.3 "Clausen et al. (1979) estimated the current (1954-1975) accumulation rate at the summit of Roosevelt Island to be 0.20 m w.e yr-1, whereas we here find the current accumulation rate (average of the last 50 years) to be 0.22±0.06 m w.e yr-

The value of 6.6cm/century is derived from the RICE accumulation rate history, which shows a distinct decrease in recent accumulation rates. We agree that this may appear contradictory to the old cores finding slightly smaller accumulation rates than the present value obtained from RICE. The difference between accumulation rates in the two cores, however, is caused by the spatial variability in accumulation rates, with the RID75 core being drilled at a location with slightly lower accumulation rates. The two statements are therefore not contradictory.

Paragraph 5.1: Most of points reported are repetitions already pointed out in Methods and Result, see above for the comment, in particular for "we noted several strong volcanic imprints that seemingly have no counterpart in the WAIS Divide ice core data, and thus most likely originate from local West Antarctic volcanoes.

We have significantly reorganized the paper, so that we now in Discussion discuss the implications of using total acidity instead of sulfate, and how it impacts the volcanic record from RICE.

Page 18, Line 31-44: The dipole effect change during the time, see Bertler paper, are this occurs in correspondence with presence or absence of RICE-WAIS volcanic event synchronization?

It would be interesting to investigate the effect directly from a comparison of the two volcanic records, but it not possible to say from our matching between the two ice cores. Given the general challenge of establishing volcanic march-points in the cores, the identification of these partly depended on the density of reliable matches in the surrounding core sections. In other words, with a higher density of reliable match points, the more additional acidity peaks were sufficiently convincing to be annotated as a match-point. This positive feedback loop significantly influenced the frequency of identified match-points, overwhelming any effect caused by the dipole strength.

Page 18, line 38: "Absence of sulfate in RICE" with a higher background of 200 ng/g, exactly the opposite

We have changed this to:

Absence of volcanic signal in the RICE core

Page 19, line 1-7: The tephra number of RICE is not unusual as presence compared to TALDICE or west Antarctic core, as the Authors have written few line after. Moreover, RICE present "several strong volcanic imprints that seemingly have no counterpart in the WAIS Divide ice core data, and thus most likely originate from local West Antarctic volcanoes.", but not tephra, this is very unusual if the volcanic event reported in Table 2 are true

We have removed the sentence about the number of visible tephra layers in RICE.

Page 19, line 3: "Only one exists within the last 2700 yr", but on the base of manuscript the tephra are two: Raoul 1964 and Pleiade 1252

Correct. This paragraph has been removed.

Page 19, line 22: "longer-term trends are significantly different between the two locations" the text after describe similar trend with higher accumulation in the past respect to the present and change trend close at secular scale

We agree that this is not formulated very clearly. The text has been rewritten to clarify that while part of the long-term trends differ at the two locations (increasing at RICE until 1250CE, decreasing at WAIS Divide), the two records also show some similarities. For instance, the decline in WAIS accelerates around the same time that RICE accumulation rates starts to decline.

Paragraph 5.3: The result of RICE does not provide new information for the mass balance of RIS, taking in account the previous cores with similar SMB value and the high spatial variability of the rise and RIS

We have deleted this paragraph from the paper.

Answers to reviewer 2

We thank the reviewer for the comments and suggestions to the manuscript. Based on the reviewer comments, we have significantly restructured and revised the paper. We will not provide a detailed summary of these structural revisions below, but hope to be allowed to submit a revised version of the paper.

In the revised version of the manuscript, we have moved the section on timescale validation by comparison to WAIS Divide to "Results". We believe that with this structural change, it should become clearer that the RICE17 timescale is NOT synchronized to WAIS Divide, and that our matching of the two cores only forms basis for a comparison between the two timescales.

A point-to-point reply to the reviewer's comments are provided below (in blue), along with a short description of the adjustments to the paper relating to these comments.

The timescale is extensively compared to the WD2014 timescale which is one aspect not so clear from this manuscript: is this timescale tuned or not to WD2014?

The timescale is not tuned to WD2014. This has been clarified in the current version of the manuscript.

Finally, there is a discussion on the accumulation rate reconstruction and its evolution over the last 2700 years. Because of the strong uncertainties associated with the reconstruction, only the recent decrease can faithfully be discussed.

We found an error in the calculation of uncertainty on accumulation rates in the previous version of the manuscript, which has now been corrected. With this correction the uncertainties have been significantly reduced, allowing us to discuss the observed changes in accumulation over time with much more confidence.

The dating strategy is not clear. There is a mixing of layer counting constraints as well as use of volcanic peaks (+ nuclear bomb tests) but the uncertainty is only defined from layer counting at least on the upper part. It thus seems that the uncertainty is a bit overestimated?

The top part of the RICE17 timescale is manually counted while using constraints from historical events (incl. volcanic peaks) observable in the RICE ice core records. These constraints reduce the uncertainty of the most recent part of the timescale (corresponding to the upper 42.5m of the core). As we account for age constraints when developing the uncertainty of the age scale, we do not consider the uncertainty in the top part to be overestimated. We have revised the text to clarify this point, and now write:

A confidence interval was assigned to the timescale by classifying layers as certain or uncertain (Fig. 4), while accounting for age constraints from marker horizons.

In the deeper part, for which the timescale has not been constrained, we use the statistically-produced StratiCounter results for the age uncertainty.

Below 42.5 m, WD2014 seems to be taken as reference for the dating of the volcanic peaks as well as for adjusting the StratiCounter algorithm. Then WD2014 is used for "validation" of the timescale. By reading the methodology, it thus seems that there is something circular in the approach if WD2014 is used both for construction and validation of the timescale – could you please explain this better?

We hope that our approach is better explained in the revised version of the manuscript.

First of all; RICE17 and WD2014 are independent timescales.

In the top part, we used historical events to constrain the RICE timescale. Below 42.5m, the timescale has not been constrained.

The only "circularity" in our approach is that we used the Pleiades tephra horizon in the RICE core to select the optimal settings for StratiCounter. This tephra horizon has previously been dated to 1251+-2 years according to WD2014, but is also found in other ice cores with similar age. It happened to be that one version of the StratiCounter output produced exactly the same age of the Pleiades tephra horizon as found in WD2014, and we decided to select those settings for the algorithm.

However, we note that our adjustments to the StratiCounter settings gave rise to very small age differences (<10 years) at the depth of this tephra layer, and that all the StratiCounter-derived timescales were in very good agreement with each other. Hence, for all practical purposes, the RICE17 and WD2014 timescales are independent of each other.

We recognize that this essential aspect was not sufficiently clear from the previous version of the manuscript, and we have made several revisions and structural changes to the text for clarification.

The methane constraint for the RICE timescale is not clear. First, it refers heavily to a paper that is in preparation (Lee et al., 2017).

The details of the approach used for matching the RICE and WAIS Divide ice cores using their respective high-resolution methane records will be described in the Lee et al paper, which is ready to be submitted any day now, and will soon be accessible as discussion paper in Climate of the Past Discussions. In the present manuscript, we have revised the wording of the section to improve its readability on its own.

Second, the uncertainties associated with such tie-points are large and it is thus complicated to use them faithfully for timescale validation.

It is true that the uncertainties associated with the individual methane match-points are relatively large. It should be noted, however, that for the RICE and WAIS Divide ice cores, these uncertainties are much smaller than for most other Antarctic ice cores (P13, L9-14).

Despite of the uncertainty on the individual match points, it is worthwhile to validate the RICE17 timescale to WD2014 based on the methane synchronization of the two cores. For instance, in Figure 6 (now: Figure 9) we observe that all methane match points below 280m are associated with older ages in WD2014 than in RICE, which corroborates the volcanic synchronization between the two ice cores.

Due to the associated uncertainties, we only use the methane match points for validation of the absolute ages of the RICE17 timescale.

Finally, the procedure mixing Monte-Carlo technique and manual adjustment is rather unclear. I imagine that everything will be in the Lee paper but details are missing to really make use of this part which is not very robust as written here.

After matching the two methane records using a Monte Carlo approach, we observed that the two records in this top part would fit slightly better if the match-points were slightly adjusted. These adjustments fall

within the uncertainty of the gas-derived age control points. We report comparisons of the age-scale relative to the automated as well as the manually-adjusted methane match-points.

The new version reads:

Ice cores can be stratigraphically matched using records of trapped gasses, which reflect global changes in atmospheric composition. Centennial-scale variations in methane concentrations observed in the RICE gas records are also found in similar records from WAIS Divide (WAIS Divide Project Members 2015; Mitchell et al. 2011). Matching up these records allows a comparison of the two ice-core timescales.

The gas records from RICE and WAIS Divide were matched using a Monte Carlo technique reported in Lee et al. (2018). The feature matching routine employed discretely-measured records of methane as well as isotopic composition of molecular oxygen ($\delta^{18}O_{atm}$). Over recent millennia, however, the $\delta^{18}O_{atm}$ concentrations are stable, and hence provided minimal matching constraints. An average spacing of 26 years between successive RICE methane samples contributes to the matching uncertainty. The matching routine identified 18 match-points over the past 2700 years, i.e. an average spacing of 150 years. Subsequent visual comparison of the methane profiles suggested minor manual refinements of the match-points (8 years on average, maximum 23 years; all within the uncertainty of the automated matching). These adjustments resulted in a slightly improved fit.

Some parts are very long and not useful (most of section 3.2.3.2, part of section 3.3 on l. 10 or p. 15) – I suggest to reduce these sections and better concentrates on the method and associated uncertainties.

As suggested by the reviewer, we have significantly shortened these sections.

Accumulation rate is certainty an input of the firn model described in p. 13 while only forcing using a site temperature history is mentioned. It is very surprising that accumulation forcing is not mentioned here since one of the aim of this paper is to provide an accumulation scenario. We are thus expecting the use (or at least validation that everything is coherent with Dage or d15N measurements) of the accumulation rate scenario in the firn model.

It is correct that the usual form of the Herron-Langway firn densification model takes both temperature and accumulation history as an input, thereby providing lock-in-depth and delta-age as output. However, in our dynamic H-L firn model, the equations have been re-organized to account for the knowledge on past lock-in depth based on measurements of d15N-N2, after correction for the existence of a convective surface zone. Consequently, the H-L model used here is forced by the temperature history (based on water isotopes) and past firn column thickness based on measurements of d15N-N2 (P13, L2-5). Additional parameters include the surface density (fitted to the modern density profile) and density at the lock-in-depth (here estimated from the temperature). With this formulation of the H-L model, we obtain as output: 1) the age at the lock-in depth (Δage), and 2) a low-frequency accumulation history.

The section has been revised as follows:

Methane feature matching allows a transfer of WAIS Divide ages to the RICE gas records, i.e. the RICE gas ages. To obtain the corresponding ice-core ice ages relevant for this study, Δage was calculated using a dynamic Herron-Langway firn densification model (Herron & Langway 1980) following Buizert et al. (2015), as described in detail in Lee et al. (2018). The model is forced using a site temperature history derived from the RICE stable water isotopes, and the firn column thickness is constrained by the isotopic

composition of molecular nitrogen ($\delta^{15}N$ of N_2). In addition to Δage, this formulation of the Herron-Langway densification model produces as output a low-resolution accumulation rate history.

In the new version of the manuscript, we have included the firn-model based accumulation history as well as the measured d15N-N2 values in figure 9c (now: figure 10e, dashed line and black dots):

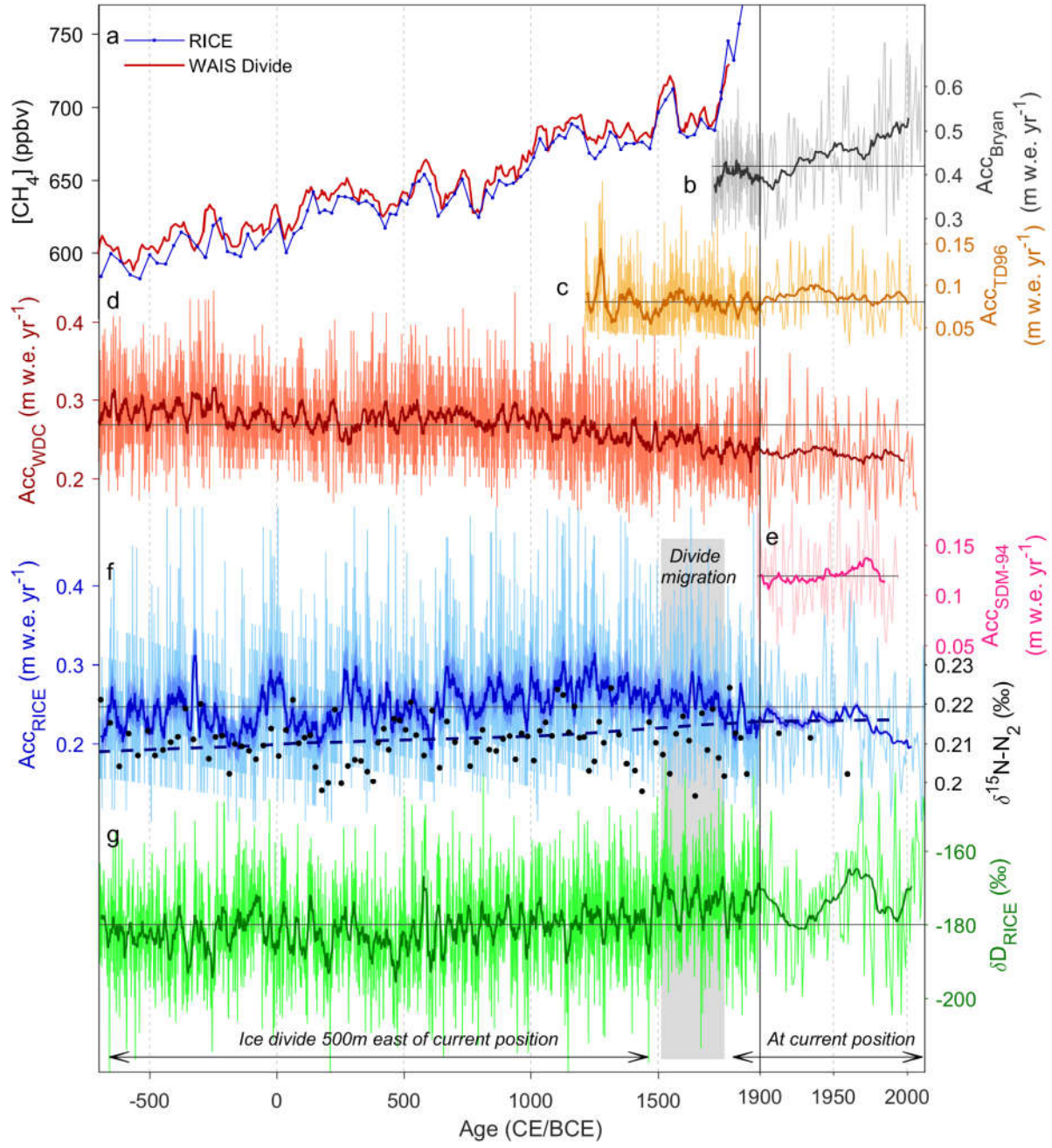

Figure 10: a) *Measured methane concentrations from RICE (blue, on the RICE17 timescale) and from WAIS Divide (red, on the WD2014 timescale).* ***b)*** *Bryan, Antarctic Peninsula (grey) (Thomas et al. 2015),* ***c)*** *Talos Dome (TD96, orange) (Stenni et al. 2002),* ***d)*** *WAIS Divide (WDC, red) (Fudge et al. 2016),* ***e)*** *Siple Dome (SDM-94, pink) (Kaspari et al. 2004), and* ***f)*** *RICE (blue) accumulation histories over the past 2700 years, in annual resolution and 20-year smoothed versions (thick lines). WAIS Divide accumulation rates have been corrected for ice advection. The shaded blue area indicates the 95% confidence interval of the RICE accumulation rates.* The short-lived peak in accumulation rates around 320 BCE is likely to partly be an artefact caused by timescale inaccuracies in this period, during which RICE17 diverges from WD2014 (Fig. 9b). *Also shown are the gas-derived accumulation rates for this time interval (f, blue dashed line), and measurements of $\delta^{15}N$ of N_2 informing on past firn column thickness (f, black dots; on the RICE gas timescale).* ***g)*** *RICE stable water isotope record (δD). Thick green line is a 20-year smoothed version of the isotope profile. Thin grey horizontal lines denote mean values of accumulation rates and δD over the displayed period. The migration period of the Roosevelt Island ice divide is marked with a grey box.*

We note some discrepancy between this accumulation history and the one derived from the RICE17 layer counts and thinning function, and we discuss these differences in the manuscript:

The RICE17 accumulation history shows reasonable agreement with low-resolution accumulation rate output from the dynamic Herron-Langway firn densification model (Fig. 10f, dashed line). The gas-based accumulation rate history does not resolve high-frequency variations, but shows a slow increase in accumulation rates of 0.16cm/century, similar to that obtained from the ice core chronology prior to 1250 CE. In contrast to the accumulation rate history derived based on the layer thicknesses and thinning function, however, the firn-based accumulation rates continue to increase until present-day. Further, the absolute value of the inferred gas-based accumulation rates tend to generally underestimate the accumulation rates by ~4cm (16%).

We speculate that these discrepancies may have to do with the shift in RICE water isotope levels occurring around 1500 CE (Fig. 10g), which in the firn model is used to represent temperature change. It has been suggested that this shift is due to other factors than temperature (Bertler et al. 2018). Assuming that the model is based on a slightly too-cold temperature input prior to 1500 CE, the model would compensate by decreasing the accumulation rates during this time, in order to preserve a constant thickness of the firn column, as indicated by steady values of $\delta^{15}N$-N_2 (Fig. 10f, black dots).

What is the "model" mentioned in l. 45, p. 13?

The "model" referred to here is a Lliboutry vertical ice-flow velocity profile fitted to observed vertical velocities. In the new version, this sentence has been rewritten as follows:

We produce a thinning function appropriate for RICE using vertical velocity profiles obtained by fitting a simple ice-flow model (Lliboutry 1979) to englacial velocities deduced from radar measurements (Kingslake et al. 2014).

The discussion on the ASL influence on the accumulation rate in the region is both in the "Results" section and in the "Discussion". This is also the case for other ideas that are repeated several times and a reorganization and simplification of the manuscript is needed.

We have carefully gone through the manuscript and reorganized, simplified and shortened the text. All text about the influence of ASL on RICE accumulation rates has been moved to the discussion section.

The accumulation reconstruction should ideally have been compared to accumulation rate scenario used for the firn model as well as with water isotope profiles. It could strengthen the discussion and conclusion parts on the accumulation aspect that are rather short.

In the new version of the manuscript, we compare the accumulation reconstruction from the firn modelling to the accumulation history from the RICE17 timescale, see comment above.

We have further expanded the discussion regarding the accumulation rate history, which is now evaluated in context of regional climate drivers, including regional sea ice extent.

A 2700-year annual timescale and accumulation history for an ice core from Roosevelt Island, West Antarctica

Mai Winstrup[1,*], Paul Vallelonga[1], Helle A. Kjær[1], Tyler J. Fudge[2], James E. Lee[3], Marie H. Riis[1], Ross Edwards[4,5], Nancy A.N. Bertler[6,7], Thomas Blunier[1], Ed J. Brook[3], Christo Buizert[3], Gabriela Ciobanu[1], Howard Conway[2], Dorthe Dahl-Jensen[1], Aja Ellis[4], B. Daniel Emanuelsson[6,7], Richard C.A. Hindmarsh[8], Elizabeth D. Keller[7], Andrei V. Kurbatov[9], Paul A. Mayewski[9], Peter D. Neff[10], Rebecca L. Pyne[7], Marius F. Simonsen[1], Anders Svensson[1], Andrea Tuohy[6,7], Edwin D. Waddington[2], Sarah Wheatley[9]

1: Centre for Ice and Climate, Niels Bohr Institute, University of Copenhagen, Copenhagen, Denmark

2: Earth and Space Sciences, University of Washington, Seattle, WA, USA

3: College of Earth, Ocean, and Atmospheric Sciences, Oregon State University, Corvallis, OR, USA

4: Physics and Astronomy, Curtin University, Perth, Western Australia, Australia

5: Department of Civil and Environmental Engineering, University of Wisconsin-Madison, Madison, USA

6: Antarctic Research Centre, Victoria University of Wellington, Wellington, New Zealand

7: GNS Science, Lower Hutt, New Zealand

8: British Antarctic Survey, Cambridge, UK

9: Climate Change Institute, University of Maine, Orono, Maine, USA

10: Earth and Environmental Sciences, University of Rochester, Rochester, NY, USA

*: Now at: Danish Meteorological Institute, Copenhagen, Denmark

Correspondance to: Mai Winstrup (mai@nbi.ku.dk)

Abstract

We present a 2700-year annually-resolved chronology and snow accumulation history for the Roosevelt Island Climate Evolution (RICE) ice core, Ross Ice Shelf, West Antarctica.

The timescale was constructed by identifying annual cycles in high-resolution impurity records, and it constitutes the top part of the Roosevelt Island Ice Core Chronology 2017 (RICE17). The timescale was validated by volcanic and methane matching to the WD2014 chronology from the WAIS Divide ice core, and the two timescales are in excellent agreement.

The RICE snow accumulation history shows that Roosevelt Island experienced slightly increasing accumulation rates between 700 BCE and 1300 CE, with an average accumulation of 0.25±0.02 m water equivalent (w.e.) per year. Since 1300 CE, trends in the accumulation rate have been consistently negative, with an acceleration in the rate of decline after the mid-17th century. The current accumulation rate at Roosevelt Island is 0.211±0.002 m w.e. y^{-1} (average since 1965 CE, ±2σ), and rapidly declining with a trend corresponding to 0.8 mm yr^{-2}. The decline observed since the mid-1960s is 8 times faster than the long-term decreasing trend taking place over the previous centuries, with decadal mean accumulation rates consistently being below average.

Previous research has shown a strong link between Roosevelt Island accumulation rates and the location and intensity of the Amundsen Sea Low (ASL), with significant impact on regional

sea ice extent. The decrease in accumulation rates at Roosevelt Island may therefore be explained in terms of a recent strengthening of the ASL and expansion of sea ice in the Eastern Ross Sea. The start of the rapid decrease in RICE accumulation rates observed in 1965 CE may thus mark the onset of significant increases in regional sea ice extent.

1. Introduction

Accurate timescales are fundamental for reliable interpretation of paleoclimate archives, including ice cores. Ice-core chronologies can be produced in a variety of ways. Where annual snow deposition is sufficiently high and reasonably regular throughout the year, seasonal variations in site temperature and atmospheric impurity deposition lead to annual cycles in the ice-core water isotope and impurity records (Dansgaard, 1964; Hammer et al., 1978). By identifying and counting the annual cycles, an annual-layer-counted ice-core timescale can be produced (Sigl et al., 2016; Steig et al., 2005; Svensson et al., 2008). This technique is commonly employed for producing ice-core timescales at sites with moderate to high snow accumulation, including coastal Antarctica. Annual-layer-counted ice-core timescales have traditionally been obtained by manual counting, but this task can now be performed using machine-learning algorithms for pattern recognition (Winstrup et al., 2012).

Where possible, identification of annual layers allows the development of a high-resolution ice-core chronology, but unless constrained by other data, the uncertainty of such a timescale will increase with depth, as the number of uncertain layers accumulate to produce some age uncertainty (Andersen et al., 2006; Rasmussen et al., 2006). Marker horizons found in the ice-core records can be used to evaluate the accuracy of a layer-counted timescale, or, alternatively, to constrain the timescale. Such marker horizons carry evidence of events of global or regional nature, and may be; (a) layers of enhanced radioactivity resulting from nuclear bomb tests (Arienzo et al., 2016); (b) sulfuric acids (Hammer, 1980) and/or tephra (Abbott et al., 2012) from volcanic eruptions; or (c) enhanced flux of cosmogenic radionuclides caused by changes in solar activity, reduction of the Earth's magnetic field, or cosmic events (Muscheler et al., 2014; Raisbeck et al., 2017; Sigl et al., 2015).

Ice cores can also be stratigraphically matched using records of past atmospheric composition from trapped air in the ice (Blunier, 2001; Blunier et al., 1998; EPICA Community Members, 2006). Variations in atmospheric composition are globally synchronous. Accounting for the time required to sequester the air into the ice, the ice-core gas records can be used also for stratigraphic matching of records measured on the ice matrix. Even during periods of stable climate, the atmospheric composition displays multi-decadal fluctuations (Bender et al., 1994; Mitchell et al., 2011, 2013) allowing synchronization on sub-centennial timescales.

Annually-resolved ice-core chronologies provide long-term reconstructions of annual snow accumulation (Alley et al., 1993; Dahl-Jensen et al., 1993): Annual layer thicknesses can be converted to past accumulation rates by applying corrections due to density changes during the transformation from snow to ice (Herron and Langway, 1980), and thinning of annual layers caused by ice flow (Nye, 1963). Reconstructions of past accumulation rates are important for improving our understanding of the natural fluctuations in snow accumulation and their climate drivers. Such knowledge is essential to accurately evaluate the current and future surface mass balance of glaciers and ice sheets, a critical and currently under-constrained factor in sea level assessments (Shepherd et al., 2012).

Here we present an ice-core chronology and accumulation history for the last 2,700 years from Roosevelt Island, an ice rise located in the Eastern Ross Embayment, Antarctica (Fig. 1). The ice core was extracted as part of the Roosevelt Island Climate Evolution (RICE) project (2010-

2014) (Bertler et al., 2018). RICE forms a contribution to the Antarctica2k network (Stenni et al., 2017; Thomas et al., 2017), which seeks to produce Antarctica-wide ice-core reconstructions of temperature and snow accumulation for the past 2000 years.

ECMWF ERA-Interim (ERAi) reanalysis fields (Dee et al., 2011) indicate that precipitation at Roosevelt Island is strongly influenced by the Amundsen Sea Low (ASL) and associated ridging (Raphael et al., 2016), and anti-correlated with precipitation in Ellsworth Land and the Antarctic Peninsula (Bertler et al., 2018; Emanuelsson et al., 2018; Hosking et al., 2013). These differences emphasize the need for high spatial and temporal coverage when reconstructing regional mass balance patterns. With few other ice cores from the Ross Sea region, the RICE accumulation history adds information on past changes in mass balance from an otherwise poorly-constrained sector of the Antarctic continent.

2. Site characteristics

Roosevelt Island is located within the eastern part of the Ross Ice Shelf (Fig. 1), from which it protrudes as an independent ice dome that is grounded 214 meters below sea level. Snow accumulates locally on the ice dome, with ice originating from the Siple Coast ice streams flowing around the island in the Ross Ice Shelf. Geophysical and glaciological surveys across Roosevelt Island in the 1960s established ice thickness, surface topography, surface velocity and accumulation rate (Bentley and Giovinetto, 1962; Clapp, 1965; Jiracek, 1967). The island was revisited during 1974-75 as part of the Ross Ice Shelf Project. During this project, shallow cores (up to 70m) were collected across the ice shelf, including two firn cores from Roosevelt Island summit (Clausen et al., 1979). The shortest (11 m) firn core from near the summit was measured for water isotopes and total β-activity in high resolution; we here refer to it as RID-75 (Table 1). Results from the shallow cores show that seasonal signals of stable isotopes and ionic chemistry are well preserved in the ice (Clausen et al., 1979; Herron and Langway, 1979; Langway et al., 1974).

Ice-penetrating radar surveys of Roosevelt Island that took place in 1997 revealed a smoothly varying internal stratigraphy of isochronal reflectors (Conway et al., 1999). There was no evidence of disturbed internal layering that would indicate high strain rates or buried crevasses, suggesting the summit of the island to be a good place for an ice core. Of special interest was a distinctive arching pattern of the internal layers beneath the divide. This pattern has implications for the ice history, since isochronal layers arch upward beneath divides that are stable and frozen at the bed (Raymond, 1983). Analyses of the geometry of this so-called Raymond stack indicate that the current divide-type ice-flow regime started about 3000 years ago (Conway et al., 1999; Martín et al., 2006), and thus has been in existence throughout the time period investigated in this paper. At mid-depths, the Raymond arches are offset from the current topographic summit by ~500m towards north east, indicating a slight migration of the ice divide in past centuries. Combined with a recently-measured vertical ice velocity profile at the ice divide (Kingslake et al., 2014), the stability of the ice flow regime at Roosevelt Island facilitates interpretation of past accumulation rates from annual layers in the RICE ice core.

The RICE deep ice core was drilled at the summit of Roosevelt Island (79.364S, 161.706W, 550 m above sea level (Bertler et al., 2018)), and less than 1 km from the old RID-75 shallow core. It was drilled in austral summers of 2011/12 and 2012/13. During the first season, the core was dry-drilled down to 130 m, and then the borehole was cased. An Estisol-240/Coasol drilling fluid mixture was used to maintain core quality during the second drilling season. The ice thickness is 764.6 m. The upper 344 m of the core spans the past 2700 years; the period for which an annual-layer-counted timescale can be constructed. In addition to the deep core, several shallow cores were drilled in the vicinity. During the 2012/13 field season, a 20 m firn

core (RICE-12/13-B) was drilled near the main core, and it was used to extend the records up to the 2012/13 snow surface. Table 1 provides an overview of the relevant firn and ice cores collected at Roosevelt Island. An automated weather station near the RICE drill site recorded mean annual temperatures of -23.5°C over the duration of the RICE project (2010-2014), and an average snow accumulation of approximately 0.20 m w.e. yr^{-1} (Bertler et al., 2018).

Methods

3. Ice core processing and impurity analysis

The RICE ice cores were processed and analyzed at the GNS Science National Ice Core Facility in Lower Hutt, New Zealand. The cores were cut longitudinally to produce a 15x35 mm triangular piece for water isotope analysis and two 35x35 mm square sticks for continuous flow analysis (CFA) (Fig. 2). The second CFA piece was for use in case the core quality of the primary piece was compromised, or for repeat measurements to test measurement accuracy and system stability.

In parallel with ice core cutting and processing, CFA and electrical conductivity measurements (ECM) were carried out. ECM (Hammer, 1980) was measured using a low-power hand-held instrument from Icefield Instruments Inc. directly on the ice-core surfaces after the initial cutting of the core. In 2012, the uppermost section (8.57-40 m) of the RICE main core was processed and analyzed using the GNS Science melter system, with continuous measurements of stable water isotopes (δD, $\delta^{18}O$) and black carbon, and discrete sampling of major ion and trace element concentrations. The following year, this set-up was replaced by an expanded version of the Copenhagen CFA system (Bigler et al., 2011), providing high-resolution continuous measurements of liquid conductivity, calcium (Ca^{2+}), insoluble dust particles, acidity (H^+), and black carbon (BC), as well as stable water isotopes (δD, $\delta^{18}O$) and methane gas concentrations (Table 1). The RICE-12/13-B firn core was analyzed using this system. Next, the RICE main core was melted and analyzed from 40 m to 475 m, at which depth the ice brittle zone was reached. Subsequent repeat measurements of the top section (8.57-40 m) of the main core were made using the second, parallel CFA stick.

Primary adaptations to the Copenhagen CFA system involved: 1) Depth assignment via a digital encoder using a 1-second sampling rate (Keller et al., 2018); 2) Continuous analysis of stable water isotopes ($\delta^{18}O$, δD) using a Los Gatos Research (LGR) analyzer (Emanuelsson et al., 2015); 3) Black carbon analysis by a Single Particle Soot Photometer (Droplet Measurement Technologies, Boulder, CO; DMT SP2) following the method reported by McConnell et al. (2007); 4) Acidity measurements based on direct registration of H^+ concentrations using an optical dye method (Kjær et al., 2016); 5) Continuous methane concentration analysis using a Picarro Cavity Ring-Down Spectroscopy (CRDS) instrument (Stowasser et al., 2012); and 6) Inclusion of three fraction collectors for discrete sample analyses by, respectively, ion chromatography (IC), Inductively-Coupled Plasma Mass Spectrometry (ICP-MS), including measurements of ^{239}Pu using an ICP-SFMS technique (Gabrieli et al., 2011), and measurements of stable water isotopes on the LGR. Figure 3 shows a diagram of the CFA system set-up.

The ice was melted at a rate of 3 cm min^{-1}, producing approximately 16.8 mL contamination-free water and gas mixture per minute of melting. Air bubbles were separated in a debubbler, dried, and sent to the Picarro CRDS instrument for methane analysis. Each minute, 5 mL meltwater was directed to each of two fraction collectors (IC and ICP-MS aliquots) and 1.1 mL was used for continuous measurements of water isotopes (0.05 mL) and black carbon (1.05 mL) by the LGR and DMT SP2 instruments. The remaining 1.8 mL was sent to flow-through liquid

conductivity and insoluble particle analyzers (Bigler et al., 2011), and then split for continuous analysis of soluble calcium (Traversi et al., 2007) and acidity (Kjær et al., 2016). A third fraction collector was used to collect discrete samples for water isotopes from the melt-head overflow lines originating from the outer core section, these being used for quality assurance of the continuous measurements.

On average, 20 metres of ice were melted during a 24-hour period, including measurements, calibrations and routine maintenance. Calibrations for water isotopes, calcium, acidity and black carbon were carried out before and after each melting run, which comprised the continuous analysis of 3x1 m long ice rods. Calibrations for methane, based on standard gases with methane concentrations corresponding to glacial and preindustrial Holocene levels, were carried out twice daily. Core breaks and/or contamination in the system caused some sections of missing data. The percentage of affected core varied between chemistry species, ranging from <1% (BC) to 17% (H^+) (see supplementary Table S1), the majority being small sections of missing data that did not severely impact annual layer interpretation.

The CFA chemistry records were very densely sampled (1 data point per mm). Mixing in the tubing as the meltwater sample travelled from melt head to the analytical systems caused individual measurements to be correlated, and hence the effective depth resolution of the system was significantly less than the sampling resolution. This was especially the case for the RICE CFA set-up owing to the relatively small fraction of total meltwater directed to the continuous measurement systems. Following the technique used in Bigler et al. (2011), the effective depth resolution for the CFA measurements was estimated to range from 0.8 cm (conductivity) to 2.5 cm (Ca^{2+}) (Table S1).

4. Constructing the Roosevelt Island Ice Core Chronology, RICE17, for the last 2700 years

The Roosevelt Island Ice Core Chronology 2017, RICE17, was constructed using multiple approaches, as necessitated by changing properties and availability of data with depth. This section describes the methodology used to construct the most recent 2700 years of RICE17, the period for which annual layer identification was feasible. For the deeper part of the core, RICE17 was constructed by gas matching to the WAIS Divide ice core on the WD2014 chronology, as reported in Lee et al. (2018).

4.1. Overview of the annual-layer counting strategy

The uppermost section (0-42.34 m) of the core was dated by manual identification of annual cycles in records of water isotopes and ice impurities from the RICE main core as well as the RICE-12/13-B shallow core. For this most recent period, several distinct marker horizons from well-known historical events were used to constrain the chronology (section 4.2).

Below 42.34m (1885 CE), the timescale was augmented using the *StratiCounter* layer-counting algorithm (Winstrup et al., 2012) applied to multiple CFA impurity records from the RICE main core (section 4.3). A previously-dated tephra layer at 165 m (Pleiades; 1251.6±2 CE according to WD2014) was used to optimize the algorithm settings, but other than that, RICE17 is a fully independent layer-counted ice-core chronology.

The layer-counted part of RICE17 stops at 343.72 m (700 BCE). At this depth, the annual layers are too thin (<6 cm, i.e. less than 8 independent data points/year in the best resolved records) for reliable layer identification in data produced by the RICE CFA set-up. To extend the RICE17 timescale further back, the layer-counted timescale was combined with the gas-derived

timescale, which covers the entire core with lower resolution (Lee et al., 2018). Excellent agreement (±3 years) between the layer-counted timescale and the independent gas-derived age at 343.7m allows us to produce the combined Roosevelt Island Ice Core Chronology 2017, RICE17, by joining the two without any further adjustments.

4.2. Manual layer interpretation with historical constraints (0 - 42.34 m; 2012 - 1885 CE)

The top 42.34 m of the RICE17 chronology was obtained by manually counting annual layers in the combined set of discretely-measured IC and ICP-MS data, where available, as well as the continuous water isotope and chemistry records produced by the RICE CFA system. The RICE main core starts at 8.65 m depth, so the top part of the timescale is based exclusively on the RICE-12/13-B shallow core. At 12.5 m, both cores display a distinct peak in their isotope profiles, showing that they can be spliced directly without need for any depth adjustments. Layer marks for the top 12.5 m were placed according to the RICE-12/13-B shallow core; lower layer marks refer to the main core. In the overlap section (8.65-19.55m), we used the combined data set from both cores to reduce the risk of timescale errors caused by core breaks or bad data sections.

Layer identification in this section of the core relied predominantly on annual signals in non-sea-salt sulfate (nss-SO_4^{2-}), acidity (H^+) and iodine (I), as these records displayed the most consistent annual signals (Fig. 4). Extreme sea-salt influx events occasionally caused large sulfate peaks, necessitating the removal of the sea-salt sulfate fraction before layer identification. For the top 20 m, the water isotope records also significantly strengthened the annual layer interpretations. Smoothing through diffusion of water molecules in the firn, however, causes the annual signal in the water isotope records to diminish with depth, resulting in a loss of annual signals below 20 m.

Summers could be identified as periods with high stable water isotope ratios, high concentrations of nss-SO_4^{2-} and associated acidity [originating from phytoplankton activity in the surrounding ocean during summer (Legrand et al., 1991; Udisti et al., 1998)], and low iodine concentrations [due to summertime photolysis of iodine in the snowpack (Frieß et al., 2010; Spolaor et al., 2014)]. Layer marks were placed according to the depths of concurrent summer peaks in water isotope ratios, nss-SO_4^{2-} concentrations, and acidity levels, and assigned a nominal date of January 1st.

The uppermost 42.34 m of the RICE17 chronology was tied to several distinctly identifiable marker horizons found in the ice-core records relating to well-known historical events (sections 4.2.1-4.2.3; Table 2). A confidence interval was assigned to the timescale by classifying layers as certain or uncertain (Fig. 4), while accounting for age constraints from marker horizons. We conservatively estimated the age uncertainty of the marker horizons to be ±1 year, thereby allowing for some uncertainty in timing of deposition of e.g. volcanic material. Some uncertain layers were counted as a year in the timescale, while others were not. In this way, a most likely timescale was constructed along with an uncertainty estimate, which we interpret as the 95% confidence interval of the age at a given depth, similar to that obtained from automated layer identification deeper in the core (section 4.3).

4.2.1. The 1974/75 snow surface

The uppermost age constraint was established by successfully matching the RICE water isotope profile to that from the RID-75 firn core (Fig. 5). Drilled in austral summer 1974/75, the snow surface in RID-75 provided the first tie-point for the RICE17 chronology at a depth of 14.62m (Table 2).

4.2.2. Nuclear bomb peaks

High-resolution ^{239}Pu measurements on the upper part of the RICE core show a significant rise in plutonium levels, starting from very low background levels at 22m and reaching peak values at 21.6m. This increase can be attributed to atmospheric nuclear bomb testing during the Castle Bravo Operation, Marshall Islands, in March 1954, which globally caused large amounts of nuclear fallout over the following year (see e.g. Arienzo et al. (2016)).

Total specific β-activity levels in the RID-75 core show the same evolution (Clausen et al., 1979), confirming both the isotopic matching between the two cores, and the age attribution of this event (Fig. 5). The abrupt increase in ^{239}Pu-fallout at 22m was used as age constraint for the RICE17 chronology. Subsequent peaks in the ^{239}Pu and β-activity records can be attributed to successive nuclear tests and subsequent test ban treaties (Table 2). These changes were much less distinct, and were therefore not used during development of the timescale.

4.2.3. Recent volcanic eruptions

A couple of volcanic horizons in RICE during this most recent part could be related to well-known volcanic eruptions. Rhyolitic tephra located between 18.1-18.2m was found to have a similar geochemical composition as a tephra layer found in the WAIS Divide core deposited late 1964 CE (Wheatley and Kurbatov, 2017). The tephra likely originates from Raoul Island, New Zealand, which erupted from November 1964 to April 1965. This is consistent with the RICE17 chronology, according to which the tephra is located in early 1965 CE (Table 2).

Only two volcanic eruptions could be unambiguously identified in the acidity records over this period; the historical eruptions of Santa Maria (1902 CE; 37.45m) and Krakatau (1883 CE; 42.34m) (Table 2). These two horizons were used to constrain the deeper part of the manually-counted interval of RICE17, which terminates at the Krakatau acidity peak. Deposition age of volcanic material for these events was assumed identical to those observed in the WAIS Divide ice core (Sigl et al., 2013). Imprints from other large volcanic eruptions taking place during recent historical time, such as Agung and Pinatubo, did not manifest themselves sufficiently in the RICE records to be confidently identified.

4.3. Automated annual layer identification (42.34 - 343.7 m; 1885 CE – 700 BCE)

For the section 42.34-343.7 m (1885 CE - 700 BCE), the RICE17 annual layer-counted timescale was produced using the StratiCounter algorithm (Winstrup et al., 2012), extended to interpret the annual signal based on multiple chemistry series in parallel (Winstrup, 2016).

StratiCounter is a Bayesian algorithm built on machine-learning methods for pattern recognition, using a Hidden Markov Model (HMM) framework (Rabiner, 1989; Yu, 2010). StratiCounter computes the most likely timescale and the associated uncertainty by identifying annual layers in overlapping data batches stepwise down the ice core. For each batch, the layering is inferred by combining prior information on layer appearance with the observed data, thereby obtaining a posteriori probability distributions for the age at a given depth. The output of StratiCounter is the most likely annual timescale, along with a 95% confidence interval for the age as function of depth. The confidence interval assumes the timescale errors to be unbiased, implying that uncertainties in layer identification partly cancel out over longer distances.

StratiCounter was applied to the full suite of CFA records: black carbon, acidity, insoluble dust particles (42.3-129m), calcium, and conductivity. See supplementary S2 for the specifics of the algorithm set-up. Annual cycles in the high-resolution black carbon (BC) record became more distinct prior to 1900 CE, and it was one of the most reliable annual proxies in the core (section

6). As observed in the topmost part of the core, acidity also displayed a distinct annual signal, although the relatively low effective depth resolution of the acidity record (Table S1) made it much less useful with depth. From 0 to 129 m, an irregular annual signal was also observed in the insoluble particle record, but data below 129 m was corrupted by the presence of drill fluid in the CFA system, which forced us to exclude the deeper part of this record. The calcium and conductivity records frequently displayed multiple peaks per year, limiting their contribution to the annual layer interpretations. The discretely-sampled ICP-MS data records did not have sufficient resolution to resolve annual layers.

Decreasing layer thicknesses caused the annual signal in the impurity records to become increasingly difficult to identify with depth, and the layer-counted timescale stops at 343m (700 BCE).

5. Reconstructing past accumulation rates

The accumulation rate history at Roosevelt Island can be inferred from depth profiles of annual-layer thicknesses in the RICE core, when corrected for firn densification and thinning of layers due to ice flow.

5.1. Changes in density with depth

Bag-mean densities were measured on the main RICE core for the interval 8-130 m, at which depth ice densities were reached (see supplementary S3). A steady-state Herron-Langway density model (Herron and Langway, 1980) fitted to the measurements was used to extend the density profile to the surface. Using an initial snow density of 410 kg m^{-3}, a surface temperature of -23.5°C, and an accumulation rate of 0.22 m w.e yr^{-1}, the modelled density profile fits well the observed values (Fig. S2). At 8 m depth, the model agrees with the measured values, providing a smooth transition between observed and modelled densities.

5.2. Thinning of annual layers due to ice flow

The annual layer thickness profile must be corrected for the amount of vertical strain experienced by the ice. This correction factor can be represented by a thinning function, which informs on the cumulative effects of ice flow on the thickness of an ice layer after it was deposited at the surface (this being the ice equivalent accumulation rate at that time). A thinning function appropriate for RICE was produced using vertical velocity profiles obtained by fitting a simple ice-flow model (Lliboutry, 1979) to englacial velocities deduced from repeat radar measurements (Kingslake et al., 2014), while (a) constraining the model parameters to match the present-day accumulation rate and ice-sheet thinning, and (b) accounting for velocity changes caused by the shift in position of the ice divide at Roosevelt Island within the past centuries.

Near-surface vertical strain rates are more compressive near ice divides than on the flanks. Hence, due to migration of the ice divide at Roosevelt Island, ice recovered from different depths in the RICE core has experienced different regimes of vertical strain. Informed by the architecture of the Raymond stack (Fig. 6c), we assumed the following divide-migration history: Until 500 years before ice core drilling (1512 CE), the divide was located 500 m east of the present position, as indicated by the position of the deeper Raymond arches. Since 500 years ago, the divide migrated westward, arriving at its present position by 1762 CE (250 years ago).

Radar measurements of near-surface vertical strain rates (Fig. 6b in Kingslake et al. 2014) show that the transition from divide- to flank-type flow at Roosevelt Island occurs over a distance of

~900 m. For the older part of the ice core (prior to 1512 CE; ice originating 500 m east of the current divide) we used a vertical velocity profile appropriate for divide/flank transitional-type ice flow. While the ice divide migrated to its present position over the following 250 years (1512-1762 CE), the vertical velocity profile transitioned to the present divide-type flow (Fig. 6a).

Following Kingslake et al. (2014), the vertical velocity profiles (w) at normalized depth (ζ) was parameterized using a shape factor (p) and the vertical velocity at the surface (w_s) (Lliboutry, 1979):

$$w(\zeta) = w_s \left(1 - \frac{p+2}{p+1}\zeta + \frac{1}{p+1}\zeta^{p+2}\right)$$

The long repeat interval (3 years) for the radar measurements meant that no vertical velocity measurements were obtained in the firn layer (Fig 6a). The velocity profile was therefore linearly extended to the surface, starting at 155m ice equivalent depth. The vertical surface velocity was taken to be 0.26 m ice eq. yr^{-1}, obtained as the sum of the modern accumulation rate (0.24 m ice eq. yr^{-1}, i.e. 0.22 m w.e yr^{-1}) and recent ice-sheet thinning (0.02m ice eq. yr^{-1}; estimated using an ice-flow model to match the dated architecture of the Raymond stack). For divide-type flow with w_s = 0.26, the overall misfit to the measured vertical velocity measurements was minimized using p = -1.22. For flank-type flow, we used p = 4.16 (Kingslake et al., 2014). For the divide/flank transitional-type flow prior to 1512 CE was used a linear combination with divide-type velocities weighted by 0.7 and flank-type velocities weighted by 0.3. As the divide migrated, the weighting was changed linearly to obtain full divide-type ice flow velocities by 250 years ago.

Figure 6b shows the resulting thinning function derived for the RICE core site. It decreases from 1.0 at the surface (no strain thinning) to 0.24 at 344 m depth. Past annual accumulation rates in water equivalents can be calculated as the annual layer thicknesses divided by the thinning function and multiplied with the firn/ice density.

5.3. Uncertainties in the accumulation history

Uncertainties in the inferred accumulation history originate from three sources: (i) identification of the annual layers; (ii) the density profile; (iii) the derived thinning function. Except for the uppermost part of the record, uncertainty in the thinning function dominates the total uncertainty, and only this factor will be considered here.

At the surface, uncertainty in the thinning function is zero (no strain thinning). Increasing uncertainty with depth (Fig. 6b; grey area) arises from: (a) the lack of measurements in the upper 90 m of the ice sheet to constrain the near-surface vertical velocity; (b) variation of the vertical velocity profile over time in ways not accounted for. The second source of uncertainty is partly mitigated because the amplitudes of the Raymond stack constrain the onset of divide flow to about 3000 years ago (Conway et al., 1999; Martín et al., 2006), i.e. prior to the period considered here, and the existence of the Raymond stack reveals that flow conditions have been stable since. Hence, we believe that most uncertainty arises from the lack of vertical velocity measurements in the upper part of the ice sheet.

To assess the magnitude of this uncertainty, we compared results using two alternate thinning functions. First, the same method as described above (section 5.2) was used to find the best fit to measured vertical velocities, but using a vertical surface velocity of 0.24 m ice eq. yr^{-1}, thereby neglecting the contribution from surface lowering. Second, we used the best fit derived by Kingslake et al. (2014). The mean difference between the three thinning functions is ~5%, with the largest difference (9%) at 78.5 m depth. Accounting also for unknown factors, the

uncertainty of the thinning function was set to increase from 0% at the surface to 10% at 78.5 m (1730 CE), and to remain constant at 10% deeper in the core. This translates to approximately the same percentage-wise uncertainty in derived accumulation rates. We suggest to interpret this uncertainty as a 95% (2σ) confidence interval. As the strain increases continuously with depth, the relative uncertainty on the accumulation rates is much smaller than the absolute values.

Results

6. Seasonality of impurity influx to Roosevelt Island

Using the RICE17 timescale, we can quantify the seasonality of impurity influx to Roosevelt Island visible in the five RICE CFA records: acidity, calcium, conductivity, black carbon and insoluble dust particles. Figure 7 shows the average seasonal pattern of the impurities at different depths, assuming constant snowfall through the year.

6.1. Acidity

The CFA acidity record is driven primarily by the influx of non-sea-salt sulfur-containing compounds, as evident by its high resemblance to the IC non-sea-salt sulfate and ICP-MS non-sea-salt sulfur records in the top part of the core (Fig. 4). Sulfur-containing compounds have a variety of sources, one of which is dimethylsulfide (DMS) emissions by phytoplankton activity during summer (Legrand et al., 1991; Udisti et al., 1998). Correspondingly, acidity displays a regular summer signal, with maximum values in late austral summer (January/February), and minimum values from June through October. This is similar in timing to the seasonal pattern of non-sea-salt sulfate at Law Dome (Curran et al., 1998) and WAIS Divide (Sigl et al., 2016). The acidity contains a faint annual signal even in the deepest part of the layer-counted timescale (Fig. 7a-c).

Episodic influxes of sulfuric acids from explosive volcanic eruptions are overprinted on the annual acidity signal. Biogenic peak values of up to 200ppb non-sea-salt sulfate are of the same order as the expected sulfate deposition from large volcanic eruptions, causing the seasonal signal to effectively obscure the volcanic contributions to the non-sea-salt sulfate concentrations. Volcanic signals are slightly more prominent in the acidity record (Fig. 8a). This may be explained by only a fraction of the biogenic sulfur emissions being oxidized to acids, whereas volcanic SO_2 emissions are almost completely oxidized to H_2SO_4 (a strong acid).

6.2. Sea-salt derived species: Calcium and conductivity

As previously noted by Kjær et al. (2016), the RICE conductivity record is almost identical to the mostly sea-salt-derived calcium record (Figs. 4, 8), suggesting sea spray to be responsible also for peaks in liquid conductivity. We hence consider these two records to be representative of sea salt deposition at Roosevelt Island.

Both records typically peak during early-to-mid-winter (June/July), but with large spread in magnitude and timing from year to year (Fig. 7d-i), and oftentimes there are multiple peaks per year. The timing of peak values is approximately similar to sea-salt tracers in WAIS Divide (Sigl et al., 2016), and a few months earlier than peak values in Law Dome (Curran et al., 1998). During the most recent period (1900-1990 CE), we observe a summer peak in the average seasonal conductivity signal, which is not present in the calcium record. This is likely the steady summer contribution to conductivity from biogenic acidity, the seasonality of which being sufficiently prominent to show up in seasonal averages of conductivity in the top part of the core.

6.3. Black carbon

Seasonal deposition of black carbon (BC) in Antarctic snow is primarily driven by biomass burning and fossil fuel combustion in the Southern Hemisphere, modulated by changes in efficiency of the long-range atmospheric transport (Bisiaux et al., 2012). Southern Hemispheric fossil fuel emissions have increased since the l950s (Lamarque et al., 2010), but are still believed to be a minor contributor to total black carbon deposition in Antarctica (Bauer et al., 2013).

Biomass burning in the Southern Hemisphere peaks towards the end of the dry season, e.g. late summer (Schultz et al., 2008). Given the distinct annual signal in the black carbon record (Fig. 7j-l), StratiCounter was set up to assign peaks in BC a nominal date of January 1st (mid-summer). We note that peaks in BC approximately coincide with peaks in acidity (similar to observed in WAIS Divide), thus ensuring consistency of nominal dates throughout the core. Minimum concentration values are reached in Austral winter (June/July).

The annual signal in black carbon changes with depth in the RICE core. During the 20th century, annual cycles exist, but are not very prominent (Fig. 7j). Prior to 1900 CE, the signal is much more distinct, with larger seasonal amplitude as well as higher annual mean concentrations (Fig. 7k-l). A recent decrease in BC concentrations has been observed also in the WAIS Divide and Law Dome ice cores, and attributed to a reduction in biofuel emissions from grass fires (Bisiaux et al., 2012). At WAIS Divide and Law Dome, however, the shift takes place several decades later than observed in RICE.

With increasing depth in the ice core, thinner annual layers cause the amplitude of the seasonal signal to slowly be reduced. Yet, aided by the high effective depth resolution of the black carbon record, the seasonal cycle persists to great depths in the RICE core, with the deepest part of the layer-counted RICE17 timescale primarily relying on the annual signal in this parameter.

6.4. Dust

The seasonal pattern in insoluble dust particle concentrations showed a weak annual signal, with a tendency to peak in summer. The simultaneous deposition of black carbon and dust is consistent with both tracers arriving via long-range transport from southern hemispheric continental sources. The dust record showed large non-annual variability, and had limited contribution to the annual layer identification in RICE17.

7. The layer-counted RICE17 chronology

The layer-counted timescale was constructed back to 700 BCE (0-343.72 m), and it forms the most recent part of the Roosevelt Island Ice Core Chronology 2017 (RICE17). It is an independent timescale, constrained only by a few well-known historical events over the last hundred years. Its independence is reflected in the timescale uncertainty: Age confidence intervals show an approximately linear increase with depth (Fig. 8b), reaching a maximum age uncertainty of ±45 years (95% confidence) at 700 BCE, the end of the layer-counted timescale.

RICE17 was evaluated by comparing to the highly accurate annual-layer-counted WD2014 chronology from WAIS Divide (Sigl et al., 2015, 2016). Timescale comparison was aided by the relative proximity of the two ice cores, and accomplished using two complementary approaches: 1) matching multi-decadal variations in the RICE methane record to a similar record from WAIS Divide; and 2) by matching volcanic marker horizons in the two cores. The two matching procedures were performed independently, and are described in the following sections.

Volcanic matching allows very precise age comparisons, but suffers from the risk of incorrect event attribution. Erroneous alignment is less likely to occur when matching records of methane concentration variability. This approach does not allow as high precision, however, due to the multi-decadal nature of the methane variations, as well as the need to account for the gas-age-ice-age difference. Combining the two lines of evidence, the methane match points were used to validate the absolute ages of the timescale (relative to WD2014), and to confirm the independently-obtained volcanic match points. Based on the volcanic matches, a high-precision comparison to WD2014 was achieved, allowing an in-depth quality assessment of the RICE17 chronology.

7.1. Timescale validation using multi-decadal variability in methane concentrations

Centennial-scale variations in methane concentrations observed in the RICE gas records can also be found in similar records from WAIS Divide (Mitchell et al., 2011; WAIS Divide Project Members, 2015). Stratigraphic matching of these records allowed a comparison of the respective ice-core timescales.

The gas records from RICE and WAIS Divide were matched using a Monte Carlo technique reported in Lee et al. (2018). The feature matching routine employed discretely-measured records of methane as well as isotopic composition of molecular oxygen ($\delta^{18}O_{atm}$). Over recent millennia, however, the $\delta^{18}O_{atm}$ concentrations have been stable, and hence provided minimal matching constraints. An average spacing of 26 years between successive RICE methane samples contributed to the matching uncertainty. The matching routine identified 18 match-points over the past 2700 years, i.e. an average spacing of 150 years. Subsequent visual comparison of the methane profiles suggested minor manual refinements of the match-points (8 years on average, maximum 23 years; all within the uncertainty of the automated matching). These adjustments resulted in a slightly improved fit.

Through methane feature matching, WAIS Divide ages could be transferred to the RICE gas records, i.e. provide an estimate for the RICE gas ages. During the snow densification process, there is a continuous transfer of contemporary air down to the gas lock-in depth, resulting in an offset (Δage) between the ages of ice and gas at a given depth (Schwander and Stauffer, 1984). To obtain the corresponding ice-core ice ages relevant for this study, Δage was calculated using a dynamic Herron-Langway firn densification model (Herron and Langway, 1980) following Buizert et al. (2015). The approach is described in detail in Lee et al. (2018). The model is forced using a site temperature history derived from the RICE stable water isotopes, and the firn column thickness is constrained by the isotopic composition of molecular nitrogen ($\delta^{15}N$ of N_2). In addition to Δage, this formulation of the Herron-Langway densification model produces as output a low-resolution accumulation rate history (section 8.3).

Compared to most other Antarctic sites, the relatively high surface temperature and accumulation rate at Roosevelt Island give rise to low Δage values (averaging 160 years over recent millennia) associated with small uncertainties (~36 years; 1σ). Combined with the feature matching uncertainty (average: 48 years), total age uncertainty (1σ) in the transfer of WD2014 to the RICE core is on average 64 years (maximum: 101 years) over the last 2700 years.

The RICE17 timescale is consistent with the WD2014 age of the methane match points (Fig. 8b). Based on the automatic matching routine, agreement of RICE17 to the gas-matched WD2014 ages is better than 33 years for all age markers, with a root-mean-square (RMS) difference of 17 years. Agreement between the two timescales is even better when using the

manually-adjusted match-points, for which the RMS difference is reduced to 13 years. We observe, however, that all methane match points below 275 m are associated with older ages in WD2014 than in RICE, suggesting a small bias in the deeper part of RICE17.

7.2. Timescale evaluation from volcanic matching

Using the layer counts in RICE17 as guide, volcanic horizons identified in RICE could be linked to the WAIS Divide volcanic record (Sigl et al., 2013, 2015), allowing a detailed comparison of their respective timescales. Identification of volcanic eruptions in the RICE records was non-trivial, but feasible after the introduction of two new volcanic tracers, described below.

7.2.1. New and conventional ice-core tracers for volcanic activity

With its coastal location and low altitude, the RICE drilling site receives significant seasonal influx of sulfuric acids from biological oceanic sources, which tends to obscure sulfur deposition from volcanic eruptions (section 6.1). Traditional volcanic ice-core tracers, ECM and sulfur, were generally of limited value for identifying volcanic horizons. The ECM record was very noisy, with few peaks extending above the noise level. Resolution of the discretely-sampled sulfur record was too low (below 67m: 5 cm, i.e. less than 4 samples/year), and even large volcanoes only left a vague imprint in form of slightly increased sulfur levels over a multi-year period (Fig. 9a). Detection of volcanic horizons in the RICE core therefore primarily relied on two new high-resolution tracers for volcanic activity: direct measurements of total acidity and estimated non-sea-salt liquid conductivity.

Peaks in the RICE liquid conductivity record were caused primarily by sea salts, and thus this record could not on its own be used as volcanic tracer. However, from the close similarity of the conductivity and the mostly sea-salt-derived calcium record (Figs. 4, 9), we could extract a signal of non-sea-salt conductivity, obtained as the conductivity-to-calcium excess. Being a secondary product, this tracer is prone to measurement errors, calibration and co-registration uncertainties, and further complicated by differences in measurement resolution. Nevertheless, peaks in the conductivity-to-calcium excess showed high consistency with peaks in total acidity, and it proved to be a reliable tracer for volcanic activity.

Based on the combined evidence from all proxies, we were able to identify volcanic horizons in RICE. A sequence of volcanic signals is shown in Figure 9a. Compared to acidic peaks resulting from unusually high biogenic summer activity, volcanic imprints could be distinguished as more prominent and/or broader features. Small and short-lived volcanic eruptions, however, were not easily identified.

7.2.2. The Pleiades: A tephra-chronological marker horizon

A visible tephra layer was found in RICE at 165m depth, with a RICE17 age of 1251.5±13 CE. Geochemistry of the tephra particles is consistent with an eruption from the Pleiades (Kalteyer, 2015; Kurbatov et al., 2015), a volcanic group located in Northern Victoria Land, Antarctica (Fig. 1). Tephra of similar geochemistry has been found in several other Antarctic cores dated to approximately the same time, including WAIS Divide (1251.6±2 CE; Dunbar et al. 2010) and Talos Dome/TALDICE (1254±2 CE; Narcisi, Proposito, and Frezzotti 2001; Narcisi et al. 2012). The Pleiades tephra horizon allowed a firm volcanic matching of the RICE and WAIS Divide ice cores at this depth (Fig. 9).

The Pleiades tephra horizon was used to select the optimal settings for the StratiCounter algorithm, seeking to reproduce the WD2014 age of the tephra layer as well as possible. The observed compliance of the two age-scales at this depth is therefore to be expected. However, we note that our use of this layer as chronological marker had little impact on the resulting

RICE17 timescale: All StratiCounter solutions produced very similar ages for the tephra horizon, and, within the age-scale uncertainties, all were in agreement with the WD2014 age of the tephra.

7.2.3. Volcanic matching to WAIS Divide

Based on the layer counts in RICE17, we could match up volcanic horizons observed in RICE with the WAIS Divide volcanic record (Sigl et al., 2013, 2015). The matching relied on identifying sequences of volcanic events in the two cores with similar age spacing according to their respective timescales. Taking this approach was especially important due to the few prominent volcanic horizons in the RICE core, and the risk of confounding volcanic and biogenic signals. Reliability increased with density of match points in the volcanic sequence. In some sections such sequences were hard to identify, either due to timescale differences, too many or too few volcanic events. For sections without CFA data, a tentative attribution was made based on the limited evidence from the non-sea-salt sulfur and ECM records, where possible. The volcanic matches are provided in Table 2.

The volcanic matching was in excellent agreement with the independently-obtained methane matching, especially when using the manually-adjusted match points (Fig. 8b). A majority of the volcanic links identified between the RICE and WAIS Divide ice cores have previously been classified as bipolar signals, originating from large tropical volcanoes (Sigl et al., 2013, 2015). This further strengthens our trust in the volcanic matching, since these large eruptions usually deposit acids over an extended area and period, and therefore are expected to be recognizable from the RICE volcanic records.

7.2.4. Quality assessment of RICE17

The volcanic matching to WAIS Divide allowed a detailed evaluation of RICE17. The WD2014 counting uncertainty is merely 7 years over the last 2700 years, much less than the uncertainty associated with RICE17, and we hence consider it to be the more accurate of the two. Within their respective uncertainties, the RICE17 and WD2014 chronologies are in full agreement at all volcanic marker horizons (Table 2; Fig. 8b). Indeed, the age differences are much less than the accumulated RICE17 age uncertainties. We hence conclude that the inferred confidence bounds on the RICE17 chronology are reliable, if somewhat conservative.

Agreement between the two ice-core timescales is particularly remarkable down to 285 m (~150 CE). For this most recent part of the RICE17 timescale, the age discrepancy is less than 7 years at all marker horizons, with a RMS age difference of 3 years. Below 285 m, the volcanic matches indicate that RICE17 may be slightly biased (~3%) towards younger ages. This is corroborated by the methane match points (section 7.1). At 285 m, the effective depth resolution of the CFA impurity records (1-2 cm) becomes marginal compared to the annual layer thicknesses (7 cm at 285 m), and we suspect that this has caused the thinnest fraction of annual layers to be indiscernible in the ice core records.

Consequently, the deepest section of the layer-counted RICE17 chronology slowly diverges from WD2014, reaching a maximum age difference of 30 years at the oldest identified volcanic marker horizon (343.3 m, 691 BCE ±45 years; Table 2). This age offset is of similar magnitude to the uncertainty of the methane-derived RICE17 ages at this depth.

8. Roosevelt Island accumulation history

Annual layer thicknesses in the RICE ice core smoothly decrease with depth, starting from more than 40 cm at the surface to ~6 cm at 344 m (Fig. 9a). After corrections for density changes and

ice flow thinning of annual layers with depth (section 5), an annual accumulation rate history for Roosevelt Island over the last 2700 years was obtained (Fig. 10f).

8.1. Long-term accumulation trends

Mean accumulation rates at Roosevelt Island over the entire 2700 year period was 0.25±0.02 m w.e. yr^{-1}. From 700 BCE to ~1300 CE, the accumulation rate at Roosevelt Island shows a slightly increasing trend (Fig. 10f; Table 3), and in 1250 CE, the 20-year running mean accumulation rate reached its maximum over the last 2700 year (0.32 m w.e. yr^{-1}). Since then, accumulation rates have decreased: very slowly until ~1650 CE, then more rapidly (0.10 mm/yr^2 from 1650-1965 CE; Table 3). A continued acceleration in the decline of accumulation rates is observed towards the present. Change points and trend estimates with their associated uncertainties were identified using a break function regression analysis (Mudelsee, 2009). The analysis revealed that high inter-annual variability in accumulation rates prohibited a very accurate determination of the breakpoints.

8.2. Significant decrease in recent accumulation rates

The Roosevelt Island accumulation history reveals a distinct and rapid accumulation decrease in recent decades (Fig. 11): Since the mid-1960s, the annual accumulation has decreased with a rate corresponding to 0.8 mm/yr^2, i.e. 8 times faster than the average over previous centuries. We note, however, that the relatively short time period for conducting the trend analysis, combined with the large inter-annual variability in accumulation rates, causes significant uncertainty in the precise timing of the change-point as well as the trend estimate.

Considering the period since 1700 CE, the lowest decadal mean value of the accumulation rate is observed in the 1990s (0.194 ± 0.001 m w.e. yr^{-1}). Except for very low accumulation rates during the 1850s and 1800s, the remaining top six decades of lowest mean accumulation take place after 1950 CE (Table 4). Indeed, over the last 50 years, only one decade (1960s) stands out as not having experienced below-average accumulation at Roosevelt Island.

The current accumulation rate at Roosevelt Island of 0.211±0.002 m w.e. y^{-1} (average since 1965 CE, $\pm 2\sigma$) is 34% less than the peak accumulation rates around 1250 CE, and 16% below the average of the last 2700 years.

8.3. Comparison to the gas-based accumulation rates

The RICE17 accumulation history is in reasonable agreement with the low-resolution accumulation rate output from the dynamic Herron-Langway firn densification model (section 7.1; Fig. 10f, dashed line). The gas-based accumulation rate history does not resolve high-frequency variations, but shows a slow increase in accumulation rates of 0.02 mm/yr^2, similar to the trend obtained from the annual layer thicknesses prior to 1300 CE. However, in contrast to the accumulation rate history derived here, the firn-based accumulation rates continue to increase until present. Further, the absolute value of the inferred gas-based accumulation rates tend to generally underestimate the accumulation rates by ~0.04 m w.e. yr^{-1} (16%).

We speculate that the discrepancies may have to do with the shift in RICE water isotope levels occurring around 1500 CE (Fig. 10g), which in the firn model is used to represent temperature change. It has been suggested that this shift is due to other factors than temperature (Bertler et al., 2018), and it coincides with commencement of the divide migration period. By using δD to estimate temperature change, the firn densification model will produce an increase in accumulation rates towards present in order to preserve a constant thickness of the firn column, as indicated by relatively steady values of $\delta^{15}N\text{-}N_2$ (Fig. 10f, black dots). Further, the model

showed a tendency to underestimate the firn column thickness during the earlier part of the period, which may explain the generally lower level of the modelled accumulation rates here.

8.4. Spatial consistency in recent accumulation rates

Spatial representativeness of the RICE accumulation rates was evaluated by comparing year-to-year profiles of layer thicknesses obtained for the overlap sections of the three available cores: RICE main core, RICE-12/13-B, and RID-75 (Fig. 12), with RID-75 located less than 1 km away from the two RICE cores. All cores were corrected for density changes and ice flow thinning using the density and thinning profile from the main RICE core.

Annual accumulation records from the three cores are very strongly correlated (correlation coefficients ranging between 0.85 and 0.87), indicating the spatial accumulation pattern across Roosevelt Island to be stable through recent time. The spatial consistency of snow deposition at Roosevelt Island is further confirmed by the agreement between their measured water isotope records (Fig. 5a). We may therefore disregard depositional noise, and consider the temporal variability in RICE annual layer thicknesses as representative of local snow accumulation.

This consistency in accumulation history is in contrast to a high spatial variability in mean accumulation rates across Roosevelt Island ice divide. Repeat surveys over three years (2010-2013) of 144 survey stakes set across Roosevelt Island showed a strong spatial gradient in snow accumulation across the ice divide: Accumulation rates of up to 0.32 m w.e. yr^{-1} were measured on the north eastern flank, decreasing to 0.09 m w.e. yr^{-1} on the south western flank (Bertler et al., 2018). In accordance with these stake measurements, the absolute accumulation rate is found to be significantly less (~7%) for RID-75 than for the two RICE cores. Insignificant differences in accumulation rate were present between the two RICE cores. Spatial variability in mean accumulation rates, combined with different averaging periods, may explain why previous estimates of Roosevelt Island accumulation rates have varied quite significantly (Bertler et al., 2018; Conway et al., 1999; Herron and Langway, 1980; Kingslake et al., 2014).

The representativeness of the Roosevelt Island accumulation rates is corroborated by high spatial correlation of the RICE accumulation rates to gridded ERA-interim precipitation data during recent decades (Bertler et al., 2018). These results suggest that precipitation variability at Roosevelt Island is representative for an extended area, which includes the Ross Ice Shelf, the Southern Ross Sea, and the western part of West Antarctica.

8.5. Influence of ice divide migration on the accumulation history

The recent period (~1500-1750 CE) of divide migration at Roosevelt Island may impact interpretation of the climate records from the RICE core. Ice recovered in the deeper part of the RICE core, deposited before divide migration, have originated west of the ice divide. Present accumulation rates show a distinct decrease on the downwind (western) side of the ice divide with a gradient of $\sim 5 \cdot 10^{-3}$ m w.e./km yr^{-1}, although muted around the summit area. Assuming a stable snowfall pattern through time relative to the divide, its migration would have caused reduced accumulation rates to be observed during the early part (until 1500 CE) of the RICE accumulation history. With the ice originating up to 500m west of the divide at time of deposition, our estimates of Roosevelt Island accumulation rates during this early period may therefore have a small negative bias of up to $2.5 \cdot 10^{-3}$ m w.e. yr^{-1}.

Correcting for the influence of ice divide migration, the main impact on the Roosevelt Island accumulation history is an earlier onset of the period with more rapid decrease in accumulation rates. The differences are small, however, and the overall pattern of trends in accumulation rate

through time remains the same. In particular, ice divide migration has no impact on accumulation rate trends observed before and after the migration period.

Discussion

9. The RICE accumulation history in a regional perspective

9.1. Past accumulation trends across West Antarctica

Regional differences in accumulation, from Northern Victoria Land across West Antarctica to Ellsworth Land, may be evaluated by accumulation reconstructions based on ice core records (Fig. 10).

The RICE accumulation history (Fig. 10f) is much more variable on inter-annual and decadal scales than the accumulation rate reconstruction from e.g. WAIS Divide (Fig. 10d). Snowfall at Roosevelt Island is dominated by large and episodic precipitation events (Emanuelsson et al., 2018), which likely contributes to the high inter-annual variability in RICE accumulation rates. A highly dynamic synoptic-scale system brings this precipitation to Roosevelt Island: Positive RICE precipitation anomalies have been linked to the increased occurrence of Eastern Ross Sea/Amundsen Sea blocking events associated with a weak state of the quasi-stationary Amundsen Sea Low (ASL) pressure system. These blocking events impede the prevailing westerly winds, and direct on-shore winds towards the Eastern Ross Sea, thereby increasing the precipitation at Roosevelt Island and Western Marie Byrd Land (Emanuelsson et al., 2018).

Only the WAIS Divide and RICE ice cores are available for evaluating multi-millennial-scale accumulation trends and corresponding change points in West Antarctica. Over the past 2700 years, WAIS Divide accumulation rates (Fudge et al., 2016) have continuously decreased from a level approximately 25% higher than today (Fig. 10d). Accumulation rates declined slowly (-0.01 mm/yr^2) until around 900 CE, after which the decline became more rapid (-0.04 mm/yr^2). This change took place a few centuries before the trend in RICE accumulation rates turned from positive to negative (1300 CE). Covering the last 800 years, the Talos Dome accumulation record (Fig. 10c) shows a relatively constant level during this early period, albeit with large decadal variability (Stenni et al., 2002).

Considering accumulation changes over the last century, more ice-core accumulation records are available from across West Antarctica; from Victoria Land through to Ellsworth Land. Most West Antarctic ice cores display decreasing accumulation rates over recent decades, but timing and strength of the decrease is location-dependent. The strongest and most recent decrease is observed at RICE (rate change at 1965 CE, this work), with Siple Dome accumulation rates starting to decrease slightly later (1970 CE, Fig. 10e; Kaspari et al., 2004). The WAIS Divide site displays the latest and weakest change of rate (ca. 1975 CE; estimated from nearby firn cores; Burgener et al., 2013). An extension of the Talos Dome accumulation record to 2010CE using snow stakes (Fig. 10c), suggests a recent decrease in accumulation rate also at this location (Frezzotti et al., 2007). In contrast, significant increases in accumulation rates are observed in ice cores from Ellsworth Land, where accumulation rates have shown a steady and marked increase during the 20th century (Fig. 10b, Thomas et al. 2015).

The difference in accumulation rate trends across West Antarctica may to a large extent be explained by changes in location and intensity of the ASL over time. The ASL influences accumulation rates in a dipole pattern: By reducing the number of blocking events, a strong

state of the ASL leads to less accumulation over the Ross Ice Shelf area, and greater accumulation over Ellsworth Land and the Antarctic Peninsula (Emanuelsson et al., 2018; Raphael et al., 2016). Thus, imposed on West Antarctic-wide accumulation trends, the RICE accumulation history likely reflects the state of the ASL back in time. The accumulation dipole is centered at the West Antarctic ice divide. Hence, the WAIS Divide ice core should be minimally influenced by the strength of the ASL, and may therefore be considered representative for West Antarctica as a whole (Fudge et al., 2016). The Northern Victoria Land region, located west of the Ross Ice Shelf, appears to be relatively unaffected by this ASL-induced dipole effect which influences Ellsworth Land and West Antarctica. The recent accumulation decrease observed at Talos Dome has been suggested to be caused partly by increased wind-driven sublimation after deposition, due to an increase in mean wind velocities associated with the deepened ASL (Frezzotti et al., 2007).

9.2. Connection to sea ice variability in the Ross Sea

Throughout the satellite era, RICE accumulation rates are strongly correlated (Bertler et al., 2018) with sea ice extent in the Ross-Amundsen Sea (Jones et al., 2016): Years of reduced sea ice extent are associated with higher accumulation of more isotopically enriched snow and above-normal air temperatures (Bertler et al., 2018).

The expansion of sea ice in the Ross Sea during recent decades has taken place concurrently with a marked reduction of sea ice in the Bellingshausen Sea (Comiso and Nishio, 2008), and both trends have been associated with a strengthening of the ASL: The deepened pressure system causes warm poleward-flowing air masses to cross the Bellingshausen Sea, while the returning cold air passes over the Ross Sea, allowing conditions favorable for sea ice expansion (Hosking et al., 2013; Raphael et al., 2016; Turner et al., 2016). The strength of the ASL concurrently affects RICE accumulation rates (section 9.1), with a deep pressure system causing less accumulation at Roosevelt Island. In addition, an extended regional sea ice cover reduce the availability of local moisture sources. With ~40-60% of the precipitation arriving to Roosevelt Island originating from local sources in the Southern Ross Sea (Tuohy et al., 2015), the relationship between sea ice extent and accumulation rate at Roosevelt Island may also be ascribed a longer distillation pathway of moist air masses during periods of extended sea ice (Kuttel et al., 2012; Noone and Simmons, 2004).

The rapid recent decline in Roosevelt Island accumulation rates likely reflects the recent increase in regional sea ice extent, and we suggest 1965 CE to mark the modern onset of rapid sea ice expansion in the region. Further investigations are required to determine if the strong relationship between Roosevelt Island accumulation rates and Western Ross Sea sea-ice extent holds over longer timescales. However, the decline in RICE accumulation rates observed since 1300 CE is consistent with previous research indicating that the present increase in sea ice extent in the Ross-Amundsen Seas is part of a long-term trend, having lasted at least the past 300 years (Thomas and Abram, 2016).

9.3. Large-scale circulation changes and implications for recent and future trends in Roosevelt Island accumulation

The ASL is sensitive to large-scale circulation patterns, in particular the Southern Annual Mode (SAM) [positive SAM: stronger ASL (e.g. Hosking et al., 2013)] and via teleconnections to the tropical El Niño-Southern Oscillation (ENSO) [stronger ASL during La Niña phase (e.g. Yuan & Martinson 2000)], and the degree to which the two are acting in phase (Clem and Fogt, 2013). A recent strengthening of SAM has been reported (Marshall 2003), consistent with the recent deepening of the ASL (e.g. Raphael et al. 2016).

It is not clear whether the recent trends in ASL and Ross Sea sea-ice extent can be ascribed to natural variability. Some studies have attributed the positive trend of SAM in recent decades to Antarctic stratospheric ozone depletion and/or global warming from greenhouse gas emissions (Kushner et al., 2001; Turner et al., 2009), thus suggesting that anthropogenic forcing may play a role. In the future, the competing effects of the two (Arblaster et al., 2011) may define the future state of the ASL, and thereby the accumulation trends observed at Roosevelt Island and across West Antarctica.

Most other coastal Antarctic sites have experienced a significant increase (~10%) in accumulation rates since the 1960s (Frezzotti et al., 2013). The broad similarities and differences noted here raise the question of whether West Antarctic accumulation, as a whole, is decreasing, or whether the observed trends merely represent a redistribution of precipitation. It highlights the issue that the current trend in total Antarctic mass balance can only be fully understood pending large spatial data coverage.

10. The RICE volcanic record

10.1. A record biased towards regional volcanism

The coastal setting of Roosevelt Island challenged the identification of volcanic eruptions in the RICE records, as high background levels of marine sulfate efficiently masked the presence of sulfate from volcanic eruptions. The RICE volcanic proxy records contained a large number of significant peaks without counterpart in WAIS Divide. While some of these may be explained as extreme events of seasonal biogenic sulfur influx, others may have been produced by regional volcanism.

Apart from sulfate, many volcanoes emit acidic compounds based on halogens, e.g. bromine, chlorine and fluoride. The halide acids are highly soluble, and will be removed from the atmosphere relatively quickly during transport. Hence, they will contribute to increased ice acidity in ice cores located close to the eruption site, whereas only sulfate is deposited from distant volcanic eruptions. By focusing on acidity as volcanic tracer instead of sulfur, the RICE volcanic proxies may thus be more sensitive to regional volcanism than to larger far-field eruptions. Such geographical bias may be particularly important for the Roosevelt Island ice core record, since there is a prevalence of quiescent regional volcanism with relatively high halogen content in West Antarctica (Zreda-Gostynska et al., 1997).

10.2. Dipole effect in deposition of volcanic tracers across West Antarctica

Differences in snow deposition across West Antarctica, influenced by the ASL, may further complicate volcanic matching between ice cores in this region. The ASL dipole acts to direct storm systems either toward the Antarctic Peninsula/Ellsworth Land region, or toward the western Marie Byrd Land/Ross Ice Shelf region. As these storm tracks are associated with snowfall and wet deposition of ions, this is likely to favor deposition and preservation of volcanic signals in one location (e.g. Antarctic Peninsula) at expense of the other (RICE, Siple Dome).

An anti-phase in snow accumulation may be part of the explanation for the difference between the WAIS Divide and RICE volcanic records. While most of the major volcanic signals in WAIS Divide also exist in RICE, they are not necessarily associated with a prominent signal. Absence of volcanic signal in the RICE core from these large far-field volcanic eruptions may be due to a particularly strong ASL state at the time, directing precipitation and sulfate ions away from Roosevelt Island. A detailed comparison of volcanic records from multiple ice cores

is required to evaluate the importance of the ASL for deposition of volcanic tracers across West Antarctica.

10.3. Volcanic synchronization of low-elevation coastal ice cores

A range over obstacles were overcome to carry out volcanic identification in the RICE core. Similar difficulties will likely challenge volcanic synchronization for other low-elevation coastal Antarctic ice cores (Philippe et al., 2016), for which many drilling projects are planned within the near future. The methods proposed here may be relevant also for these cores.

Robust volcanic matching of RICE and WAIS Divide was possible only by the aid of accurate, high-resolution ice-core timescales for both cores. This demonstrates the importance of building an Antarctic-wide network of accurately-dated volcanic reference horizons, based on tephra, sulfate and acidity. Particular emphasis should be placed on the production of annually-counted timescales for Antarctic ice cores, especially as new and/or improved measurement methods allow the production of high-resolution impurity records for relatively high-accumulation Antarctic sites, such as RICE.

Conclusions

The upper part of the RICE ice core from Roosevelt Island, Ross Ice Shelf, West Antarctica, was dated by annual layer counting back to 700 BCE based on multiple high-resolution impurity records. The timescale covers a period of stable ice flow after establishment of an ice divide at Roosevelt Island. The chronology was validated by comparison to the timescale from the WAIS Divide ice core, West Antarctica, by matching sequences of volcanic events visible primarily in direct measurements of ice-core acidity and non-sea-salt conductivity. The maritime environment at Roosevelt Island gave rise to challenging conditions for identifying volcanic signatures in the ice core, and the volcanic matching was confirmed by matching centennial-scale variability in atmospheric methane concentrations measured in the two ice cores. The RICE17 and WD2014 timescales were found to be in excellent agreement.

Based on the layer thickness profile, we produced an annual accumulation record for Roosevelt Island for the past 2700 years. Similar accumulation histories are observed in three Roosevelt Island ice cores covering recent times, giving confidence that RICE is a reliable climate archive suitable for further understanding of climate and geophysical variability across West Antarctica.

Roosevelt Island accumulation rates were slightly increasing from 700 BCE until 1300 CE, after which accumulation rates have consistently decreased. Current accumulation trends at Roosevelt Island indicate a rapid decline of 0.8 mm/yr^2, starting in the mid-1960s. The modern accumulation rate of 0.211 m w.e yr^{-1} (average since 1965CE) is at the low extreme of observed values during the past several thousands of years. The low present-day accumulation rate has been linked to a strengthening of the Amundsen Sea Low, and expansion of sea ice in the Western Ross Sea. The current increase of sea ice in the Ross Sea is therefore likely part of a long-term increasing trend, although the rapid increase since the mid-1960s may have an anthropogenic origin.

Data availability:

The following data will be made available on the Centre for Ice and Climate website (http://www.iceandclimate.nbi.ku.dk/data/) as well as public archives PANGAEA and NOAA paleo-databases: RID-75 isotope and beta-activity records; RICE-12/13-B and RID-75 accumulation rates; RICE17 timescale; RICE accumulation rates; and volcanic match points

between RICE and WAIS Divide. Roosevelt Island GPS and radar data have been archived at the U.S. Antarctic Program Data Center, available at: https://gcmd.gsfc.nasa.gov/search/Metadata.do?entry=USAP0944307&subset=GCMD.

Acknowledgements

This work is a contribution to the Roosevelt Island Climate Evolution (RICE) Program, funded by national contributions from New Zealand, Australia, Denmark, Germany, Italy, China, Sweden, UK and USA. The main logistic support was provided by Antarctica New Zealand (K049) and the US Antarctic Program. We thank all the people involved in the RICE logistics, fieldwork, sampling and analytical programs. The Danish contribution to RICE was funded by the Carlsberg Foundation's North-South Climate Connections project grant. The research also received funding from the European Research Council under the European Community's Seventh Framework Programme (FP7/2007-2013) ERC grant agreement 610055 as part of the Ice2Ice project. The RICE Program was supported by funding from NSF grants (PLR-1042883, ANT-0837883, ANT-0944021, ANT-0944307 and ANT-1643394) and New Zealand Ministry of Business, Innovation, and Employment grants issued through Victoria University of Wellington (RDF-VUW-1103, 15-VUW-131), GNS Science (540GCT32, 540GCT12) and Antarctica New Zealand (K049). Figure 1 was made using Quantarctica2 (Norwegian Polar Institute) basemaps and QGIS software.

We have presented here ice core data collected and analyzed by Henrik Clausen, Willi Dansgaard, Steffen Bo Hansen and Jan Nielsen under the Ross Ice Shelf Project (RISP) carried out between 1973 and 1978. We acknowledge the pioneering work conducted by these researchers and the ongoing international collaborations they established.

References

Abbott, P. M., Davies, S. M., Steffensen, J. P., Pearce, N. J. G., Bigler, M., Johnsen, S. J., Seierstad, I. K., Svensson, A. and Wastegård, S.: A detailed framework of Marine Isotope Stages 4 and 5 volcanic events recorded in two Greenland ice-cores, Quat. Sci. Rev., 36, 59–77, doi:10.1016/j.quascirev.2011.05.001, 2012.

Alley, R. B., Meese, D. A., Shuman, C. A., Gow, A. J., Taylor, K. C., Grootes, P. M., White, J. W. C., Ram, M., Waddington, E. D., Mayewski, P. A. and Zielinski, G. A.: Abrupt increase in Greenland snow accumulation at the end of the Younger Dryas event, Nature, 362(6420), 527–529, doi:10.1038/362527a0, 1993.

Andersen, K., Svensson, A., Johnsen, S., Rasmussen, S., Bigler, M., Röthlisberger, R., Ruth, U., Siggaard-Andersen, M.-L., Steffensen, J., Dahl-Jensen, D., Vinther, B. and Clausen, H.: The Greenland Ice Core Chronology 2005, 15–42ka. Part 1: constructing the time scale, Quat. Sci. Rev., 25(23–24), 3246–3257, doi:10.1016/j.quascirev.2006.08.002, 2006.

Arblaster, J. M., Meehl, G. A. and Karoly, D. J.: Future climate change in the Southern Hemisphere: Competing effects of ozone and greenhouse gases, Geophys. Res. Lett., 38(L02701), 1–6, doi:10.1029/2010GL045384, 2011.

Arienzo, M. M., McConnell, J. R., Chellman, N., Criscitiello, A. S., Curran, M., Fritzsche, D., Kipfstuhl, S., Mulvaney, R., Nolan, M., Opel, T., Sigl, M. and Steffensen, J. P.: A Method for Continuous 239Pu Determinations in Arctic and Antarctic Ice Cores, Environ. Sci. Technol., 50, 7066–7073, doi:10.1021/acs.est.6b01108, 2016.

Bauer, S. E., Bausch, A., Nazarenko, L., Tsigaridis, K., Xu, B., Edwards, R., Bisiaux, M. and McConnell, J.: Historical and future black carbon deposition on the three ice caps: Ice core measurements and model simulations from 1850 to 2100, J. Geophys. Res. Atmos., 118(14), 7948–7961, doi:10.1002/jgrd.50612, 2013.

Bender, M. L., Sowers, T., Barnola, J. M. and Chappellaz, J.: Changes in the O2/N2 ratio of the atmosphere during recent decades reflected in the composition of air in the firn at Vostok Station, Antarctica, Geophys. Res. Lett., 21(3), 189–192, doi:10.1029/93GL03548, 1994.

Bentley, C. R. and Giovinetto, M. B.: Ice-flow studies on the ice dome of Roosevelt Island, Antarctica, Trans. Am. Geophys. Union, 43(3), 369–372, doi:10.1029/TR043i003p00345, 1962.

Bertler, N. A. N., Conway, H., Dahl-Jensen, D., Emanuelsson, D. B., Winstrup, M., Vallelonga, P. T., Lee, J. E., Brook, E. J., Severinghaus, J. P., Fudge, T. J., Keller, E., Baisden, W. T., Hindmarsh, R. C. A., Neff, P. D., Blunier, T., Edwards, R., Mayewski, P. A., Kipfstuhl, S., Buizert, C., Canessa, S., Dadic, R., Kjær, H. A., Kurbatov, A. V., Zhang, D., Waddington, E. D., Baccolo, G., Beers, T., Brightley, H. J., Carter, L., Clemens-Sewall, D., Ciobanu, V. G., Delmonte, B., Eling, L., Ellis, A. A., Ganesh, S., Colledge, N., Haines, S. A., Handley, M., Hawley, R. L., Hogan, C. M., Johnson, K. M., Korotkikh, E., Lowry, D. P., Mandeno, D., McKay, R. M., Menking, J. A., Naish, T. R., Noerling, C., Ollive, A., Orsi, A., Proemse, B. C., Pyne, A. R., Pyne, R. L., Renwick, J., Scherer, R. P., Semper, S., Simonsen, M., Sneed, S. B., Steig, E. J., Tuohy, A., Ulayottil Venugopal, A., Valero-Delgado, F., Venkatesh, J., Wang, F., Wang, S., Winski, D. A., Winton, V. H. L., Whiteford, A., Xiao, C., Yang, J. and Zhang, X.: The Ross Dipole - temperature, snow accumulation, and sea ice variability in the Ross Sea Region, Antarctica, over the past 2700 years, Clim. Past, 14, 193–214, doi:10.5194/cp-14-193-2018, 2018.

Bigler, M., Svensson, A., Kettner, E., Vallelonga, P., Nielsen, M. E. and Steffensen, J. P.: Optimization of high-resolution continuous flow analysis for transient climate signals in ice cores, Environ. Sci. Technol., 45(10), 4483–4489, doi:10.1021/es200118j, 2011.

Bisiaux, M. M., Edwards, R., McConnell, J. R., Curran, M. A. J., Van Ommen, T. D., Smith, A. M., Neumann, T. A., Pasteris, D. R., Penner, J. E. and Taylor, K.: Changes in black carbon deposition to Antarctica from two high-resolution ice core records, 1850-2000 AD, Atmos. Chem. Phys., 12(9), 4107–4115, doi:10.5194/acp-12-4107-2012, 2012.

Blunier, T.: Timing of Millennial-Scale Climate Change in Antarctica and Greenland During the Last Glacial Period, Science, 291(5501), 109–112, doi:10.1126/science.291.5501.109, 2001.

Blunier, T., Chappellaz, J., Schwander, J., Dällenbach, A., Stauffer, B., Stocker, T. F., Raynaud, D., Jouzel, J., Clausen, H. B., Hammer, C. U. and Johnsen, S. J.: Asynchrony of Antarctic and Greenland climate change during the last glacial period, Nature, 394, 739–743, doi:10.1038/29447, 1998.

Buizert, C., Cuffey, K. M., Severinghaus, J. P., Baggenstos, D., Fudge, T. J., Steig, E. J., Markle, B. R., Winstrup, M., Rhodes, R. H., Brook, E. J., Sowers, T. a., Clow, G. D., Cheng, H., Edwards, R. L., Sigl, M., McConnell, J. R. and Taylor, K. C.: The WAIS Divide deep ice core WD2014 chronology - Part 1: Methane synchronization (68–31 ka BP) and the gas age–ice age difference, Clim. Past, 11, 153–173, doi:10.5194/cp-11-153-2015, 2015.

Burgener, L., Rupper, S., Koenig, L., Forster, R., Christensen, W. F., Williams, J., Koutnik, M., Miège, C., Steig, E. J., Tingey, D., Keeler, D. and Riley, L.: An observed negative trend in

West Antarctic accumulation rates from 1975 to 2010: Evidence from new observed and simulated records, J. Geophys. Res. Atmos., 118(10), 4205–4216, doi:10.1002/jgrd.50362, 2013.

Clapp, J. L.: Summary and Discussion of Survey Control for Ice Flow Studies on Roosevelt Island, Antarctica, Univ. Wisconsin Res. Rep., 65(1), 1965.

Clausen, H. B., Dansgaard, W., Nielsen, J. O. and Clough, J. W.: Surface accumulation on Ross Ice Shelf, Antarct. J. United States, 14(5), 68–74, 1979.

Clem, K. R. and Fogt, R. L.: Varying roles of ENSO and SAM on the Antarctic Peninsula climate in austral spring, J. Geophys. Res. Atmos., 118, 11481–11492, doi:10.1002/jgrd.50860, 2013.

Comiso, J. C. and Nishio, F.: Trends in the sea ice cover using enhanced and compatible AMSR-E, SSM/I, and SMMR data, J. Geophys. Res. Ocean., 113(C02S07), 1–22, doi:10.1029/2007JC004257, 2008.

Conway, H., Hall, B., Denton, G., Gades, A. and Waddington, E.: Past and future grounding-line retreat of the West Antarctic ice sheet, Science, 286(280), 280–283, doi:10.1126/science.286.5438.280, 1999.

Curran, M. A. J., van Ommen, T. D. and Morgan, V.: Seasonal characteristics of the major ions in the high-accumulation Dome Summit South ice core, Law Dome, Antarctica, Ann. Glaciol., 27, 385–390, doi:10.3189/1998AoG27-1-385-390, 1998.

Dahl-Jensen, D., Johnsen, S., Hammer, C., Clausen, H. and Jouzel, J.: Past accumulation rates derived from observed annual layers in the GRIP ice core from Summit, Central Greenland, in NATO ASI Series, vol. I12, edited by W. R. Peltier, pp. 517–532, Springer-Verlag Berlin Heidelberg, doi: 10.1007/978-3-642-85016-5, 1993.

Dansgaard, W.: Stable isotopes in precipitation, Tellus, 16(4), 436–468, doi:10.3402/tellusa.v16i4.8993, 1964.

Dee, D. P., Uppala, S. M., Simmons, A. J., Berrisford, P., Poli, P., Kobayashi, S., Andrae, U., Balmaseda, M. A., Balsamo, G., Bauer, P., Bechtold, P., Beljaars, A. C. M., van de Berg, L., Bidlot, J., Bormann, N., Delsol, C., Dragani, R., Fuentes, M., Geer, A. J., Haimberger, L., Healy, S. B., Hersbach, H., Hólm, E. V., Isaksen, L., Kållberg, P., Köhler, M., Matricardi, M., Mcnally, A. P., Monge-Sanz, B. M., Morcrette, J. J., Park, B. K., Peubey, C., de Rosnay, P., Tavolato, C., Thépaut, J. N. and Vitart, F.: The ERA-Interim reanalysis: Configuration and performance of the data assimilation system, Q. J. R. Meteorol. Soc., 137(656), 553–597, doi:10.1002/qj.828, 2011.

Dunbar, N. W., Kurbatov, A. V., Koffman, B. G. and Kreutz, K. J.: Tephra Record of Local and Distal Volcanism in the WAIS Divide Ice Core, in WAIS Divide Science Meeting September 30th-October 1st, La Jolla, CA, USA. [online] Available from: https://geoinfo.nmt.edu/staff/dunbar/publications/abstracts/dakk2010.html, 2010.

Emanuelsson, B. D., Baisden, W. T., Bertler, N. A. N., Keller, E. D. and Gkinis, V.: High-resolution continuous-flow analysis setup for water isotopic measurement from ice cores using laser spectroscopy, Atmos. Meas. Tech., 8(7), 2869–2883, doi:10.5194/amt-8-2869-2015, 2015.

Emanuelsson, B. D., Bertler, N. A. N., Neff, P. D., Renwick, J. A., Markle, B. R., Baisden, W. T. and Keller, E. D.: The role of Amundsen–Bellingshausen Sea anticyclonic circulation in

forcing marine air intrusions into West Antarctica, Clim. Dyn., 1–18, doi:10.1007/s00382-018-4097-3, 2018.

EPICA Community Members: One-to-one coupling of glacial climate variability in Greenland and Antarctica., Nature, 444, 195–198, doi:10.1038/nature05301, 2006.

Frezzotti, M., Urbini, S., Proposito, M., Scarchilli, C. and Gandolfi, S.: Spatial and temporal variability of surface mass balance near Talos Dome, East Antarctica, J. Geophys. Res. Earth Surf., 112(2), doi:10.1029/2006JF000638, 2007.

Frieß, U., Deutschmann, T., Gilfedder, B., Weller, R. and Platt, U.: Iodine monoxide in the Antarctic snowpack, Atmos. Chem. Phys., 2439–2456, doi:10.5194/acp-10-2439-2010, 2010.

Fudge, T. J., Markle, B. R., Cuffey, K. M., Buizert, C., Taylor, K. C., Steig, E. J., Waddington, E. D., Conway, H. and Koutnik, M.: Variable relationship between accumulation and temperature in West Antarctica for the past 31,000 years, Geophys. Res. Lett., 3795–3803, doi:10.1002/2016GL068356, 2016.

Gabrieli, J., Cozzi, G., Vallelonga, P., Schwikowski, M., Sigl, M., Eickenberg, J., Wacker, L., Boutron, C., Gäggeler, H., Cescon, P. and Barbante, C.: Contamination of Alpine snow and ice at Colle Gnifetti, Swiss/Italian Alps, from nuclear weapons tests, Atmos. Environ., 45(3), 587–593, doi:10.1016/j.atmosenv.2010.10.039, 2011.

Hammer, C.: Acidity of polar ice cores in relation to absolute dating, past volcanism, and radio-echoes, J. Glaciol., 25, 359–372, doi:10.3189/S0022143000015227, 1980.

Hammer, C. ., Clausen, H. B., Dansgaard, W., Gundestrup, N., Johnsen, S. and Reeh, N.: Dating of Greenland ice cores by flow models, isotopes, volcanic debris, and continental dust, J. Glaciol., 20(82), 3–26, doi:10.3189/S0022143000021183, 1978.

Haran, T., Bohlander, J., Scambos, T., Painter, T. and Fahnestock, M.: MODIS Mosaic of Antarctica 2003-2004 (MOA2004) Image Map, National Snow and Ice Data Center, Boulder, Colorado, USA, 2013.

Herron, M. M. and Langway, C. C.: Dating of Ross Ice Shelf Cores by Chemical Analysis, J. Glaciol., 24(90), 345–356, doi:10.3189/S0022143000014866, 1979.

Herron, M. M. and Langway, C. C.: Firn densification: an empirical model, J. Glaciol., 25(93), 373–385, doi:10.3189/S0022143000015239, 1980.

Hosking, J. S., Orr, A., Marshall, G. J., Turner, J. and Phillips, T.: The influence of the amundsen-bellingshausen seas low on the climate of West Antarctica and its representation in coupled climate model simulations, J. Clim., 26(17), 6633–6648, doi:10.1175/JCLI-D-12-00813.1, 2013.

Jiracek, G. R.: Radio sounding of Antarctic ice, Univ. Wisconsin Res. Rep., 67(1), 1967.

Jones, J. M., Gille, S. ., Goosse, H., Abram, N. J., Canziani, P., Charman, D., Clem, K., Crosta, X., Lavergne, C. de, Eisenman, G., England, M. H., Fogt, R., Frankcombe, L. M., Marshall, G., Masson-delmotte, V., Morrison, A. K., Orsi, A., Raphael, M. N., Renwick, J. A., Schneider, D. P., Simpkins, G. R., Steig, E. J., Stenni, B., Swingedouw, D. and Vance, T. R.: Assessing recent trends in high-latitude Southern Hemisphere surface climate, Nat. Clim. Chang., 6, 917–926, doi:10.1038/nclimate3103, 2016.

Kalteyer, D. A.: Tephra in Antarctic Ice Cores, Master Thesis, University of Maine, 2015.

Kaspari, S., Mayewski, P. A., Dixon, D. A., Spikes, V. B., Sneed, S. B., Handley, M. J. and Hamilton, G. S.: Climate variability in West Antarctica derived from annual accumulation-rate records from ITASE firn/ice cores, Ann. Glaciol., 39, 585–594, doi:10.3189/172756404781814447, 2004.

Keller, E. D., Baisden, W. T., Bertler, N. A. N., Emanuelsson, B. D., Canessa, S. and Phillips, A.: Calculating uncertainty for the RICE ice core continuous flow analysis water isotope record, Atmos. Meas. Tech. Discuss., 2018, 1–20, doi:10.5194/amt-2017-387, 2018.

Kingslake, J., Hindmarsh, R. C. A., Adalgeirsdottir, G., Conway, H., Pritchard, H. D., Corr, H. F. J., Gillet-Chaulet, F., Martin, C., King, E. C., Mulvaney, R. and Pritchard, H. D.: Full-depth englacial vertical ice sheet velocities measured using phase-sensitive radar, J. Geophys. Res. Earth Surf., 119, 2604–1618, doi:10.1002/2014JF003275, 2014.

Kjær, H. A., Vallelonga, P., Svensson, A., Elleskov Kristensen, M. L., Tibuleac, C., Winstrup, M. and Kipfstuhl, S.: An Optical Dye Method for Continuous Determination of Acidity in Ice Cores, Environ. Sci. Technol., 50(19), 10485–10493, doi:10.1021/acs.est.6b00026, 2016.

Kurbatov, A. V., Kalteyer, D. A., Dunbar, N. W., Yates, M. G., Iverson, N. A. and Bertler, N. A.: Major element analyses of visible tephra layers in the Roosevelt Island Climate Evolution Project ice core (Antarctica), Interdiscip. Earth Data Alliance, doi:10.1594/IEDA/100554, 2015.

Kushner, P. J., Held, I. M. and Delworth, T. L.: Southern Hemisphere Atmospheric Circulation Response to Global Warming, J. Clim., 14(10), 2238–2249, doi:10.1175/1520-0442(2001)014<0001:SHACRT>2.0.CO;2, 2001.

Kuttel, M., Steig, E. J., Ding, Q., Monaghan, A. J. and Battisti, D. S.: Seasonal climate information preserved in West Antarctic ice core water isotopes : relationships to temperature, large-scale circulation, and sea ice, Clim. Dyn., 39, 1841–1857, doi:10.1007/s00382-012-1460-7, 2012.

Lamarque, J. F., Bond, T. C., Eyring, V., Granier, C., Heil, A., Klimont, Z., Lee, D., Liousse, C., Mieville, A., Owen, B., Schultz, M. G., Shindell, D., Smith, S. J., Stehfest, E., Van Aardenne, J., Cooper, O. R., Kainuma, M., Mahowald, N., McConnell, J. R., Naik, V., Riahi, K. and Van Vuuren, D. P.: Historical (1850-2000) gridded anthropogenic and biomass burning emissions of reactive gases and aerosols: Methodology and application, Atmos. Chem. Phys., 10(15), 7017–7039, doi:10.5194/acp-10-7017-2010, 2010.

Langway, C. C., Herron, M. and Cragin, J. H.: Chemical Profile of the Ross Ice Shelf at Little America V, Antarctica, J. Glaciol., 13(69), 431–435, doi:10.3189/S0022143000023200, 1974.

Lee, J., Brook, E. J., Bertler, N. A. N., Buizert, C., Baisden, W. T., Blunier, T., Ciobanu, G., Conway, H., Dahl-Jensen, D., Fudge, T. J., Hindmarsh, R. C. A., Keller, E. D., Parrenin, F., Severinghaus, J. P., Vallelonga, P., Waddington, E. D. and Winstrup, M.: A 83,000 year old ice core from Roosevelt Island, Ross Sea, Antarctica, Clim. Past Discuss., 1–44, doi:10.5194/cp-2018-68, 2018.

Legrand, M., Feniet-Saigne, C., Saltzman, E. S., Germain, C., Barkov, N. I. and Petrov, V. N.: Ice-core record of oceanic emissions of dimethylsulphide during the last climate cycle, Nature, 350(6314), 144–146, doi:10.1038/350144a0, 1991.

Lliboutry, L. A.: A critical review of analytical approximate solutions for steady state velocities and temperatures in cold ice sheets, Gletscherkd. Glazialgeol, 15(2), 135–148, 1979.

Marshall, G. J.: Trends in the Southern Annular Mode from Observations and Reanalyses, J. Clim., 16(24), 4134–4143, doi:10.1175/1520-0442(2003)016<4134:TITSAM>2.0.CO;2, 2003.

Martín, C., Hindmarsh, R. C. A. and Navarro, F. J.: Dating ice flow change near the flow divide at Roosevelt Island, Antarctica, by using a thermomechanical model to predict radar stratigraphy, J. Geophys. Res. Earth Surf., 111(1), 1–15, doi:10.1029/2005JF000326, 2006.

McConnell, J. R., Edwards, R., Kok, G. L., Flanner, M. G. and Zender, C. S.: 20th-Century industrial black carbon emissions altered Arctic climate forcing, Science, 317(5843), 1381–1384, doi:10.1126/science.1144856, 2007.

Mitchell, L. E., Brook, E. J., Sowers, T., McConnell, J. R. and Taylor, K.: Multidecadal variability of atmospheric methane, 1000-1800 C.E., J. Geophys. Res. Biogeosciences, 116(2), 1–16, doi:10.1029/2010JG001441, 2011.

Mitchell, L. E., Brook, E. J., Lee, J. E., Buizert, C. and Sowers, T.: Constraints on the Late Holocene Anthropogenic Contribution to the Atmospheric Methane Budget, Science, 342(6161), 964–966, doi:10.1126/science.1238920, 2013.

Mudelsee, M.: Ramp function regression: A tool for quantifying climate transitions, Computers, 26, 293–307, doi:10.1140/epjst/e2009-01089-3, 2000.

Mudelsee, M.: Break function regression, Eur. Phys. J. Spec. Top., 174(1), 49–63, doi:10.1140/epjst/e2009-01089-3, 2009.

Muscheler, R., Adolphi, F. and Knudsen, M. F.: Assessing the differences between the IntCal and Greenland ice-core time scales for the last 14,000 years via the common cosmogenic radionuclide variations, Quat. Sci. Rev., 106, 81–87, doi:10.1016/j.quascirev.2014.08.017, 2014.

Narcisi, B., Proposito, M. and Frezzotti, M.: Ice record of a 13th century explosive volcanic eruption in northern Victoria Land, East Antarctica, Antarct. Sci., 13(2), 174–181, doi:10.1017/S0954102001000268, 2001.

Narcisi, B., Petit, J. R., Delmonte, B., Scarchilli, C. and Stenni, B.: A 16,000-yr tephra framework for the Antarctic ice sheet: A contribution from the new Talos Dome core, Quat. Sci. Rev., 49, 52–63, doi:10.1016/j.quascirev.2012.06.011, 2012.

Noone, D. and Simmons, I.: Sea ice control of water isotope transport to Antarctica and implications for ice core interpretation, J. Geophys. Res., 109, 1–13, doi:10.1029/2003JD004228, 2004.

Nye, J. F.: Correction Factor for Accumulation Measured by the Thickness of the Annual Layers in an Ice Sheet, J. Glaciol., 4(36), 785–788, doi:10.3189/S0022143000028367, 1963.

Philippe, M., Tison, J. L., Fjøsne, K., Hubbard, B., Kjær, H. A., Lenaerts, J. T. M., Drews, R., Sheldon, S. G., De Bondt, K., Claeys, P. and Pattyn, F.: Ice core evidence for a 20th century increase in surface mass balance in coastal Dronning Maud Land, East Antarctica, Cryosph., 10(5), 2501–2516, doi:10.5194/tc-10-2501-2016, 2016.

Rabiner, L. R.: A Tutorial on Hidden Markov Models and Selected Applications in Speech Recognition, Proc. IEEE, 77(2), 257–286, doi:10.1109/5.18626, 1989.

Raisbeck, G. M., Cauquoin, A., Jouzel, J., Landais, A., Petit, J.-R., Lipenkov, V. Y., Beer, J., Synal, H.-A., Oerter, H., Johnsen, S. J., Steffensen, J. P., Svensson, A. and Yiou, F.: An

improved north–south synchronization of ice core records around the 41 kyr 10Be peak, Clim. Past, 13(3), 217–229, doi:10.5194/cp-13-217-2017, 2017.

Raphael, M. N., Marshall, G. J., Turner, J., Fogt, R. L., Schneider, D., Dixon, D. A., Hosking, J. S., Jones, J. M. and Hobbs, W. R.: The Amundsen sea low: Variability, change, and impact on Antarctic climate, Bull. Am. Meteorol. Soc., 97(1), 111–121, doi:10.1175/BAMS-D-14-00018.1, 2016.

Rasmussen, S. O., Andersen, K. K., Svensson, A. M., Steffensen, J. P., Vinther, B. M., Clausen, H. B., Siggaard-Andersen, M. L., Johnsen, S. J., Larsen, L. B., Dahl-Jensen, D., Bigler, M., Röthlisberger, R., Fischer, H., Goto-Azuma, K., Hansson, M. E. and Ruth, U.: A new Greenland ice core chronology for the last glacial termination, J. Geophys. Res. Atmos., 111(6), doi:10.1029/2005JD006079, 2006.

Raymond, C. F.: Deformation in the Vicinity of Ice Divides, J. Glaciol., 29(103), 357–373, doi:10.3189/S0022143000030288, 1983.

Schultz, M. G., Heil, A., Hoelzemann, J. J., Spessa, A., Thonicke, K., Goldammer, J. G., Held, A. C., Pereira, J. M. C. and van Het Bolscher, M.: Global wildland fire emissions from 1960 to 2000, Global Biogeochem. Cycles, 22(2), 1–17, doi:10.1029/2007GB003031, 2008.

Schwander, J. and Stauffer, B.: Age difference between polar ice and the air trapped in its bubbles, Nature, 311, 45–47, doi:10.1038/311045a0, 1984.

Shepherd, A., Ivins, E. R., A, G., Barletta, V. R., Bentley, M. J., Bettadpur, S., Briggs, K. H., Bromwich, D. H., Forsberg, R., Galin, N., Horwath, M., Jacobs, S., Joughin, I., King, M. A., Lenaerts, J. T., Li, J., Ligtenberg, S. R. M., Luckman, A., McMillan, M., Meister, R., Milne, G., Mouginot, J., Muir, A., Nicolas, J., Paden, J., Payne, A. J., Pritchard, H. D., Rignot, E., Rott, H., Sørensen, L. S., Scambos, T. A., Scheuchl, B., Schrama, E. J. O., Smith, B., Sundal, A. V, Angelen, J. H. van, Berg, W. J. van der, Broeke, M. R. van der, Vaughan, D. G., Velicogna, I., Wahr, J., Whitehouse, P. L., Wingham, D. J., Yi, D., Young, D. and Zwally, H. J.: A Reconciled Estimate of Ice-Sheet Mass Balance, Science, 338, 1183–1190, doi:10.1126/science.1228102, 2012.

Sigl, M., McConnell, J. R., Layman, L., Maselli, O., McGwire, K., Pasteris, D., Dahl-Jensen, D., Steffensen, J. P., Vinther, B., Edwards, R., Mulvaney, R. and Kipfstuhl, S.: A new bipolar ice core record of volcanism from WAIS Divide and NEEM and implications for climate forcing of the last 2000 years, J. Geophys. Res. Atmos., 118(3), 1151–1169, doi:10.1029/2012JD018603, 2013.

Sigl, M., Winstrup, M., McConnell, J. R., Welten, K. C., Plunkett, G., Ludlow, F., Büntgen, U., Caffee, M., Chellman, N., Dahl-Jensen, D., Fischer, H., Kipfstuhl, S., Kostick, C., Maselli, O. J., Mekhaldi, F., Mulvaney, R., Muscheler, R., Pasteris, D. R., Pilcher, J. R., Salzer, M., Schüpbach, S., Steffensen, J. P., Vinther, B. M. and Woodruff, T. E.: Timing and climate forcing of volcanic eruptions for the past 2,500 years., Nature, 523(7562), 543–9, doi:10.1038/nature14565, 2015.

Sigl, M., Fudge, T. J., Winstrup, M., Cole-Dai, J., Ferris, D., McConnell, J. R., Taylor, K. C., Welten, K. C., Woodruff, T. E., Adolphi, F., Bisiaux, M., Brook, E. J., Buizert, C., Caffee, M. W., Dunbar, N. W., Edwards, R., Geng, L., Iverson, N., Koffman, B., Layman, L., Maselli, O. J., McGwire, K., Muscheler, R., Nishiizumi, K., Pasteris, D. R., Rhodes, R. H. and Sowers, T. A.: The WAIS Divide deep ice core WD2014 chronology - Part 2: Annual-layer counting (0-31 ka BP), Clim. Past, 12(3), 769–786, doi:10.5194/cp-12-769-2016, 2016.

Spolaor, A., Vallelonga, P., Gabrieli, J., Martma, T., Björkman, M. P., Isaksson, E., Cozzi, G., Turetta, C., Kjær, H. A., Curran, M. A. J., Moy, A. D., Schönhardt, A., Blechschmidt, A. M., Burrows, J. P., Plane, J. M. C. and Barbante, C.: Seasonality of halogen deposition in polar snow and ice, Atmos. Chem. Phys., 14(18), 9613–9622, doi:10.5194/acp-14-9613-2014, 2014.

Steig, E. J., Mayewski, P. A., Dixon, D. A., Kaspari, S. D., Frey, M. M., Schneider, D. P., Arcone, S. A., Hamilton, G. S., Spikes, V. B., Albert, M., Meese, D., Gow, A. J., Shuman, C. A., White, J. W. C., Sneed, S., Flaherty, J. and Wumkes, M.: High-resolution ice cores from US ITASE (West Antarctica): development and validation of chronologies and determination of precision and accuracy, Ann. Glaciol., 41(1), 77–84, doi:10.3189/172756405781813311, 2005.

Stenni, B., Proposito, M., Gragnani, R., Flora, O., Jouzel, J., Falourd, S. and Frezzotti, M.: Eight centuries of volcanic signal and climate change at Talos Dome (East Antarctica), J. Geophys. Res., 107(D9), 1–13, doi:10.1029/2000JD000317, 2002.

Stenni, B., Curran, M. A. J., Abram, N. J., Orsi, A., Goursaud, S., Masson-Delmotte, V., Neukom, R., Goosse, H., Divine, D., van Ommen, T., Steig, E. J., Dixon, D. A., Thomas, E. R., Bertler, N. A. N., Isaksson, E., Ekaykin, A., Frezzotti, M. and Werner, M.: Antarctic climate variability at regional and continental scales over the last 2000 years, Clim. Past, 13, 1609–1634, doi:10.5194/cp-2017-40, 2017.

Stowasser, C., Buizert, C., Gkinis, V., Chappellaz, J., Schapbach, S., Bigler, M., Fan, X., Sperlich, P., Baumgartner, M., Schilt, A. and Blunier, T.: Continuous measurements of methane mixing ratios from ice cores, Atmos. Meas. Tech., 5(5), 999–1013, doi:10.5194/amt-5-999-2012, 2012.

Svensson, A., Andersen, K. K., Bigler, M., Clausen, H. B., Dahl-Jensen, D., Davies, S. M., Johnsen, S. J., Muscheler, R., Parrenin, F., Rasmussen, S. O., Rothlisberger, R., Seierstad, I., Steffensen, J. P. and Vinther, B. M.: A 60 000 year Greenland stratigraphic ice core chronology, Clim. Past, 4, 47–57, doi:10.5194/cpd-3-1235-2007, 2008.

Thomas, E. R. and Abram, N. J.: Ice core reconstruction of sea ice change in the Amundsen-Ross Seas since 1702 A.D., Geophys. Res. Lett., 43(10), 5309–5317, doi:10.1002/2016GL068130, 2016.

Thomas, E. R., Hosking, J. S., Tuckwell, R. R., Warren, R. A. and Ludlow, E. C.: Twentieth century increase in snowfall in coastal West Antarctica, Geophys. Res. Lett., 42(21), 9387–9393, doi:10.1002/2015GL065750, 2015.

Thomas, E. R., van Wessem, J. M., Roberts, J., Isaksson, E., Schlosser, E., Fudge, T., Vallelonga, P., Medley, B., Lenaerts, J., Bertler, N., van den Broeke, M. R., Dixon, D. A., Frezzotti, M., Stenni, B., Curran, M. and Ekaykin, A. A.: Regional Antarctic snow accumulation over the past 1000 years, Clim. Past, 13, 1491–1513, doi:10.5194/cp-2017-18, 2017.

Traversi, R., Becagli, S., Castellano, E., Maggi, V., Morganti, A., Severi, M. and Udisti, R.: Ultra-sensitive Flow Injection Analysis (FIA) determination of calcium in ice cores at ppt level, Anal. Chim. Acta, 594(2), 219–225, doi:10.1016/j.aca.2007.05.022, 2007.

Tuohy, A., Bertler, N., Neff, P., Edwards, R., Emanuelsson, D., Beers, T. and Mayewski, P.: Transport and deposition of heavy metals in the Ross Sea Region, Antarctica, J. Geophys. Res. Atmos., 120(20), 10996–11011, doi:10.1002/2015JD023293, 2015.

Turner, J., Comiso, J. C., Marshall, G. J., Lachlan-cope, T. A., Bracegirdle, T., Maksym, T., Meredith, M. P., Wang, Z. and Orr, A.: Non-annular atmospheric circulation change induced by stratospheric ozone depletion and its role in the recent increase of Antarctic sea ice extent, Geophys. Res. Lett., 36(L08502), 1–5, doi:10.1029/2009GL037524, 2009.

Turner, J., Hosking, J. S., Marshall, G. J., Phillips, T. and Bracegirdle, T. J.: Antarctic sea ice increase consistent with intrinsic variability of the Amundsen Sea Low, Clim. Dyn., 46(7), 2391–2402, doi:10.1007/s00382-015-2708-9, 2016.

Udisti, R., Traversi, R., Becagli, S. and Piccardi, G.: Spatial distribution and seasonal pattern of biogenic sulphur compounds in snow from northern Victoria Land, Antarctica, Ann. Glaciol., 27, 535–542, doi:10.3189/1998AoG27-1-535-542, 1998.

WAIS Divide Project Members: Precise interpolar phasing of abrupt climate change during the last ice age, Nature, 520(7549), 661–665, doi:10.1038/nature14401, 2015.

Wheatley, S. and Kurbatov, A. V.: Antarctic Ice Core Tephra Analysis, U.S. Antarct. Progr. Data Center. Dataset., doi:10.15784/601038, 2017.

Winstrup, M.: A Hidden Markov Model Approach to Infer Timescales for High-Resolution Climate Archives, in Proceedings of the 30th AAAI Conference on Artificial Intelligence and the 28th Innovative Applications of Artificial Intelligence Conference, pp. 4053–4061, AAAI Press, Palo Alto, California, February 12 – 17, 2016, Phoenix, Arizona USA., 2016.

Winstrup, M., Svensson, A. M., Rasmussen, S. O., Winther, O., Steig, E. J. and Axelrod, A. E.: An automated approach for annual layer counting in ice cores, Clim. Past, 8(6), 1881–1895, doi:10.5194/cp-8-1881-2012, 2012.

Yu, S. Z.: Hidden semi-Markov models, Artif. Intell., 174(2), 215–243, doi:10.1016/j.artint.2009.11.011, 2010.

Yuan, X. and Martinson, D. G.: Antarctic sea ice extent variability and its global connectivity, J. Clim., 13(10), 1697–1717, doi:10.1175/1520-0442(2000)013<1697:ASIEVA>2.0.CO;2, 2000.

Zreda-Gostynska, G., Kyle, P. R., Finnegan, D. and Meeker Prestbo, K.: Volcanic gas emissions from Mount Erebus and their impact on the Antarctic environment, J. Geophys. Res., 102055(10), 39–15, doi:10.1029/97JB00155, 1997.

Figures

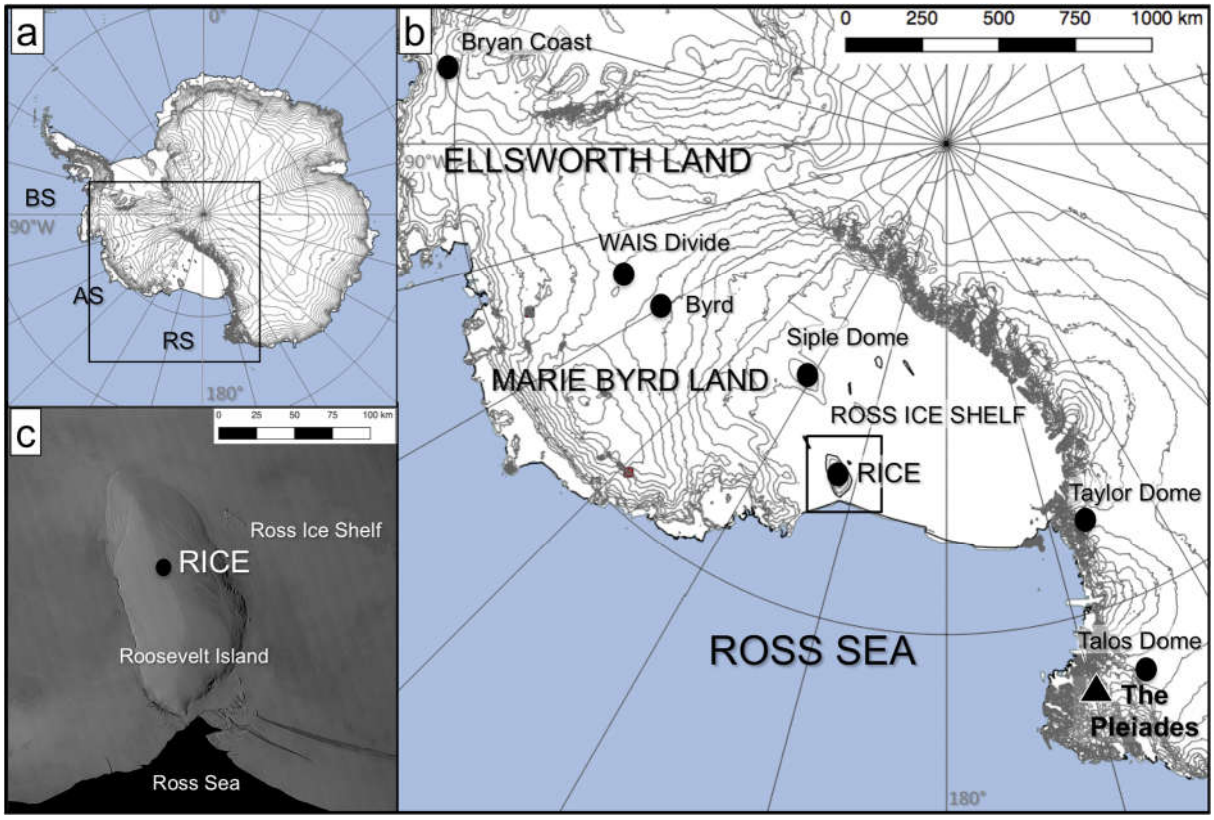

Figure 1: a, b): Roosevelt Island is located in the eastern sector of the Ross Ice Shelf embayment. Locations discussed in the text are represented by triangles (volcanoes) and circles (ice cores). RS: Ross Sea; AS: Amundsen Sea; BS: Bellingshausen Sea. **c)** MODIS image of Roosevelt Island (Haran et al. 2013), protruding as an ice dome from the surrounding Ross Ice Shelf. The RICE ice core is drilled on the ice divide of Roosevelt Island.

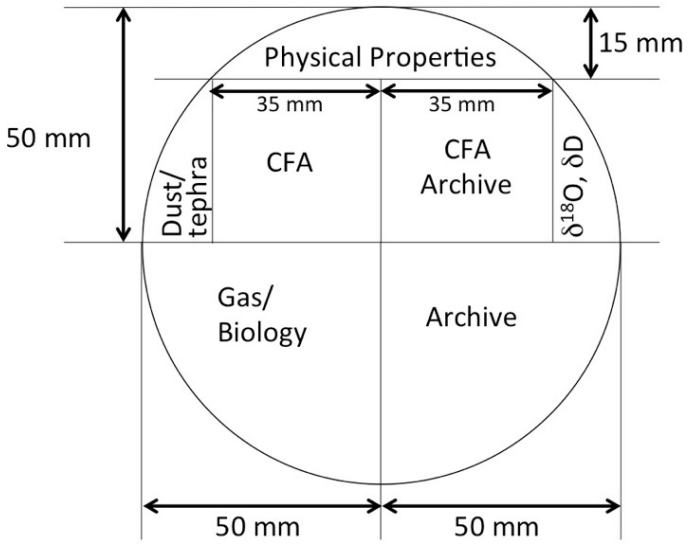

Figure 2: The RICE main core cutting plan included 2 CFA sticks of size 35x35mm.

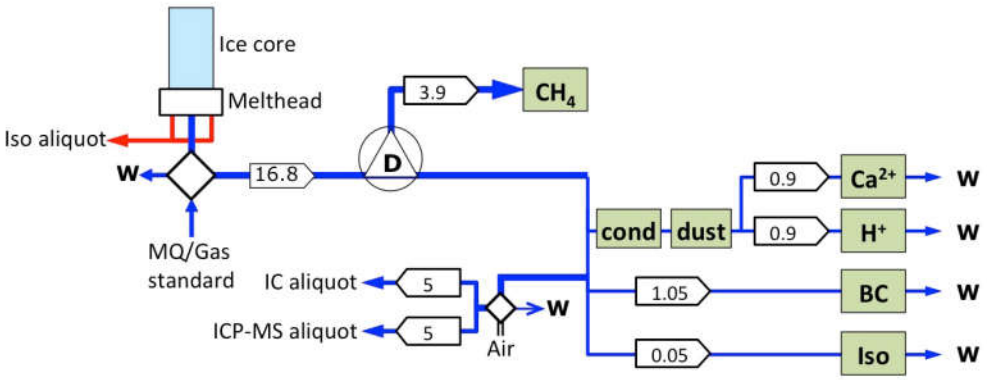

Figure 3: The RICE CFA set-up. A 1m long ice-core rod (light blue) is placed on a melt head, which separates melt water from the pristine inner part of the core from that of the more contaminated outer rim. Meltwater from the outer stream (red) is used for discrete measurements of water isotopes, while the melt water stream from the inner core section (dark blue) passes through a debubbler (D), which separates air from the melt water. The air composition is analyzed for methane concentration, while the meltwater stream is channeled to various analytical instruments for continuous impurity analysis of dust, conductivity (cond), calcium (Ca^{2+}), acidity (H^{+}), black carbon (BC), and water isotopes (Iso), as well as collected in vials for discrete aliquot sampling by IC and ICP-MS. W denotes waste water. Diamonds represent injection valves used for introduction of air or water standards when the melter system is not in use. Arrow boxes indicate liquid flow rates in mL min^{-1}. Green boxes represent analytical instruments.

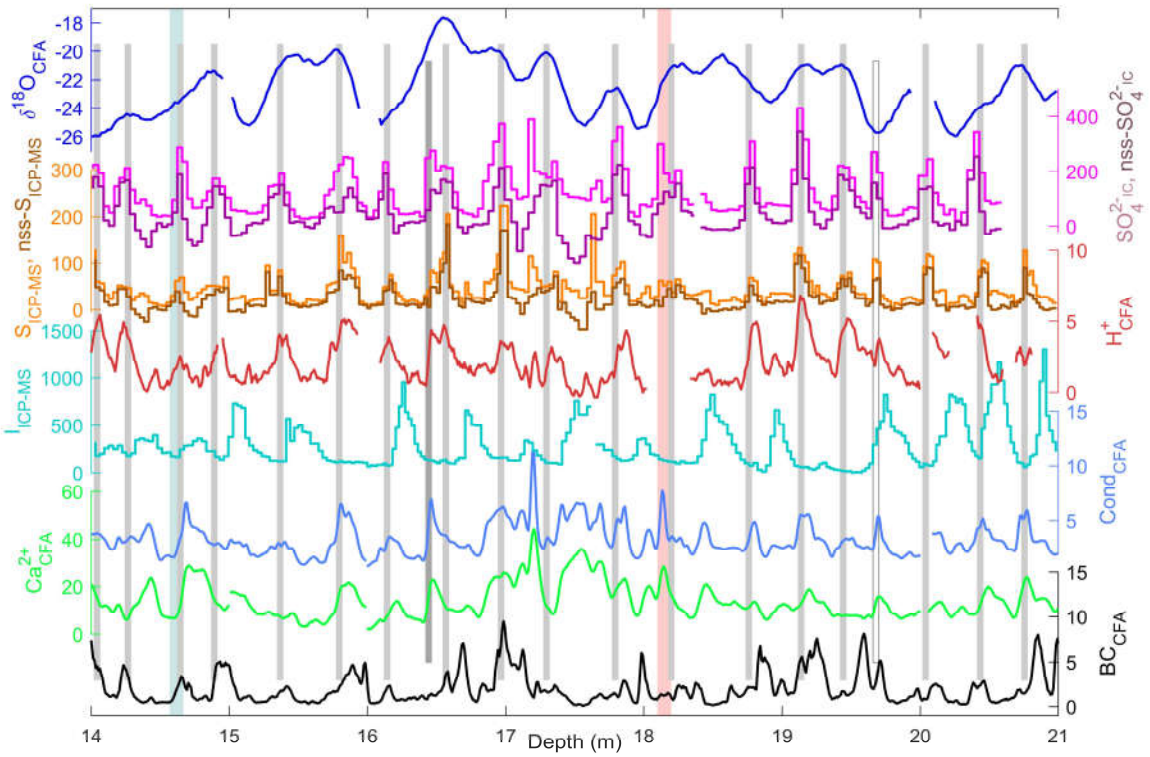

Figure 4: Assignment of annual layers in an upper section of the RICE core. All units are in ppb, except for $\delta^{18}O$ (in ‰), H^+ (in µeq L^{-1}), and conductivity (in µS cm^{-1}). The CFA chemistry records are smoothed with a 3-cm moving average filter. Two uncertain layers exist within the section: At 16.6 m, an uncertain layer is being counted as part of the timescale, in order to match the tiepoint ages corresponding to the isotope match to RID-75 (cyan bar; 14.6 m) and the Raoul tephra horizon (red bar; 18.1 m). A second uncertain layer is located at 19.7 m; the sulfate record suggest that it is an annual layer, but this is not supported by iodine and $\delta^{18}O$. This layer is not counted in the RICE17 chronology, in order to match the age of the next tie-point located at 22 m.

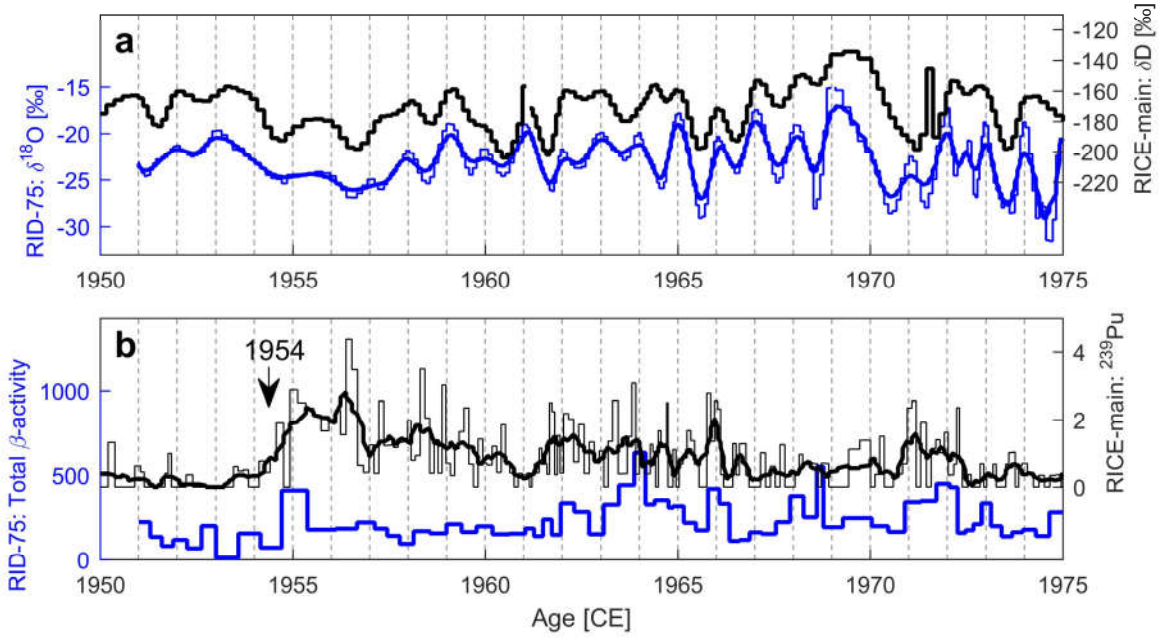

Figure 5: a) RICE water isotope profile (δD) compared to isotope data ($\delta^{18}O$) from the RID-75 core for the period 1950-1975. Diffusion causes the isotope record to smooth over time, and a smoothed version of the RID-75 isotope profile (thick blue) highlights its similarities to the RICE isotope record (black). **b)** Total specific β-activity (in disintegrations per hour, dph) for the RID-75 core compared to ^{239}Pu measurements (normalized intensities) from the RICE main core. Both cores show a sharp increase in nuclear waste deposition starting in 1954 CE, and several broader peaks hereafter.

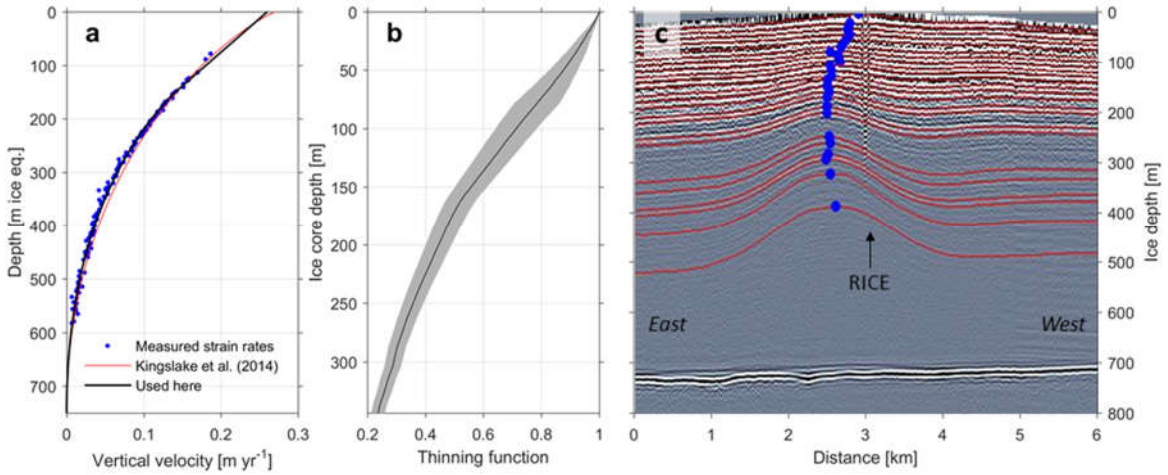

Figure 6: a) Vertical velocity measurements (Kingslake et al., 2014) and the associated fitted functions. Fit used here improves overall misfit and does not have a bias at mid-depth. **b)** Thinning function with associated uncertainties (2σ). **c)** Radar echogram (Kingslake et al.,

2014) with traced layers (red) and location of maximum amplitudes of the stack of Raymond arches (blue circles). The location of the modern topographic ice divide (and the RICE drill site) is marked by the returns from a pole west of the maximum bump amplitudes at depth, as indicated with an arrow.

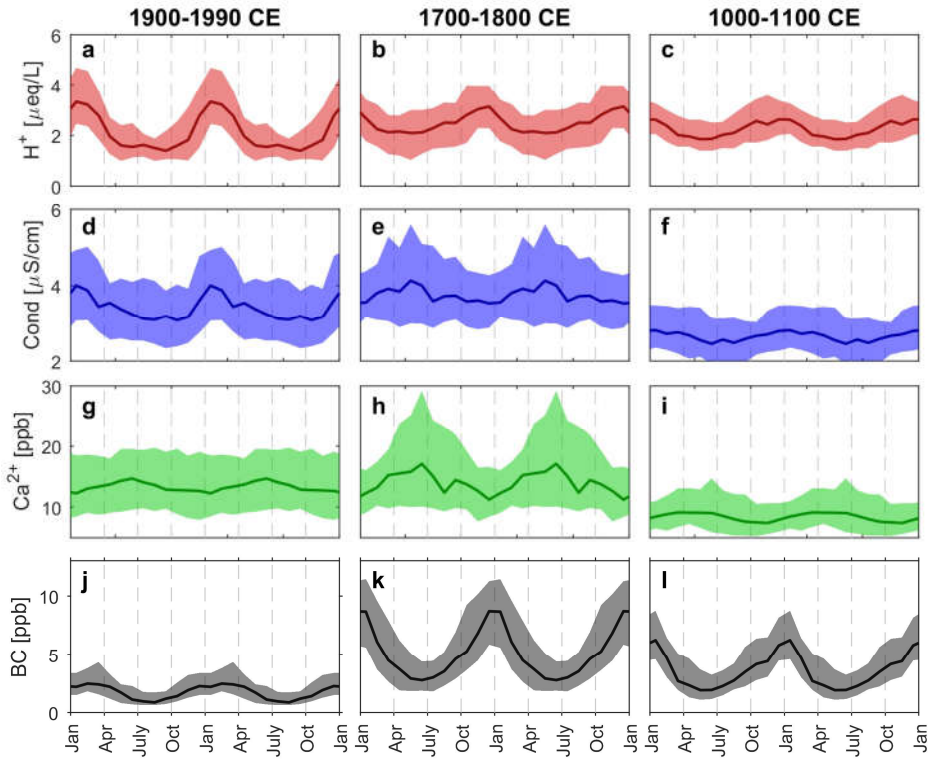

Figure 7: Average annual signals of 2 successive years in RICE **a-c)** acidity (H^+), **d-f)** conductivity (Cond), **g-i)** calcium (Ca^{2+}), and **j-l)** black carbon (BC) during three centuries, calculated under the assumption of constant snowfall through the year. The main RICE CFA data only extends to 1990CE. The line shows monthly-averaged median value of measured concentrations, and colored area signifies the 50% quantile envelope of the value distribution.

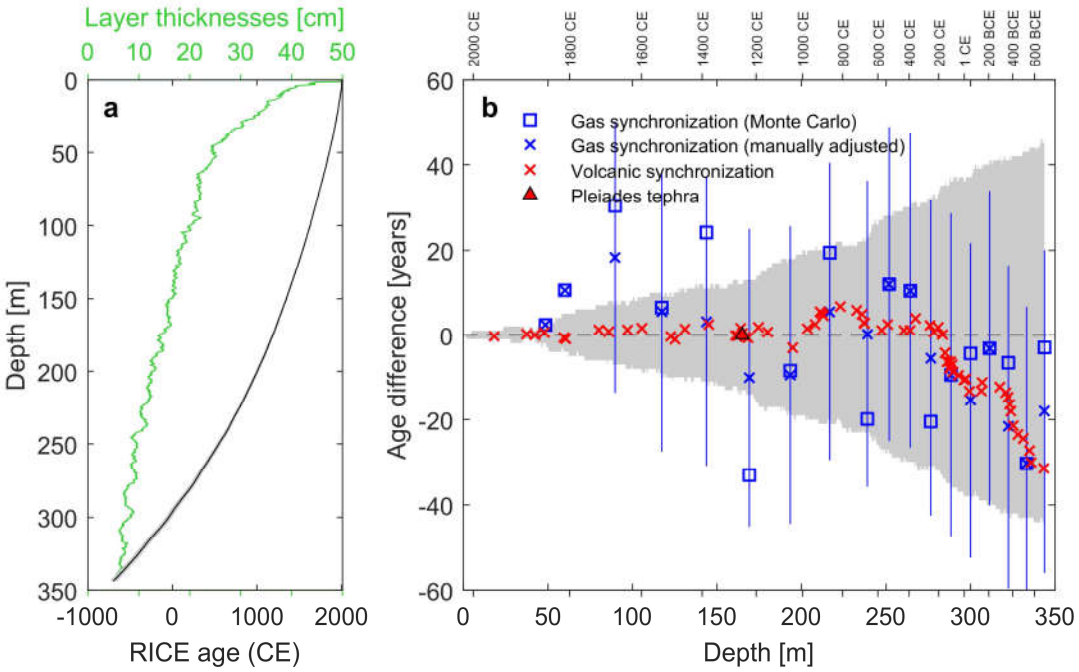

Figure 8: a) Depth evolution of RICE17 ages (black), including the associated 95% confidence interval (grey area, almost invisible due to scale), and corresponding mean layer thicknesses (50 year running mean; green). **b)** Comparison of RICE17 ages and its confidence interval (grey area) to WD2014 from volcanic (red) and gas (blue) matching to WAIS Divide. A negative age difference implies fewer layers in RICE17 than in WD2014. Blue vertical lines indicate 1σ age uncertainties on Monte Carlo methane matches. A solid red triangle indicates the Pleiades tephra layer at 165m depth.

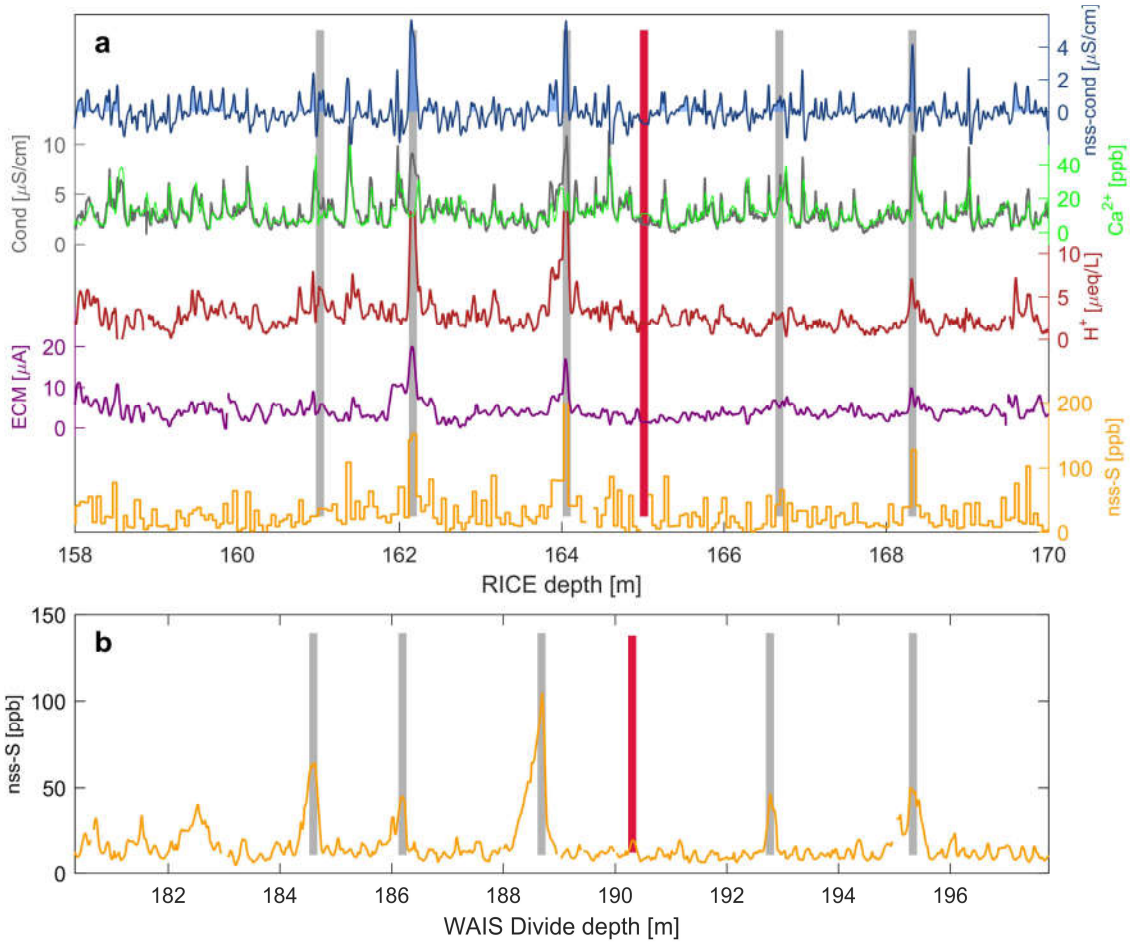

Figure 9: a) The RICE volcanic proxy records: non-sea-salt-sulfur (nss-S; orange), ECM (purple), acidity (H^+; red), and non-sea-salt conductivity (nss-cond; blue) based on the conductivity-to-calcium excess (grey, green). **b)** Matching of the RICE records to the WAIS Divide non-sea-salt sulfur record (Sigl et al., 2015). Vertical bars indicate volcanic match points (Table 2), with the red bar representing the Pleiades tephra horizon (1251 CE).

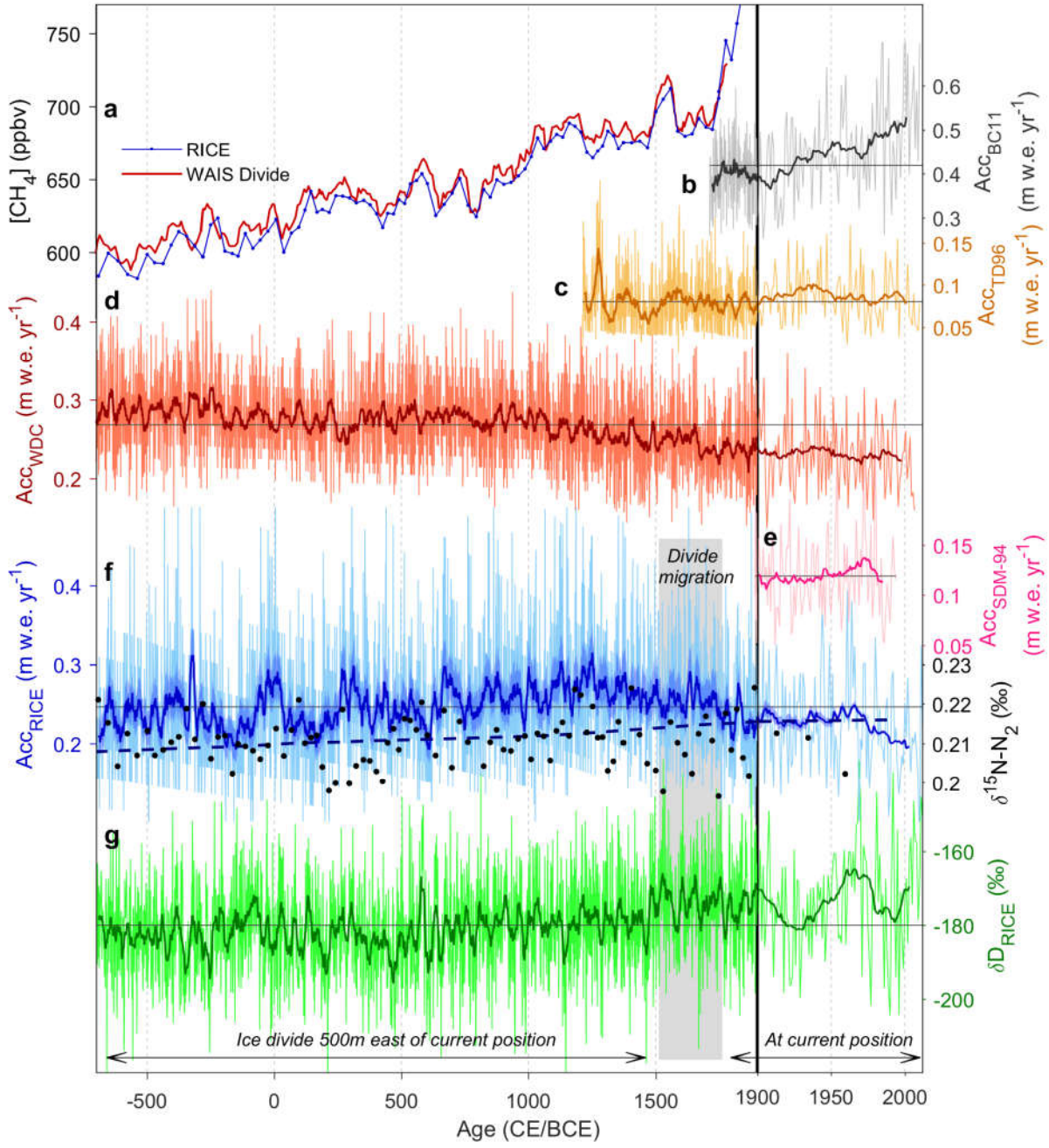

Figure 10: a) Measured methane concentrations from RICE (blue, on the RICE17 timescale) and from WAIS Divide (red, on the WD2014 timescale). **b)** Bryan Coast (BC11, grey), Ellsworth Land (Thomas et al., 2015), **c)** Talos Dome (TD96, orange), Northern Victoria Land, (Frezzotti et al., 2007; Stenni et al., 2002) (no thinning function applied, extended to 2010 CE using stakes measurements), **d)** WAIS Divide (WDC, red), Central West Antarctica (Fudge et al. 2016) (corrected for ice advection), **e)** Siple Dome (SDM-94, pink), Marie Byrd Land (Kaspari et al. 2004), and **f)** RICE (blue) accumulation histories over the past 2700 years, in annual resolution and 20-year smoothed versions (thick lines). The shaded blue area indicates the 95% confidence interval of the RICE accumulation rates. The short-lived peak in accumulation rates around 320 BCE is likely to be an artefact caused by timescale inaccuracies in this period, during which RICE17 diverges from WD2014 (Fig. 9b). Also shown are the gas-

derived accumulation rates for this time interval (f, blue dashed line), and measurements of $\delta^{15}N$ of N_2 informing on past firn column thickness (f, black dots; on the RICE gas timescale). **g)** RICE stable water isotope record (δD). Thick green line is a 20-year smoothed version of the isotope profile. Grey horizontal lines denote mean values of the respective accumulation rates and δD over the displayed period. Note that the scale changes at 1900CE (thick vertical line). The migration period of the Roosevelt Island ice divide is marked with a grey box.

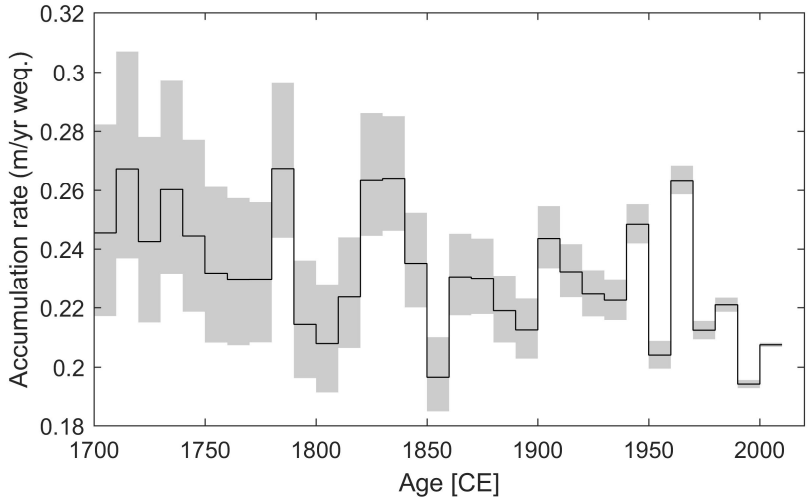

Figure 11: Decadal accumulation rates at Roosevelt Island since 1700 CE. Grey shadows indicate the 95% uncertainty bounds due to uncertainties in the thinning function.

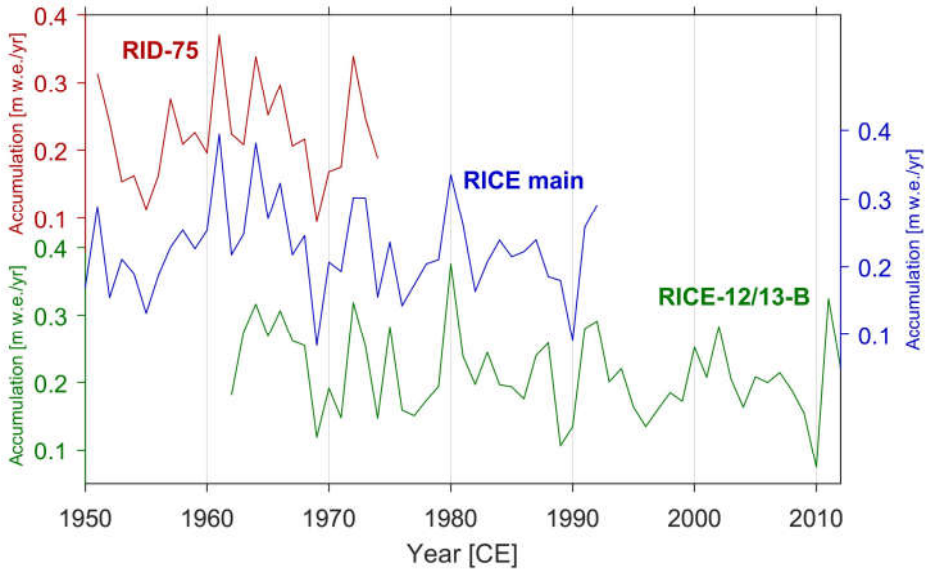

Figure 12: Accumulation reconstructions since 1950 CE for the three Roosevelt Island ice cores described in Table 1.

Tables

Ice core:	RID-75	RICE	RICE-12/13-B
Drilled	1974/75	2011/12 (0-130 m) 2012/13 (130-764.6 m)	Jan 2013
Depth	0-10.68 m	8.57-764.60 m	0-19.41 m
Location	79°22' S, 161°40' W	79°21.839' S, 161°42.387' W	79°21.726' S, 161°42.000' W
Data sets:			
β-activity	16 cm resolution (Clausen et al., 1979)	-	-
$\delta^{18}O$, δD	Only $\delta^{18}O$; 4 cm resolution (Clausen et al., 1979)	Continuous and 2 cm resolution (Bertler et al., 2018)	Continuous and 2 cm resolution (Bertler et al., 2018)
CFA	-	H^+, Ca^{2+}, conductivity, dust, BC; 8.57-344 m; continuous (this work)	H^+, Ca^{2+}, conductivity, dust, BC; continuous (this work)
ECM	-	49-344 m; continuous (this work)	-
IC	-	Na^+, Ca^{2+}, Mg^{2+}, SO_4^{2-}; 8.57-20.6 m; 4 cm resolution (pers. comm., N. Bertler)	Na^+, Ca^{2+}, Mg^{2+}, SO_4^{2-}; 4.5 cm resolution (pers. comm., N. Bertler)
ICP-MS	-	S, Na, I; 8.57-249 m; 2-7 cm resolution (pers. comm., P. Mayewski)	S, Na, I; 9.5 cm resolution (pers. comm., P. Mayewski)
	-	Pu^{239}; 8.64-40m; 4 cm resolution (pers. comm., R. Edwards)	-
CH_4 $\delta^{18}O_{atm}$	-	Discrete samples (Lee et al., 2018)	-

Table 1: The Roosevelt Island ice and firn core records used in this study.

1

Depth (m)	RICE17 age (CE)	Event	WD2014 age (CE)
0	**2013.0±0**	**Snow surface in RICE-12/13-B (Jan 2013)**	-
14.62	**1975.1±1**	**Isotope match to RID-75 snow surface (winter 74/75)**	-
16.18	1970.9±1	Radioactivity peak (winter 1970/71[1])	-
18.10-18.20★	**(1965.0-1965.2) ±1**	**Tephra likely from Raoul Island, New Zealand (Nov 1964)**	**(1964.7-1964.9) ±1**
21.98	**1954.7±1**	**Onset of high radioactivity levels from Castle Bravo, Marshall Islands (March 1954)**	-
37.45	**1903.8±1**	**Santa Maria, Guatemala (Oct 1902)**	**1904.0±1**
42.34	**1885.0±1**	**Krakatau, Indonesia (Aug 1883), bipolar**	**1885.0±1**
47.90	1863.3±2	Makian, Indonesia (Dec 1861), bipolar	1863.9±1
59.46[#]	1817.0±4	Tambora, Indonesia (April 1815), bipolar	1816.4±0
60.56[†]	1811.8±4	Unknown, bipolar	1810.9±1
80.09[#]	1722.3±6	Unknown	1723.5±1[*]
85.99	1695.0±6	Unknown, bipolar	1695.8±1
97.12	1641.2±7	Parker Peak, Philippines (Jan 1641), bipolar	1642.4±1
105.58[#]	1599.3±8	Huaynaputina, Peru (Feb 1600), bipolar	1600.9±1
122.67	1507.0±10	Unknown	1506.7±2
125.19	1493.4±10	Unknown	1492.4±2[*]
131.04	1458.4±10	Kuwae, Vanuatu, bipolar	1459.8±2
145.15	1376.2±11	Unknown	1378.7±2
161.02	1277.3±12	Unknown	1277.2±2
162.17	*1269.9±13*	*Unknown*	1269.7±2
164.06	*1257.3±13*	*Samalas, Indonesia, bipolar*	1258.9±1
165.01-165.02★	**1251.5±13**	**Tephra from the Pleiades, West Antarctica**	**1251.6±2**
166.68	1242.3±13	Unknown	1241.9±2
168.32	1231.4±13	Unknown, bipolar	1230.7±2
174.50	1190.1±14	Unknown, bipolar	1191.9±2
180.01	1152.3±16	Unknown	1153.0±2
194.81	1043.3±18	Unknown	1040.3±2
203.44	974.5±19	Unknown, bipolar	976.0±2
208.11	937.1±20	Unknown	939.6±2[*]

211.02	912.6±20	Unknown, bipolar	918.1±2
212.03[x]	903.9±20	Unknown	909.0±2[*]
212.88[x]	896.3±20	Unknown, bipolar	900.9±2
222.94	813.2±20	Unknown, bipolar	819.9±2
232.66	720.3±21	Unknown	726.1±2
235.78	693.1±22	Unknown, bipolar	698.0±2
236.94	683.0±22	Unknown, bipolar	685.9±2
237.25	680.1±22	Unknown, bipolar	682.9±2
247.49	575.1±27	Unknown, bipolar	576.2±2
250.93	539.2±27	Unknown, bipolar	541.7±3
260.59	434.3±29	Unknown, bipolar	435.4±3
264.19	394.4±30	Unknown, bipolar	395.5±3
267.41	356.9±30	Unknown, bipolar	360.8±3
276.06	*264.3±31*	*Unknown, bipolar*	266.6±3
278.41	236.4±31	Taupo (New Zealand), bipolar	237.1±3
280.82	205.3±32	Unknown	207.1±3
283.36[†]	170.9±33	Unknown, bipolar	171.0±3
284.97	148.1±34	Unknown	143.9±3
286.17	131.6±35	Unknown	125.3±4
286.40	128.1±35	Unknown	121.9±4
287.49	113.4±35	Unknown	105.5±4
288.11	105.2±35	Unknown	97.8±4[*]
288.35	102.3±35	Unknown	96.0±4
289.18	90.8±36	Unknown	83.8±4
289.54	86.2±36	Unknown	77.5±4[*]
292.80	41.2±37	Unknown	31.7±4
296.12[#]	3.1±37	Unknown	-7.5±4
297.24[#]	-10.4±37	Unknown	-20.3±4
299.30[#]	-34.0±37	Unknown	-46.3±4
306.39	-130.9±39	Unknown	-143.1±4[*]
306.89	-137.9±39	Unknown	-148.1±4
317.30	-295.9±41	Unknown	-307.2±4[*]
320.87	-344.4±41	Unknown	-357.0±5
322.15	-362.8±41	Unknown	-376.5±5
323.14	-376.7±41	Unknown	-392.1±5

323.84	-385.7±42	Unknown	-402.7±5*
325.25	-405.7±42	Unknown	-426.1±5*
328.05⌘	-446.6±42	Unknown	-469.1±5*
331.21	-496.4±43	Unknown	-519.9±5*
334.94	-554.7±43	Unknown	-581.0±5*
335.84	-567.5±43	Unknown	-596.6±5*
343.30#	-691.5±44	Unknown	-722.0±6*

1: Age from Clausen et al. (1979). ★Depths indicate the tephra sampling interval. #: CFA acidity is missing for relevant interval, attribution is based on remaining records. †CFA acidity does not record peak. x: Conductivity and Ca records missing for interval. ⌘: CFA and IC data missing, depth annotation based on ECM only. *: Eruption not identified in existing compilation of volcanic eruptions in WAIS Divide (Sigl et al., 2013).

Table 2: Marker horizons used for development and validation of the RICE17 chronology. Strata in bold were used for constraining the timescale. Volcanic matching to WAIS Divide allows comparison between RICE17 ages (with 95% confidence interval indicated) and the corresponding WD2014 ages with associated uncertainties (Sigl et al., 2015, 2016). Indicated depths and ages correspond to peaks in the volcanic proxies. Below 42.3m, decimal ages have been calculated assuming BC to peak Jan 1st. Historical eruption ages (in column 3) indicate starting date of the eruption. In column 3 is also stated whether the eruption previously has been observed to cause a bipolar signal, based on the compilation in Sigl et al. (2013), here updated to the WD2014 timescale. Since this compilation only identifies bipolar volcanoes back to 80 CE, volcanoes prior to this are not classified. Three exceptionally large volcanic signals observed in the RICE core are indicated in italics.

Change point	Time period (rounded)	Mean accumulation rate [m. w.e./yr]	Accumulation rate trend [mm w.e. yr^{-2}]
	700 BCE – 1300 CE	0.25 ± 0.02	+0.02 (0.020 ± 0.003)
1287 CE (1291 ± 135)*			
	1300 CE – 1650 CE	0.26 ± 0.03	-0.04 (-0.03 ± 0.03)
1661 CE (1675 ± 123)*			
	1650 CE – 1965 CE	0.24 ± 0.02	-0.10 (-0.08 ± 0.05)
1966 CE (1969 ± 34)			
	1965 CE – 2012 CE	0.211 ± 0.002	-0.80 (-0.84 ± 0.76)

*Change point not well-determined from bootstrap analysis.

Table 3: Mean value and trends in RICE accumulation rates during various time periods. Change points and trends are found using break-fit regression (Mudelsee, 2009). The most likely change-points and trend values are provided, as well as the associated confidence intervals (in parenthesis: median and median absolute deviation; Mudelsee (2000)) determined from block bootstrap analysis. Uncertainties (2σ) on mean accumulation rates are calculated based on the uncertainty in the accumulation reconstruction. Accumulation trends estimates from the bootstrap analysis (in parenthesis) includes uncertainties in determination of the change-point, but not uncertainties associated with the derived accumulation rate history. The analysis does not account for a potential bias due to ice divide migration, which may slightly

affect the mean accumulation rate values prior to 1750 CE, and the trend during the period of divide migration (~1500-1750 CE).

Rank	Decade	Decadal mean accumulation rate [m. w.e./yr]
1	1990-1999	0.194 ± 0.001
2	1850-1859	0.197 ± 0.010
3	1950-1959	0.204 ± 0.006
4	2000-2009	0.207 ± 0.001
5	1800-1809	0.208 ± 0.017
6	1970-1979	0.212 ± 0.004

Table 4: Ranking of decades since 1700 CE according to lowest mean accumulation. Uncertainties (2σ) on the mean values are due to uncertainties in the accumulation reconstruction.

Supplementary material

S1. Effective depth resolution of the CFA records

Effective depth resolution of the CFA records were evaluated based on the time it took for the various measurement lines in the system to respond to an abrupt change in concentration level. Following the approach in Bigler et al. (2011), response times were calculated as the average time required for the system to transition from a blank water standard to the highest calibration standard plateau, using the 10% and 90% levels of the transition curve. From the employed melt rate of 3 cm/min, response times were then converted to equivalent response depths as a measure for the effective depth resolution. For the RICE CFA set-up, the conductivity record has the highest effective resolution of 0.8 cm, closely followed by black carbon (Table S1).

	Response time (s)	Response depth (cm)	Missing data fraction
Conductivity	15 ± 2	0.8 ± 0.1	6%
Acidity	38 ± 3	1.9 ± 0.2	17%
Calcium	49 ± 6	2.5 ± 0.3	9%
Black carbon	20 ± 3	1.0 ± 0.2	<1%
Insoluble dust particles	17 ± 3	1.0 ± 0.2	8%

Table S1: Response times for the CFA system to transition between the blank water level and a calibration standard plateau, and the equivalent response depths. Core breaks, contamination, measurement errors etc. gave rise to sections of missing data, these comprising from 1% to 17% of the total length of the record. Below 129 m, the dust record was extensively contaminated by drill liquid, and the missing data fraction is calculated for the uncontaminated top part only.

S2. StratiCounter settings and procedure

StratiCounter was initialized based on a preliminary set of manual layer annotations within a selected depth interval (40-150 m). The manual annotations were used to produce a set of generalized templates for an annual layer in the various impurity records. Applying the Expectation-Maximization algorithm (e.g. Gupta and Chen 2010), StratiCounter continuously updates and refines the statistical description of an annual layer, thereby allowing for changes in layer characteristics with depth (Winstrup, 2016; Winstrup et al., 2012). To further increase the independence of the StratiCounter timescale from the preliminary manual interpretation, in a final step the entire timescale was reevaluated using an improved set of layer templates derived from the algorithm output.

Rapid thinning of layers with depth in the RICE core necessitated slight changes in StratiCounter settings with depth. We therefore divided the record into four sections: an upper (42-180 m), an upper middle (165-250 m), a lower middle (240-300 m), and a lower section (280-344 m). Overlap sections served as base for comparison between the runs, which were found to contain only minor differences. Within these sections, the results from the deeper section were used to produce the final timescale.

For the uppermost section (42-180 m), performance of the algorithm was tested using a variety of algorithm settings, which all resulted in very similar timescales (±10 years at 165 m). The final version was chosen as the timescale in best agreement with the WD2014 age of the Pleiades tephra horizon (Dunbar et al., 2010) found at 165 m depth (Kalteyer, 2015). Proceeding to the deeper sections, the algorithm settings were kept as similar as possible to those employed for the upper part (Table S2).

The main change in settings with depth was the averaging distance employed to produce a lower-resolution record from the original 1 mm resolution CFA records, performed before automatic layer identification. Section delimitations were selected based on estimated layer thicknesses obtained from methane matching to WAIS Divide ice core (Lee et al., 2018) and chosen so that an average layer consists of approximately 10-15 individual data points. Accordingly, the averaging distance was successively reduced from 1.5 cm to 0.5 cm to account for the general decrease in layer thicknesses with depth (Table S2). Note that the averaging distance applied for the deepest section is less than the effective resolution of even the highest-resolution impurity records (Table S1), meaning that successive averaged data points are significantly correlated.

StratiCounter was run based on the full suite of CFA records: Black carbon, acidity, calcium, conductivity, and dust (topmost section only). The dust record was excluded for the lower sections due to drill liquid contamination. The impurity records were weighted so that records of large similarity (e.g. the calcium and conductivity) were not treated as independent data series, and with added emphasis on the black carbon, which displayed the most pronounced annual signal (Table S2). Before analysis, extreme peaks caused by measurement noise and processing errors were removed from the data series. These were further standardized using z-scores based on the logarithm of the impurity concentrations in order to reduce inter-annual variability in layer signal.

Section	**42.34–180 m (42.34-165 m)**	**165-250 m (165-240 m)**	**240-300 m (240-280 m)**	**280-350 m (280-343.7 m)**
Depth resolution (cm)	1.5	1.0	0.75	0.5
Weights of impurity series				
Black carbon	1	1	1	1
Acidity	0.5	0.5	0.5	0.5
Dust	0.5	0	0	0
Calcium	0.25	0.25	0.25	0.25
Conductivity	0.25	0.25	0.25	0.25

Table S2: StratiCounter settings for each depth range; in parenthesis is given the interval for which the results were used to produce the final combined timescale: Interpolated depth resolution of the impurity records before automated layer identification, and weighting of the various impurity records in the StratiCounter algorithm.

S3. The RICE density profile

Measured densities for the RICE core (Fig. S1) show good agreement with a modelled density profile calculated from a steady-state Herron-Langway densification model (Herron and Langway, 1980) when using appropriate values for the initial snow density (410 kg m^{-3}; within the range measured in adjacent snow pits), surface temperature (-23.5°C; consistent with borehole temperatures (Bertler et al., 2018)), and accumulation rate (0.22 m w.e yr^{-1}). The measured density profile was extended to the surface using the modelled densities. We note that the initial densification in the Herron-Langway model is parameterized as a linear function of depth, depending only on initial snow density and surface temperature.

At intermediate depths (50-120 m), the observed density profile has slightly denser snow than predicted by the Herron-Langway model. This difference may indicate that a steady-state assumption is invalid, or it may be due to the additional vertical strain present at divide locations (Kingslake et al., 2014).

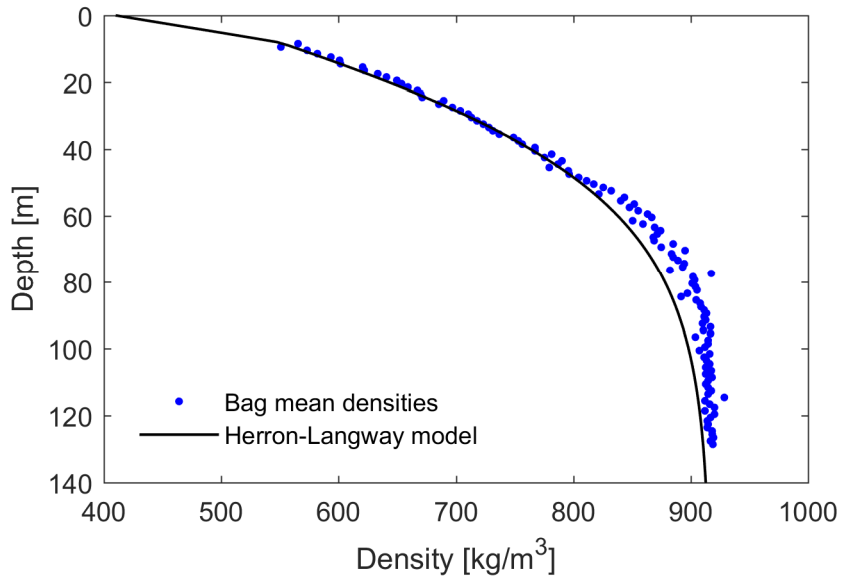

Figure S1: Measured and modelled density profile for the RICE core.

Supplementary references

Bertler, N. A. N., Conway, H., Dahl-Jensen, D., Emanuelsson, D. B., Winstrup, M., Vallelonga, P. T., Lee, J. E., Brook, E. J., Severinghaus, J. P., Fudge, T. J., Keller, E., Baisden, W. T., Hindmarsh, R. C. A., Neff, P. D., Blunier, T., Edwards, R., Mayewski, P. A., Kipfstuhl, S., Buizert, C., Canessa, S., Dadic, R., Kjær, H. A., Kurbatov, A. V., Zhang, D., Waddington, E. D., Baccolo, G., Beers, T., Brightley, H. J., Carter, L., Clemens-Sewall, D., Ciobanu, V. G., Delmonte, B., Eling, L., Ellis, A. A., Ganesh, S., Colledge, N., Haines, S. A., Handley, M., Hawley, R. L., Hogan, C. M., Johnson, K. M., Korotkikh, E., Lowry, D. P., Mandeno, D., McKay, R. M., Menking, J. A., Naish, T. R., Noerling, C., Ollive, A., Orsi, A., Proemse, B. C., Pyne, A. R., Pyne, R. L., Renwick, J., Scherer, R. P., Semper, S., Simonsen, M., Sneed, S. B., Steig, E. J., Tuohy, A., Ulayottil Venugopal, A., Valero-Delgado, F., Venkatesh, J., Wang, F., Wang, S., Winski, D. A., Winton, V. H. L., Whiteford, A., Xiao, C., Yang, J. and Zhang, X.: The Ross Dipole - temperature, snow accumulation, and sea ice variability in the Ross Sea Region, Antarctica, over the past 2700 years, Clim. Past, 14, 193–214, doi:10.5194/cp-14-193-2018, 2018.

Bigler, M., Svensson, A., Kettner, E., Vallelonga, P., Nielsen, M. E. and Steffensen, J. P.: Optimization of high-resolution continuous flow analysis for transient climate signals in ice cores, Environ. Sci. Technol., 45(10), 4483–4489, doi:10.1021/es200118j, 2011.

Dunbar, N. W., Kurbatov, A. V., Koffman, B. G. and Kreutz, K. J.: Tephra Record of Local and Distal Volcanism in the WAIS Divide Ice Core, in WAIS Divide Science Meeting September 30th-October 1st, La Jolla, CA, USA. [online] Available from: https://geoinfo.nmt.edu/staff/dunbar/publications/abstracts/dakk2010.html, 2010.

Gupta, M. R. and Chen, Y.: Theory and Use of the EM Algorithm, Found. Trends® Signal Process., 4(3), 223–296, doi:10.1561/2000000034, 2010.

Herron, M. M. and Langway, C. C.: Firn densification: an empirical model, J. Glaciol., 25(93), 373–385, doi:10.3189/S0022143000015239, 1980.

Kalteyer, D. A.: Tephra in Antarctic Ice Cores, Master Thesis, University of Maine, 2015.

Lee, J., Brook, E. J., Bertler, N. A. N., Buizert, C., Baisden, W. T., Blunier, T., Ciobanu, G., Conway, H., Dahl-Jensen, D., Fudge, T. J., Hindmarsh, R. C. A., Keller, E. D., Parrenin, F., Severinghaus, J. P., Vallelonga, P., Waddington, E. D. and Winstrup, M.: A 83,000 year old ice core from Roosevelt Island, Ross Sea, Antarctica, Clim. Past Discuss., 1–44, doi:10.5194/cp-2018-68, 2018.

Winstrup, M.: A Hidden Markov Model Approach to Infer Timescales for High-Resolution Climate Archives, in Proceedings of the 30th AAAI Conference on Artificial Intelligence and the 28th Innovative Applications of Artificial Intelligence Conference, pp. 4053–4061, AAAI Press, Palo Alto, California, February 12 – 17, 2016, Phoenix, Arizona USA., 2016.

Winstrup, M., Svensson, A. M., Rasmussen, S. O., Winther, O., Steig, E. J. and Axelrod, A. E.: An automated approach for annual layer counting in ice cores, Clim. Past, 8(6), 1881–1895, doi:10.5194/cp-8-1881-2012, 2012.